1 of 1

12/7-20-94 JSH (1)

PNL-8681
UC-702

Modeling Study of Deposition Locations in the 291-Z Plenum

L. A. Mahoney
J. A. Glissmeyer

June 1994

Prepared for the U.S. Department of Energy
under Contract DE-AC06-76RLO 1830

Pacific Northwest Laboratory
Operated for the U.S. Department of Energy
by Battelle Memorial Institute

Battelle

PNL-8681

DISCLAIMER

PACIFIC NORTHWEST LABORATORY
operated by
BATTELLE MEMORIAL INSTITUTE
for the
UNITED STATES DEPARTMENT OF ENERGY
under Contract DE-AC06-76RLO 1830

Printed in the United States of America

Available to DOE and DOE contractors from the Office of Scientific and Technical Information, P.O. Box 62, Oak Ridge, TN 37831; prices available from (615) 576-8401. FTS 626-8401.

Available to the public from the National Technical Information Service, U.S. Department of Commerce, 5285 Port Royal Rd., Springfield, VA 22161.

PNL-8681
UC-702

MODELING STUDY OF DEPOSITION LOCATIONS IN THE 291-Z PLENUM

L. A. Mahoney
J. A. Glissmeyer

June 1994

Prepared for
the U.S. Department of Energy
under Contract DE-AC06-76RLO 1830

Pacific Northwest Laboratory
Richland, Washington 99352

SUMMARY

The TEMPEST (Trent and Eyler 1991) and PART5 computer codes were used to predict the probable locations of particle deposition in the suction-side plenum of the 291-Z building in the 200 Area of the Hanford Site, the exhaust fan building for the 234-5Z, 236-Z, and 232-Z buildings in the 200 Area of the Hanford Site. The TEMPEST code provided velocity fields for the airflow through the plenum. These velocity fields were then used with TEMPEST to provide modeling of near-floor particle concentrations without particle sticking (100% resuspension). The same velocity fields were also used with PART5 to provide modeling of particle deposition with sticking (0% resuspension). Some of the parameters whose importance was tested were particle size, point of injection, and exhaust fan configuration.

The predicted locations of particle accumulation in the 291-Z building are considerably different for the 0% resuspension case (PART5) than for the 100% resuspension case (TEMPEST). We expect that for most particles, the no-resuspension results will apply because of the probable stickiness of the floor and because small particles (under 20 μm in size) tend to remain where they are deposited unless the air velocity is substantially increased. However, some large "fluffy" particles such as might come from broken filters may deposit according to the resuspension case. In addition, given a sufficient amount of condensate, some disposed contaminants would be transported further south to a low spot.

Although the two fan configurations that were tested were fairly dissimilar, the near-floor concentration patterns in the 291-Z building predicted by TEMPEST for the two configurations were very similar. In both cases the particles in the relatively slow flow from the 232/236-Z exhaust contributed a disproportionately high fraction of the deposition for any given particle size. The location of maximum concentrations also varied with particle size. For large (100-μm) depositing particles, the major estimated deposition areas included the incline below the inflow from 234-5Z, the floor just below the incline, a region running diagonally from fan EM-1 to EM-6, and a broad area of the floor opposite the inflow from 232/236-Z. Smaller particles that might be carried along some distance before depositing may accumulate along the floor from below the fan EM-7

inlet to the inflow from 232/236-Z and also in the southeast corner. The possibility that some fans may accumulate more internal contamination than others was also illustrated by the results from the PART5 model for 100-μm particles.

CONTENTS

FIGURES

TABLES

1.0 INTRODUCTION

There has been concern that plutonium-containing particulate material may have been deposited downstream of the final high-efficiency particulate air (HEPA) filters during the 40-plus years of operation of the Plutonium Finishing Plant (PFP) complex in the 200 Area of the Hanford Site. One of the potentially contaminated areas is the 291-Z building, which houses the final exhaust plenum, fans, and discharge stack for the 234-5Z (PFP), 232-Z (incinerator), and the 236-Z (plutonium reclamation) buildings. Some of the particles deposited in the plenum would have come from the very small fraction of particles that passed through the HEPA filters during normal operations. Additional material might have come from resuspension of contaminated rust in metal ducts (especially the 236-Z duct) or from the few events (such as hydrofluoric acid process excursions) that damaged the final HEPA filters.

One motivation for this study is the need to minimize personnel or equipment exposure during possible future decontamination or measurement programs in the ventilation ducts downstream of the final HEPA filters. An indication of the expected locations of maximum contaminant deposition would be an aid to planning such programs. The modeling effort reported here was concerned only with the central plenum portion of the 291-Z building where the exhaust airflows drawn from the 234-5Z, 232-Z (until December 1990), and 236-Z buildings combined together. Because of its size and the resulting low air velocity, this plenum appears to have a higher potential for the accumulation of deposited particles than other smaller (high air velocity) ducts. It is directly from this plenum that the exhaust fans draw ventilation air (from the connected buildings) for discharge through the adjacent 291-Z-1 stack. Other potential accumulating deposition sites may be the fan discharge plenums, but they are not addressed in this report.

In this study, Pacific Northwest Laboratory[(a)] staff used the TEMPEST (Trent and Eyler 1991) and PART5 computer models to estimate the locations of contaminant deposition in the central plenum of the 291-Z building. Section

---

(a) Pacific Northwest Laboratory is operated for the U.S. Department of Energy by Battelle Memorial Institute under Contract DE-AC06-76RLO 1830.

2.0 details the [illegible]um configuration. Section 3.0 presents information about the anticipated contaminant particle-size distribution, Section 4.0 presents the modeling techniques used and Section 5.0 presents the results given by the models. Finally, Section 6.0 presents the conclusions drawn from the results.

2.0 SYSTEM CONFIGURATION

Figure 2.1 shows the orientation of 291-Z relative to the other buildings in the complex. A large overhead duct brings filtered exhaust air from 234-5Z to the north end of the suction-side plenum of 291-Z. Smaller ducts carry filtered exhaust air from 232-Z and 236-Z to a common port on the east side of the suction-side plenum of 291-Z. (In December 1990, the 232-Z building was isolated from the 236-Z duct and switched over to its own new ventilation exhauster.) The figure also shows the four electric fans on the west side of the plenum. The standby steam-driven fan (obscured by the 232-Z duct) is arranged the same way as the electric fans. Figure 2.2 is a view of the east side of the suction-side plenum showing three electric fans and one standby steam-driven fan. Both the ducts from 232-Z and 236-Z discharge together into the suction-side plenum through an opening between the standby steam-driven fan and the electric fans. All of the fans discharge downward into two discharge ducts, one on the east side and the other on the west side of the plenum. The discharge ducts join together at the south end of the plenum at the base of the stack.

The standby steam-driven fans have seen limited use, but are regularly tested. To maintain the normal ventilation flow through the buildings, only four of the seven electric fans are used at any given time; however, the fan usage is rotated among the seven electric fans for maintenance reasons. One key parameter possibly affecting the location of deposits in the plenum is which of the seven fans are in use. Unfortunately, records of fan usage are retained for only a limited time period. To determine the effect of what could be called the "fan configuration," two different fan configurations were studied.

The available data indicate that common practice is to use three fans from one side and one from the opposite side of the plenum at a time, as shown in Figure 2.3. The fan usage data was obtained for the period covering July 1990 through May 1991. Fans EM1, EM2, EM3, and EM6 were operated together for 79% of that time. Fans EM2, either EM3 or EM4, EM5 and EM6 were operated together for another 21% of that time. However, because the facility has been operated for more than four decades and the available fan data cover only a

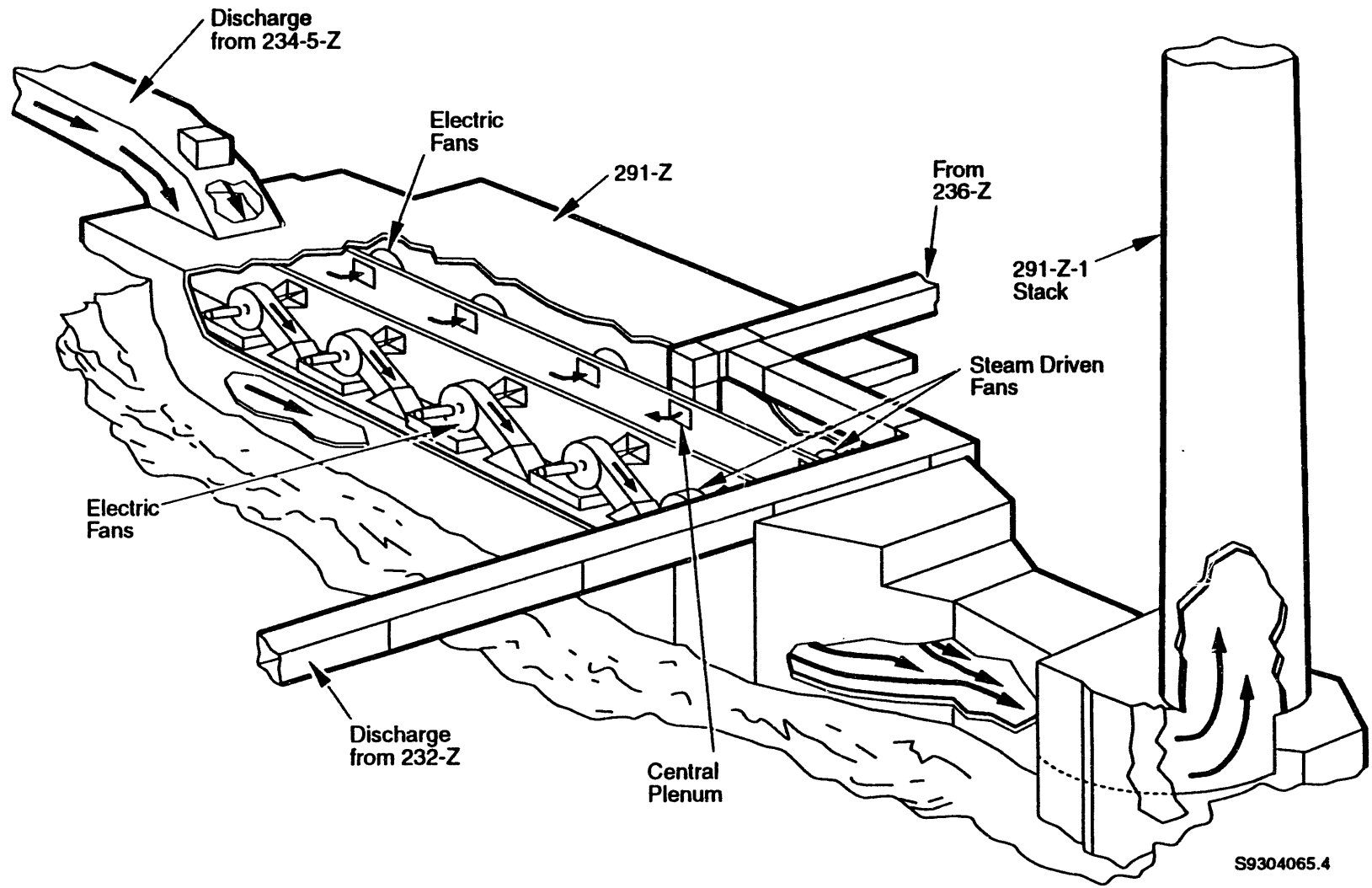

FIGURE 2.1. Cutaway View of 234-5Z and 291-Z Building Ventilation Exhaust System (from the West)

small portion of that time, it was decided to model what might reasonably be expected to be the cases that would result in the most different airflow and deposition patterns. Therefore, the first configuration modeled, Fan Configuration 1, includes the three electric fans on the east side (EM5, EM6, EM7) and the northernmost fan on the west side (EM1), as shown in Figure 2.3a. Fan Configuration 2 includes the three northernmost fans on the west side (EM1, EM2, EM3) and the second of the three electric fans on the east side (EM6), as shown in Figure 2.3b.

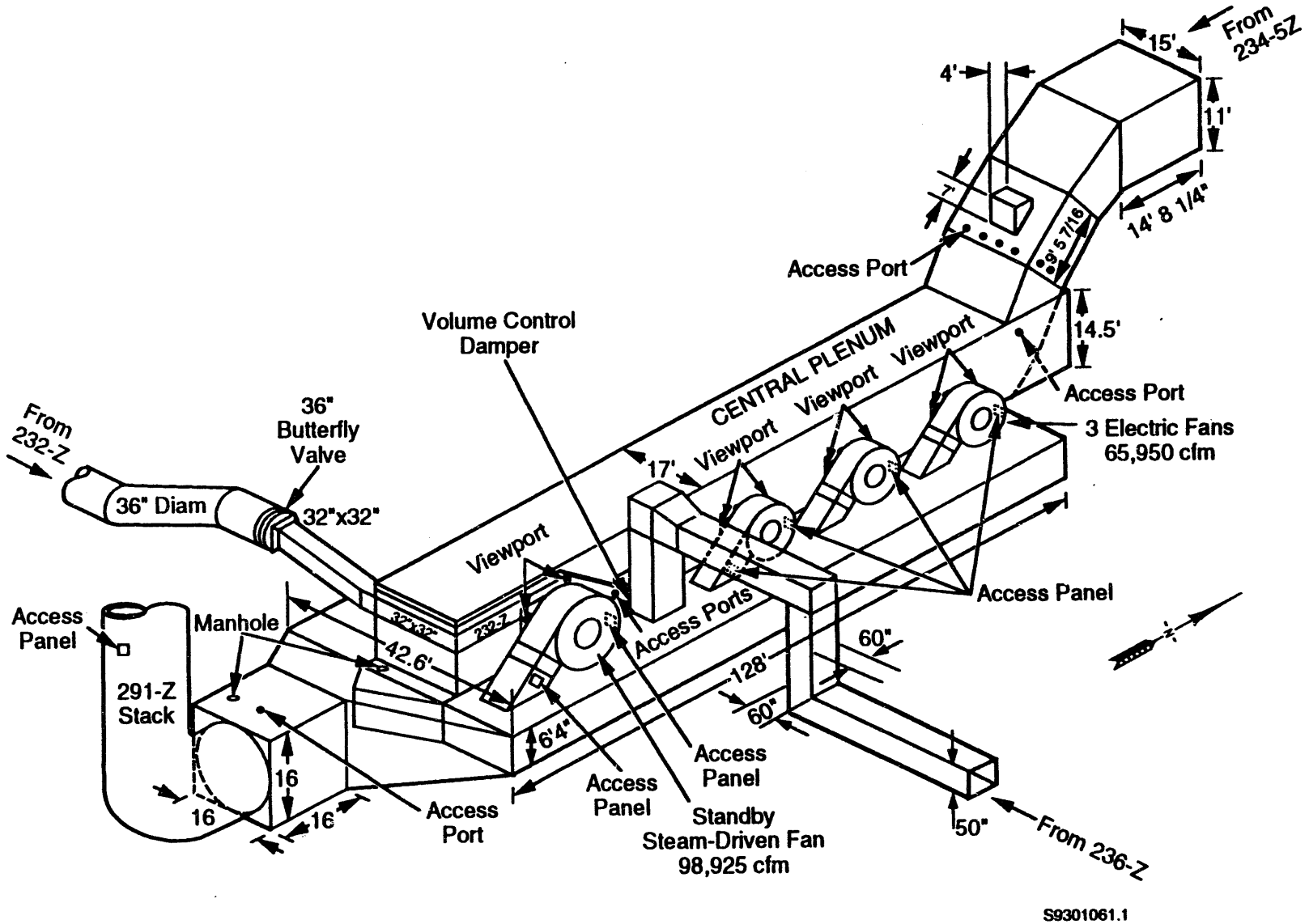

FIGURE 2.2. View of 291-Z Central Plenum, Fans, Duct, and Stack (from the East)

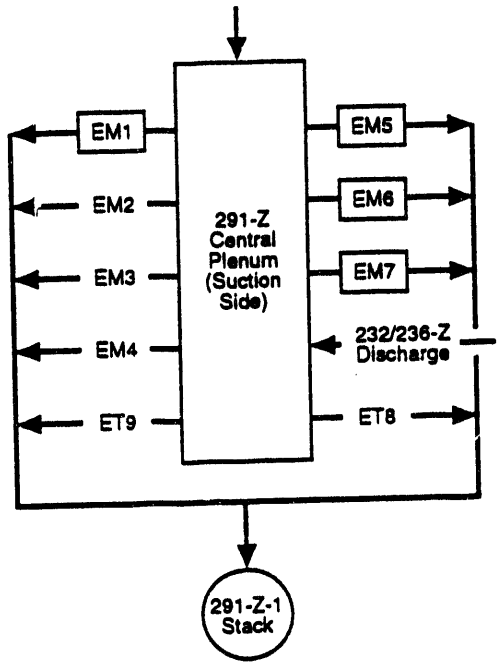

a) Fan Configuration 1

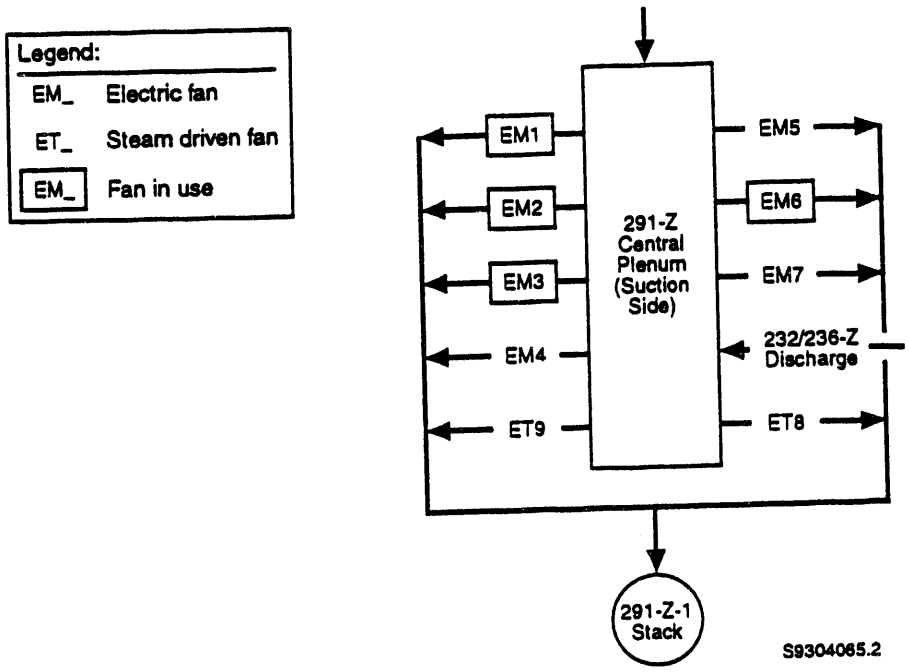

b) Fan Configuration 2

FIGURE 2.3. Fan Configurations 1 and 2 Modeled

3.0 PARTICLE-SIZE DISTRIBUTION

The data most relevant for modeling the deposition of contaminated particles in the 291-Z exhaust plenum are those obtained from characterizations of filtered exhaust air flows. During the 1970s, several studies were performed to characterize the particulate material in the PFP exhaust ventilation system. Two important relevant conclusions can be made from these studies.

First, most of the airborne radionuclides are found as contamination on particles of other materials. Some of these other materials were identified by Glissmeyer (1992), who investigated the background levels of some metals (iron, copper, zinc, tin, titanium, and manganese) in the 291-Z-1 stack to help determine a candidate tracer. While titanium and manganese were not found, the highest concentrations of iron, copper, and zinc were 8.2E-3, 9.1E-6, and 1.9E-4 $\mu g/ft^3$, respectively. The total for these metals was then 8.4E-3 $\mu g/ft^3$ or 2.97E-13 g/cm^3. During the same study, the highest measured plutonium concentration was 2.5E-12 $\mu Ci/cm^3$ or 4.1E-17 g/cm^3. The airborne concentration of plutonium was then about four orders of magnitude less than these other metals. From this and other studies, we conclude that most deposited materials will be construction- or process-derived and will bear relatively small amounts (on a mass basis) of radionuclides.

Second, depositing particles will include a broad range of sizes, much broader than might be expected in filtered air. The information supporting these two conclusions is summarized in Subsection 3.1. Subsection 3.2 describes the particle sizes used in the modeling phase.

3.1 PARTICLE-SIZE MEASUREMENTS

In a study conducted by Mishima and Schwendiman in 1970 and 1971 (1971), samples were collected from the 291-Z-1 stack and the main tributaries to the exhaust flow, the Zone 4 PFP exhaust, hydrofluoric acid (HF) system, vacuum line, 236-Z, and 232-Z. Observations were as follows:

- In the plenum downstream of the 309 filter room, the calculated activity concentrations were between 4.5E-06 and 1.0E-03 dpm/ft^3. The filtered

material was "black with shiny patches," with measured aerodynamic median activity diameters (AMAD) of 9.5 and 20 μm.

- The HF system exhaust was sampled in the winter (1970-1971). Samples were taken downstream of the final filter bank enclosure. An activity concentration of 0.06 dpm/ft^3 was measured. The AMAD of the particles was 7.4 μm, but the activity distribution of the material was bi-modal, indicating more than one mechanism of particle formation.

- The vacuum system maintained at 26-in Hg was sampled between October and December of 1970. Samples were taken from the line between the vacuum pump and the main exhaust plenum. All the interior surfaces and plates from the samples were loaded with a glassy, hard material resembling hard water deposits. An activity concentration of as high as 2.8 dpm/ft^3 was measured. The AMAD was estimated to be less than 1.6 μm with a log-normal size distribution, indicating one mechanism of particle formation.

- The 236-Z building exhaust was sampled from a duct just upstream of the entry into the 291-Z exhaust plenum. "A large quantity of moist, reddish-brown, granular material was found on the filter sample...and the rubber cement surface on impactor plates and impactor walls appeared oxidized." (Mishima and Schwendiman 1971, p. 18). The AMAD was 3 μm. The coarseness of the material pointed to generation of the particles downstream of the filters. The material could have been rust from the existing duct, which was metal and aboveground. The sample was described as having a "high salt content" (Mishima and Schwendiman 1971, p. 18). The activity concentration was low (1E-4 dpm/ft^3). Since the sampling described here, much of this duct has been replaced with a concrete, below-ground duct.

- The 232-Z duct was sampled during incinerator operations. The sample showed "highly active, coarse, red and gray particles" (Mishima and Schwendiman 1971, p. 11). The outlet for the sample was on a vertical wall of a sloped duct. The red coloring may suggest rust, gray may indicate ash. The AMAD was 8 μm with a log-normal distribution.

- The 291-Z-1 stack was sampled at the base of the stack in the last quarter of 1970. Considerable condensation was noted, and the sampled material was dark gray. The activity concentration was low (6.4E-03 dpm/ft^3). The plutonium was believed to be attached to inert particles.

Another measurement program conducted from October, 1972 to May, 1973 sampled particles at the base of the 291-Z-1 stack (Mishima and Schwendiman 1973). Seven sets of samples were taken. The AMAD from the samples ranged from 3.3 to 9.0 μm with 60 to 80% of the activity associated with particles less than 10 μm. The average activity was 0.034 dpm/ft^3. No apparent correlation was seen between building operations and measured activity.

A study using tracer particles was performed in 1976-78 on the 291-Z-1 stack to determine the adequacy of the in-place sampling system (Glissmeyer 1992). Samples were taken at the 50-ft level of the stack. All of the samples contained particles with the appearance of rust. The AMADs of plutonium-containing particles were between 3.5 and 8.6 μm. TiO_2 and ZnS tracers with aerodynamic mass mean diameters (AMMDs) of 1.3 and 8 to 9.5 μm were released into the stack to test the sampling system.

Table 3.1 summarizes the size measurements of plutonium-bearing particles taken from the 291-Z tributaries and exhaust stack.

TABLE 3.1. Summary of Particle-Size Measurements in Vent Exhaust Streams

Location	Date	Plutonium Concentration 10^{-13} µCi/ml	Reported AMAD µm	Entrance Loss %	Observations	Reference[a]
Main Stack	12/70- 1/71	1.0	3	N.M.[b]	condensation	1
236Z Exhaust	10/70 - 11/70	0.016	3	N.M.	reddish brown, granular paste	1
232Z Exhaust	12/70 -1/71	2.9	7.9	N.M.	small amount of ash	1
26-in. Vacuum Exhaust	10/70 - 11/70	37	1.6	N.M.	loaded w/ glassy hard material	1
	12/70 - 1/71	17	>0.3	N.M.		
309 Filter Room	9/70 - 10/70	0.16	9.5	N.M.		1
	12/70	0.12	≈20	N.M.		
HF Exhaust	12/70 - 1/71	9.4	7.4	N.M.		1
Main Stack	10 - 11, '72	11	6	41.5		2
	11 - 12, '72	2.1	8 - 9	41.5		2
	12/72 - 1/73	3.3	3.3	41.9		2
	1 - 3, '73	2.5	4	28.4		2
	3 - 4, '73	4.8	7	53.2		2
	4 - 5, '73	6.4	7.3	52.8		2
	5/73	3.2	8	56.0		2
	10 - 11, '77	11	6.8	46	visible rust particles in samples	3
	11/77	2.3	8.6	59		3
	1 - 2, 78	9.5	3.5	23		3

Notes and References:
(a) Numbers correspond with the following references:
1) Mishima and Schwendiman 1971,
2) Mishima and Schwendiman 1973, and
3) Glissmeyer 1992.
(b) N.M. = not measured.

Air samples were collected on filters concurrently with the cascade impactor sampling at the base of the stack during the 1972 - 1973 measurements (Mishima and Schwendiman 1973). Those results were all within a factor of two of the impactor results, indicating good recovery in the impactor samples. During this same sampling campaign, the plutonium collected in the sampling probe and transition to the impactor was analyzed. These deposits were a significant fraction of the total collection in the probe and impactor combined. Because larger particles are more inclined to deposit than smaller ones, it could be reasoned that the particles deposited in the inlet are all larger than what was collected on the first stage of the impactor. Factoring that into the analysis for the samples would have resulted in AMADs of about two to three times greater than reported. It seems more reasonable to conclude that particles of all sizes deposited, but with deposition favoring the larger sizes. This would result in a more modest, yet indeterminant, adjustment of the AMAD.

Keeping in mind the possibilities for errors in the reported particle-size measurements and the broadness of the plotted-size distributions, it seems reasonable to conclude that plutonium-bearing particles that have deposited inside the 291-Z plenum would cover a broad range of sizes.

3.2 MODELED PARTICLE SIZES

A possible major type of radionuclide-bearing particle may be iron oxide. A major source of airborne iron could be the rusty steel duct that carried exhaust air from 236-Z a short distance above ground to the 291-Z fan house. This source was first identified by Mishima and Schwendiman (1971). The duct walls had been attacked by the corrosive vapors coming from the process and condensing on the exposed, cold steel surfaces. It is unknown how long this section of duct had been a serious source of contaminated airborne rust particles, perhaps since shortly after the start of the PRF processing in the early 1960s. By 1977, the duct had rusted through and replacement occurred soon thereafter. Extrapolating from Mishima and Schwendiman's observation of a 1/4-in thick cake of rust on a 4-in air filter through which 2.65E6 ft^3 had been drawn, one finds an air concentration of 1.3E-10 g/cm^3

when a deposit diameter of 3.5-in and a bulk density of just 0.25 g/cm^3 are assumed. Extrapolating further, assuming an air flow through the duct of 46,500 cfm and a duration of just 1 year yields about 91 kg of potentially contaminated rust having passed the sampling point. This quantity of large contaminated particles could have an important impact on the deposition patterns of radionuclides.

Based on the studies summarized here, a broad range of particle sizes was selected for the TEMPEST modeling of deposition in the 291-Z plenum. The selected particle sizes and settling velocities are shown in Table 3.2. The smaller sizes represent the typical range of plutonium-bearing particles observed in most of the studies. The larger sizes represent the rust from 236-Z or the HEPA filter fragments from filter blowouts like the HF system filter accident of 1986. It is likely that on a mass basis, the 236-Z duct rust may overwhelm the contributions from other sources. The actual particle concentration value input to TEMPEST is of little importance because concentration and deposition results for the different species are evaluated separately. The concentration inputs shown in Table 3.2 for the smaller particles correlate to the measured values for metals in Glissmeyer (1992). The inputs for the larger particles roughly correspond to the airborne rust content extrapolated as above from Mishima and Schwendiman (1971).

TABLE 3.2. Particle Parameters for Modeling

Particle Diam. μm	Settling Vel. cm/s	Main Duct ng/cm^3	232/236 ng/cm^3
1	3.5E-03	4E-05	4E-05
3.4	3.5E-02	4E-05	4E-05
10	3.1E-01	4E-05	4E-05
34	3.5E+00	4E-05	1E-01
100	2.5E+01		0.1
1000	3.9E+02		0.1

4.0 MODELING TECHNIQUES

The modeling techniques available allow the prediction of relative amounts of deposition in the plenum, and so of the locations of peak deposition. However, the absolute amount of total deposition to be expected is not predictable because of gaps in information and technique. The information required for predicting the absolute amount is the complete history of the fan configuration and the size and concentration of particles entering the plenum. On the technique side, there is no method for predicting the fraction of particles that rebound from the surface immediately on contact or are resuspended later. Likewise, there is no method for assessing the movement of contaminants when there is enough condensed moisture in the plenum to wash deposits down to low points of the floor.

The modeling techniques that were employed in this study are described below. Section 4.1 describes how the central plenum's physical features were parameterized for model input. Section 4.2 describes how velocity fields were computed. The modeling of particle trajectories is described in Section 4.3. Finally, Section 4.4 describes the aerosol transport modeling in TEMPEST.

4.1 MODELING DOMAIN

The first step in the modeling process was to translate the physical description of the central plenum into model inputs. The plenum space was subdivided into three-dimensional (3D) cells sized so that key cell boundaries coincided with the physical locations of ducts and fans. Some regions were subdivided more finely than others to achieve better flow-field resolution in those areas.

Figure 4.1 shows the overall layout of the 3D computational cells, but with the west wall removed for clarity. The cell lines shown on the wall and floor project through space to form the 3D computational cells inside the plenum. The inclined plane where the duct from 234-5Z enters the plenum was approximated stair-step-wise. The steam-driven fan intakes were not included because they were not to be considered in this effort. The velocity and particle concentration are assumed uniform within each individual cell.

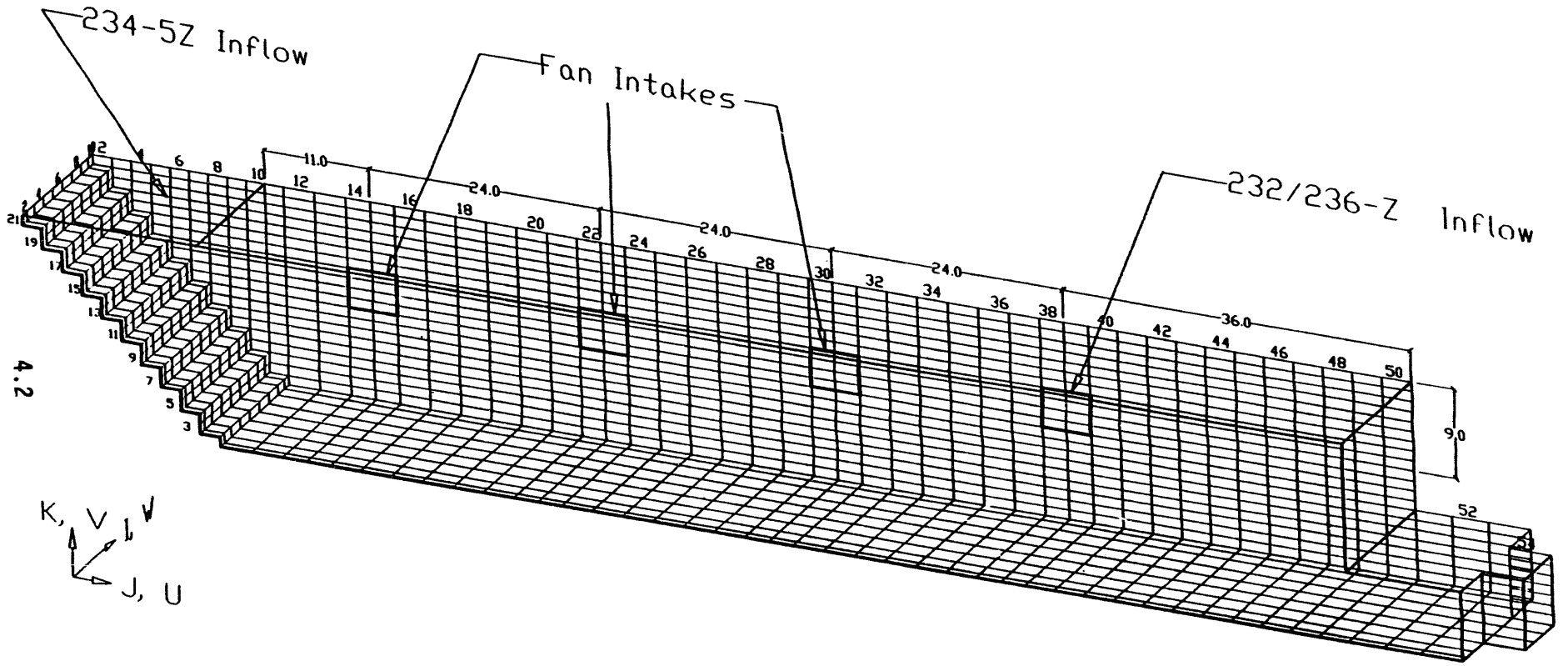

FIGURE 4.1. Diagram of Computational Mesh

Cell types were then defined for the cells along the wall. Type categories included inflow, outflow, and wall.

4.2 VELOCITY FIELDS

The next step was the calculation of air-velocity fields (the 3D matrix of velocity vectors, one for each computational cell) for the two different fan configurations shown in Figure 2.3. The TEMPEST code was used for calculating the velocity fields.

The exhibits in Appendix A are the TEMPEST input files for the two configurations. In order to attain steady-state flow, the TEMPEST model was run for 75 to 80 s of simulation time. At this point, the velocity time histories at several locations were examined to confirm that steady-state flow had been reached. These time histories are shown and discussed in Appendix B.

4.3 PARTICLE TRACKING

The steady-state velocity field produced with TEMPEST (after 80-s elapsed simulation) for one of the fan configurations was used with the particle tracking model, PART5, to find the locations of maximum deposition when no resuspension occurs. The PART5 model includes the effects of drag and settling but not of diffusive deposition or particle inertia. It also does not include resuspension or particle rebound and so can be best used to describe deposition under conditions where 100% sticking is achieved.

A burst of particles was injected into otherwise pure air at both the 232/236-Z and 234-5Z inflow areas. Table 4.1 shows the ranges of cells into which particles were placed. The coordinates refer to the cell numbers used in Figure 4.1.

The injected particles were randomly scattered throughout each range of injection cells at a density of about 100 particles per unit area so the particle flux would be areally uniform. Consequently, where there was uneven air velocity across the injection area, the particle concentration (particle number/unit volume of air) varied inversely with local air velocity. This was the case for the 234-5Z inflow. The particle concentration in the northern half of the opening of that duct into the plenum was about twice that of the southern half and the 232/236-Z inflow.

TABLE 4.1. Ranges of Cell Numbers Used as Injection Areas

Entry location	J (length)	K (height)	I (width)
232/236-Z	38-39	10-14	10
234-5Z	2-10	21	2-10

Two types of particles were considered: tracer particles (with no drag or settling) and 100-μm aerodynamic equivalent diameter (AED) particles (with drag and settling). The PART5 model provided output of the locations at which particles were deposited and of the exhaust ports through which particles were ejected, as well as the times at which deposition or ejection occurred. Runs were carried out to a long enough time (50 to 200 s after injection) to permit deposition or ejection of over 99% of the particles.

4.4 TEMPEST AEROSOL MODELING

The TEMPEST model treats aerosol concentration as a continuum property; particle settling is controlled by specifying a vertical settling velocity. There is no provision in the model for particle deposition and sticking, inertia, diffusive deposition, or vector drag. Thus, the TEMPEST model is most useful as a way of estimating particle concentrations resulting from assumed immediate 100% resuspension. The settling velocities that were specified for different particle sizes are listed in Table 4.2.

Air-velocity fields for both fan configurations were used with the TEMPEST model. The incoming airflows were given aerosol mass fractions (relative to air) of 3.4×10^{-11} (roughly corresponding to the Table 3.2 mass concentration of 4.0×10^{-5} ng/cm^3 that had been measured in 234-5Z airflows entering the plenum). The air that was initially in the plenum was free of aerosol. Aerosol injection was continuous, not a single burst as in the case of the PART5 model. TEMPEST runs were made for the particle sizes shown in Table 4.1 and were typically carried out for 30 or 60 s time. These run lengths were chosen to permit settling of heavy particles and mixing of the aerosol-laden inflow with the initially clean plenum air volume. Some characteristic settling and mixing times for the plenum are given in Table 4.2.

TABLE 4.2. Characteristic Settling and Mixing Times for the Plenum

Average air residence time in plenum (total flow/total volume)	9 s
Average residence time for plenum south of 232/236-Z	40 s
Time for 100-μm aerosol to settle from plenum top in still air	24 s
Time for 10-μm aerosol to settle from plenum top in still air	1900 s
Time for 1-μm aerosol to settle from plenum top in still air	10^5 s

5.0 RESULTS

The discussion of the modeling results is divided into velocity fields, particle tracking, and TEMPEST aerosol modeling. Section 5.1 presents and compares the velocity fields generated by TEMPEST for the two fan configurations studied. The velocity fields resulting from the two fan configurations were quite similar, with only subtle differences in the bottom of the central plenum. Because of the similarity between the velocity fields, the particle trajectory tracking model was applied to only one fan configuration. The particle tracking results for non-depositing and depositing particles are discussed in Section 5.2. Section 5.3 presents the results from using TEMPEST to model aerosol movement in the plenum. Particle settling is accounted for in this model, but actual deposition and deposit build-up are not addressed by TEMPEST. Issues relating to the validity of the approach are discussed first. Then the effects of fan configuration on where large and small particles tend to accumulate are discussed.

5.1 VELOCITY FIELDS

Figures 5.1 through 5.10 show side-by-side views of the velocity fields generated for the two fan configurations. Each of these shows a two-dimensional representation of the velocity vectors for a different plane in the plenum. The scales differ along the axes of the figures. The north-south axis, (J-axis in Figure 4.1) is compressed considerably to fit the page, with the consequence that some of the vectors depicted seem to overlap.

There are several similarities in the velocity fields produced by the two fan configurations. Figure 5.1 shows the horizontal plane at the elevation of the fan centerlines. The two fan arrangements have distinctly different patterns for the air exhausting through the fans, but there is little effect on the 232/236-Z plume entering the plenum. Figure 5.2 shows that the velocity patterns along the floor are quite similar; however, there appears to be some vorticity or an eddy in the middle of the plenum, which can

be seen in the second velocity field but not the first. There is also a region that runs diagonally from the second west fan to the third east fan where two opposing horizontal airstreams meet. The stagnant areas in the southernmost fifth or so of the plenum also exist in both velocity fields. Figure 5.3 shows that both velocity fields produced very similar patterns along the ceiling. Figure 5.2 and 5.3 both show the slow backflow from the 232/236-Z exhaust passing across the floor and ceiling of the plenum back towards the 232/236-Z entry point. Figures 5.4 through 5.6 show that most of the differences between the two fan configurations are in the vertical velocity fields. However, note the nearly stagnant conditions in the southern fifth of the plenum.

Figures 5.7 and 5.8 show the floor-level velocities in the southern part of the plenum (south of the 232/236-Z exhaust entry point). The horizontal velocities are plotted as vectors, and the vertical velocities are separately plotted as a contour plot. The velocity fields in this part of the plenum are nearly to identical for the two fan configurations.

The general similarity of the two velocity fields results from the fact that the two fan configurations are nearly the same except for being "flipped" to have the three fans on the other side of the plenum. The incoming 232/236-Z exhaust is the only part of the overall three-dimensional flow that does not share in this symmetry, but the effects of this exhaust flow are so diffuse in the north end of the plenum that little asymmetry of the flow field is produced. Since the 232/236-Z exhaust is the dominant influence on velocities in the south end of the plenum, changing the sides on which the exhaust fans operate has little effect in the south end.

5.2 PARTICLE TRACKING

Because of the similarity in the velocity fields from both fan configurations, the particle tracking model (PART5) was used for only the first fan configuration. Both tracer and depositing particles were modeled.

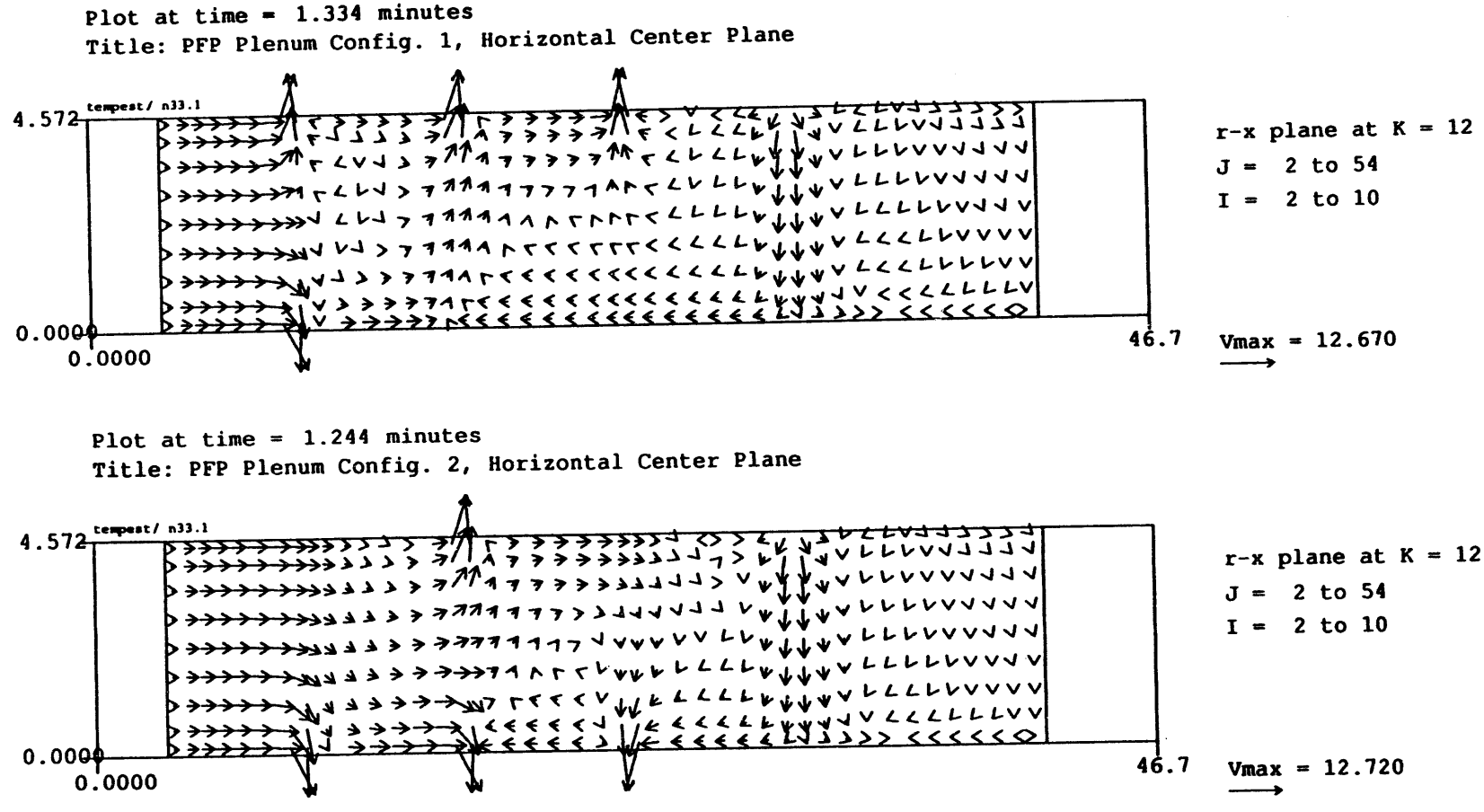

FIGURE 5.1. Velocities in the Horizontal Plane of the Exhaust Fan Centers for Fan Configurations 1 (upper figure) and 2 (lower figure)

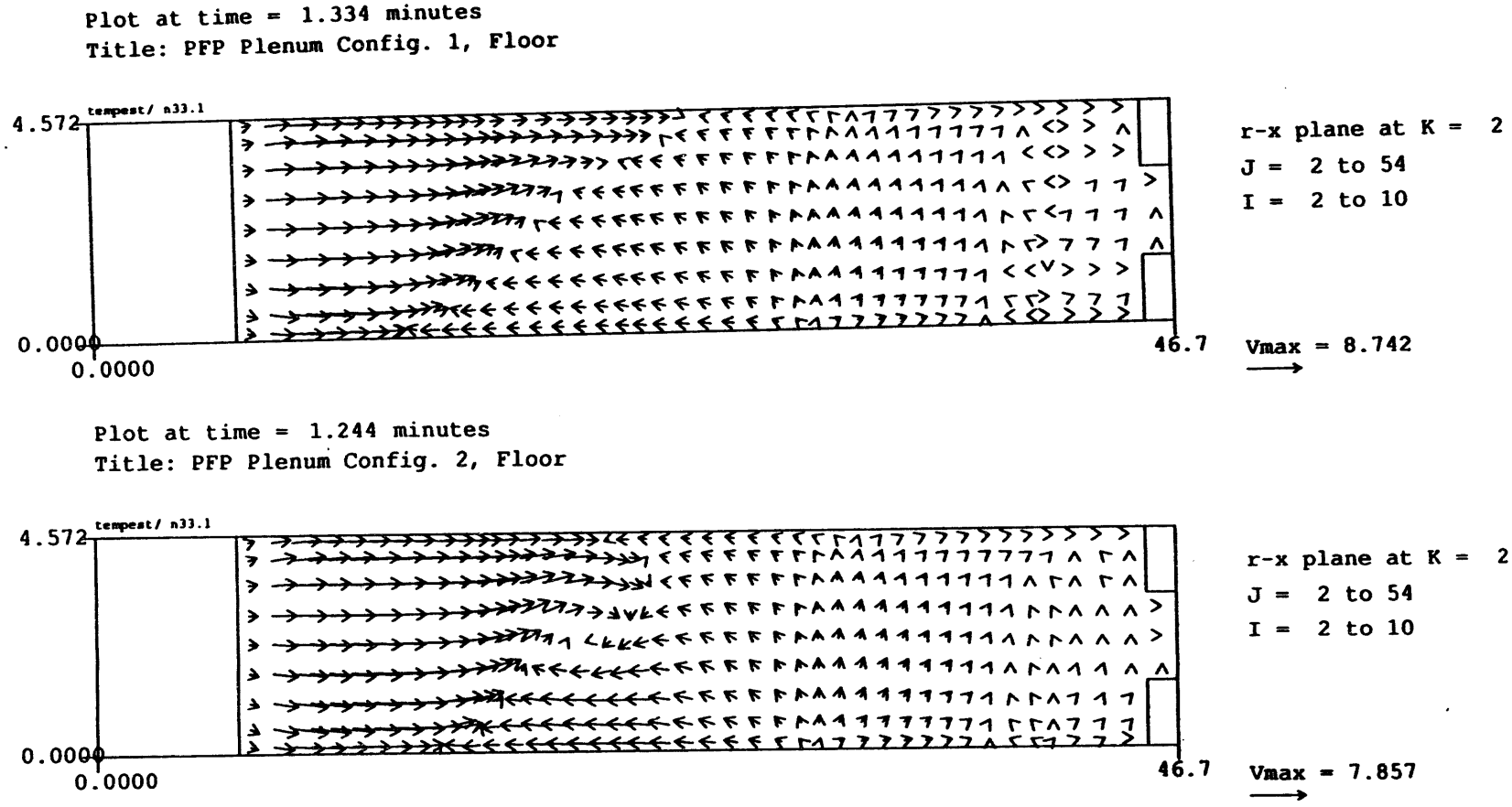

FIGURE 5.2. Velocities in the Horizontal Plane Next to the Floor for Fan Configurations 1 (upper figure) and 2 (lower figure)

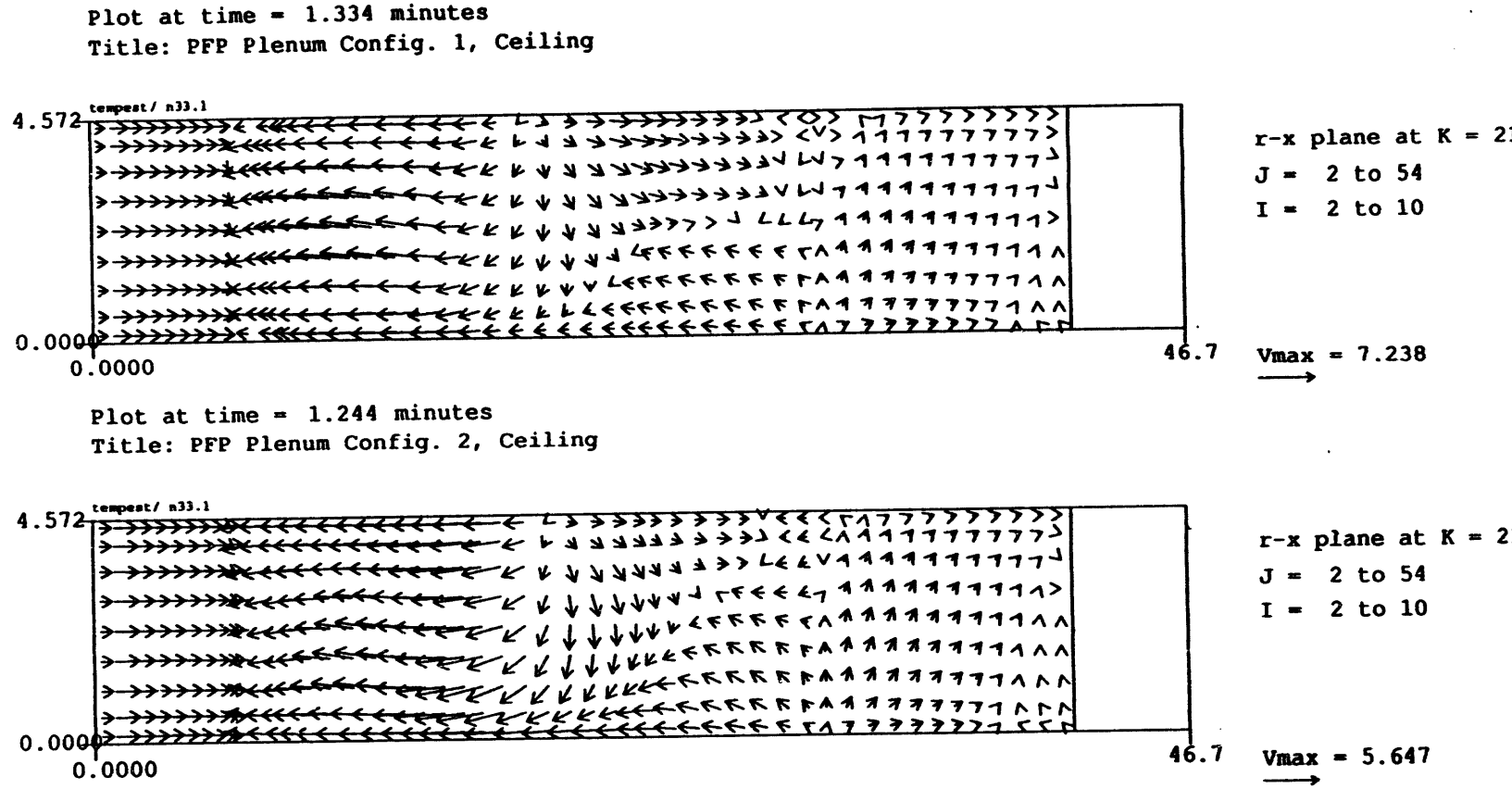

FIGURE 5.3. Velocities in the Horizontal Plane Next to the Ceiling for Fan Configurations 1 (upper figure) and 2 (lower figure)

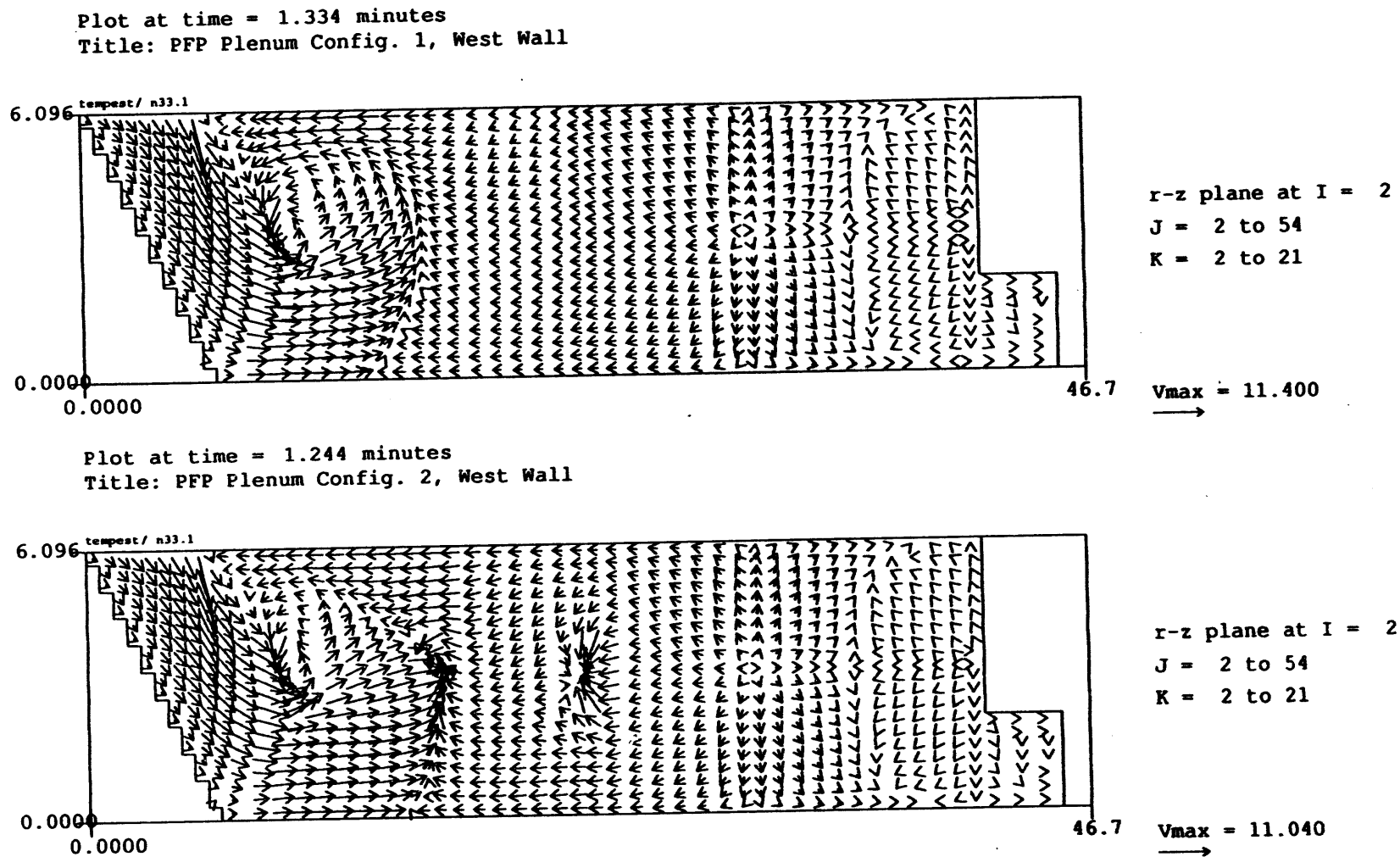

FIGURE 5.4. Velocities in the Vertical Plane Next to the West Hall for Fan Configurations 1 (upper figure) and 2 (lower figure)

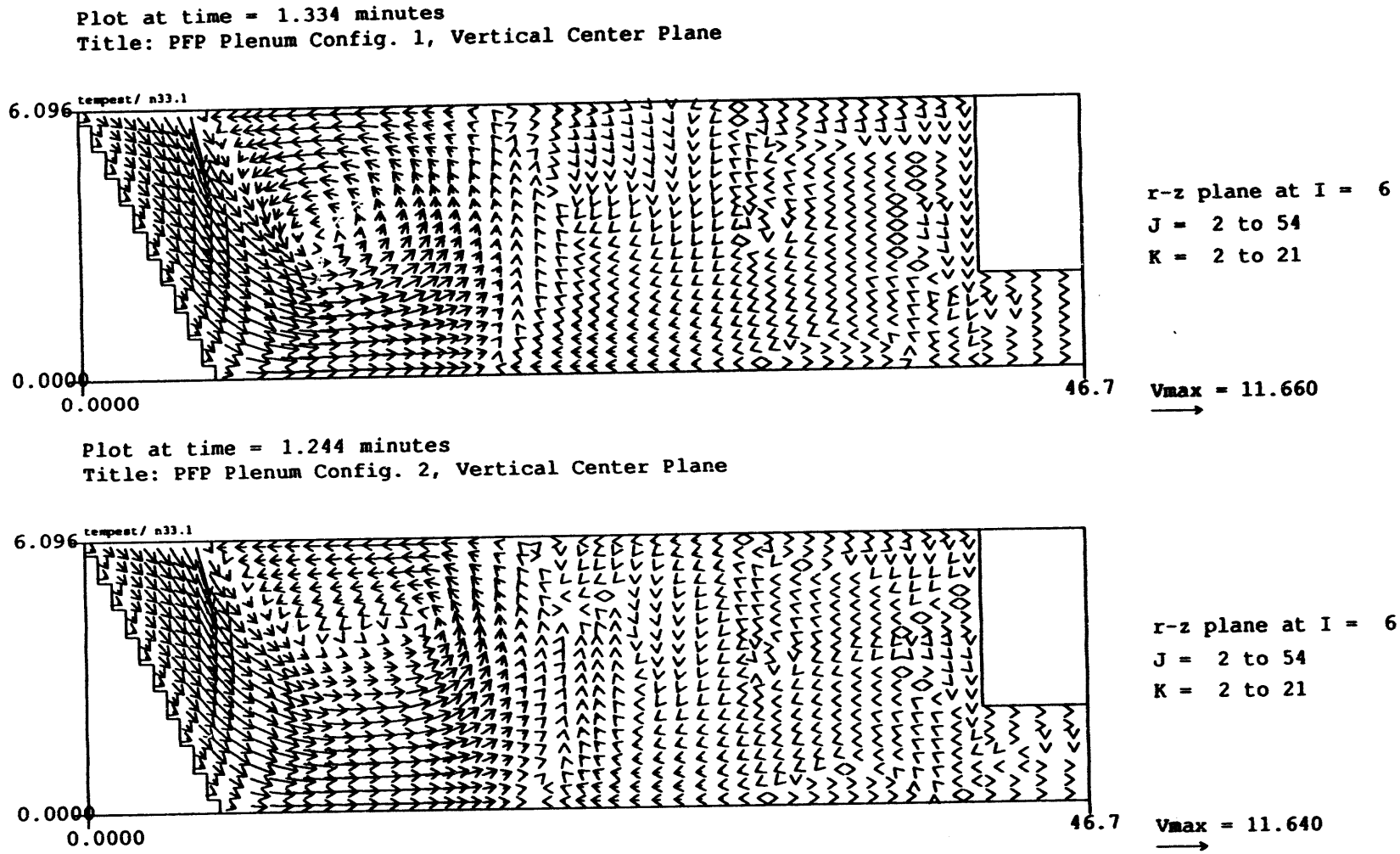

FIGURE 5.5. Velocities in the Vertical Plane at the Center of the Plenum for Fan Configurations 1 (upper figure) and 2 (lower figure)

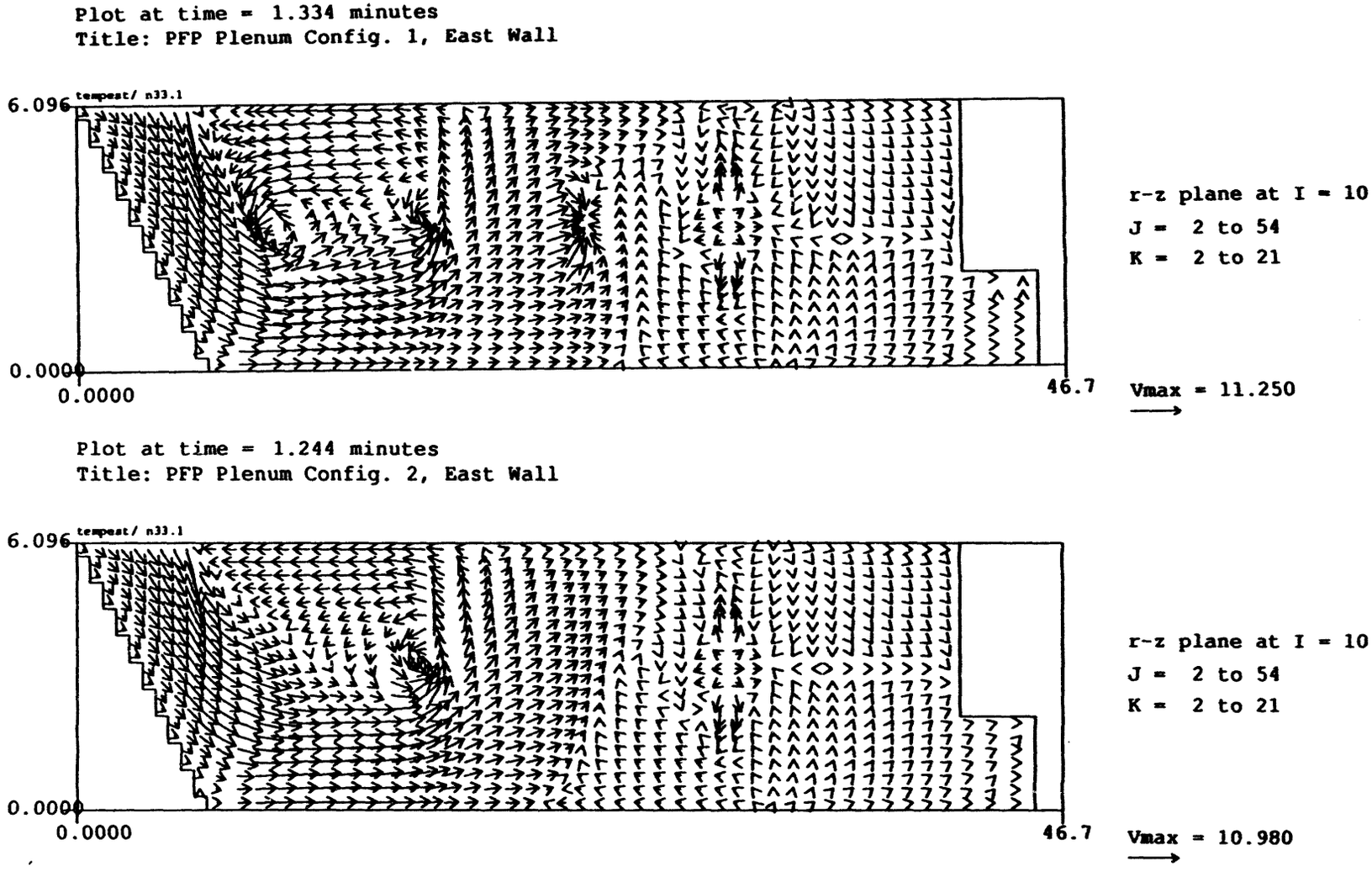

FIGURE 5.6. Velocities in the Vertical Plane Next to the East Wall for Fan Configurations 1 (upper figure) and 2 (lower figure)

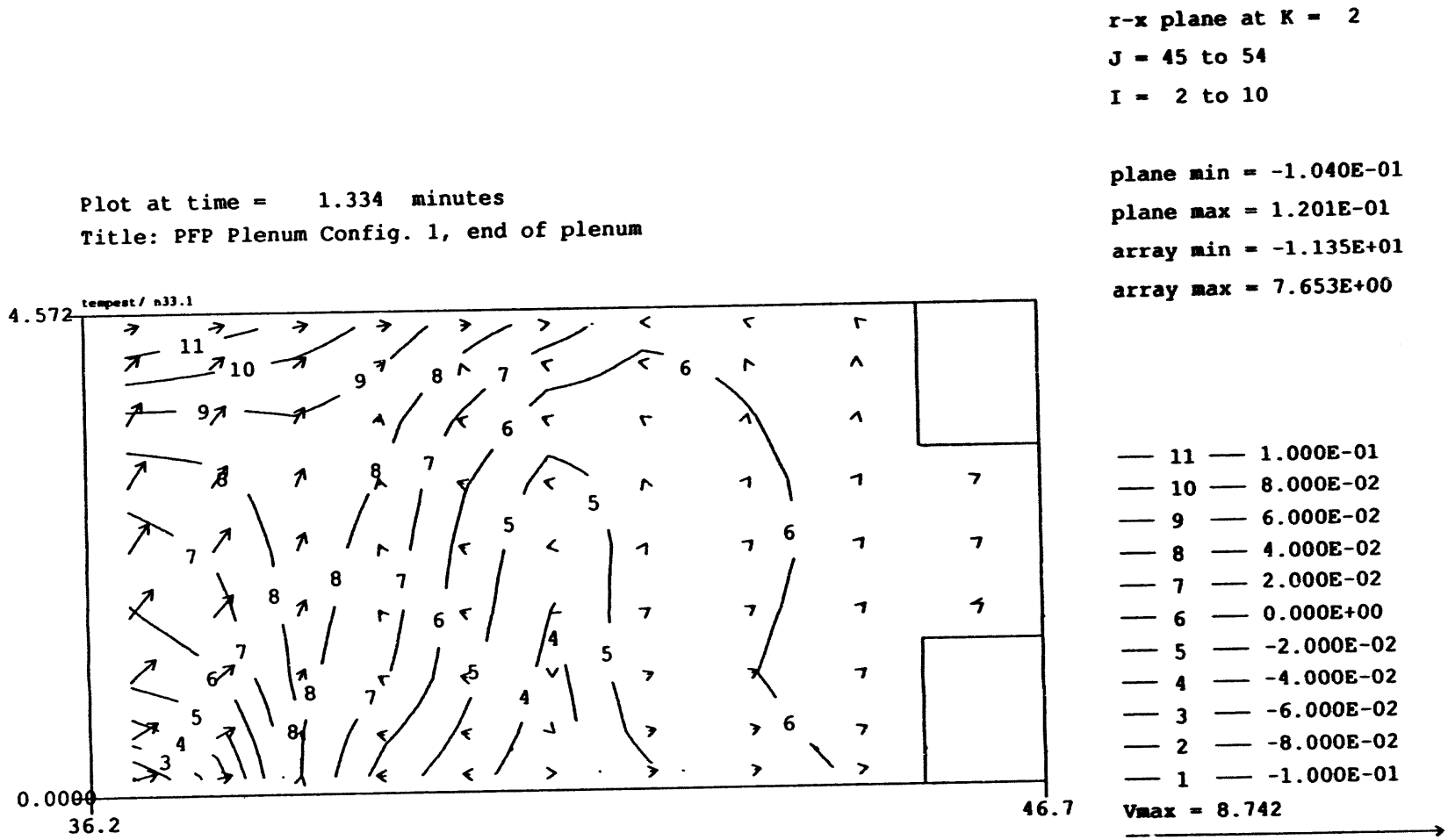

FIGURE 5.7. Floor-Level Horizontal and Vertical Velocities in the Southern Area of the Plenum for Fan Configuration 1

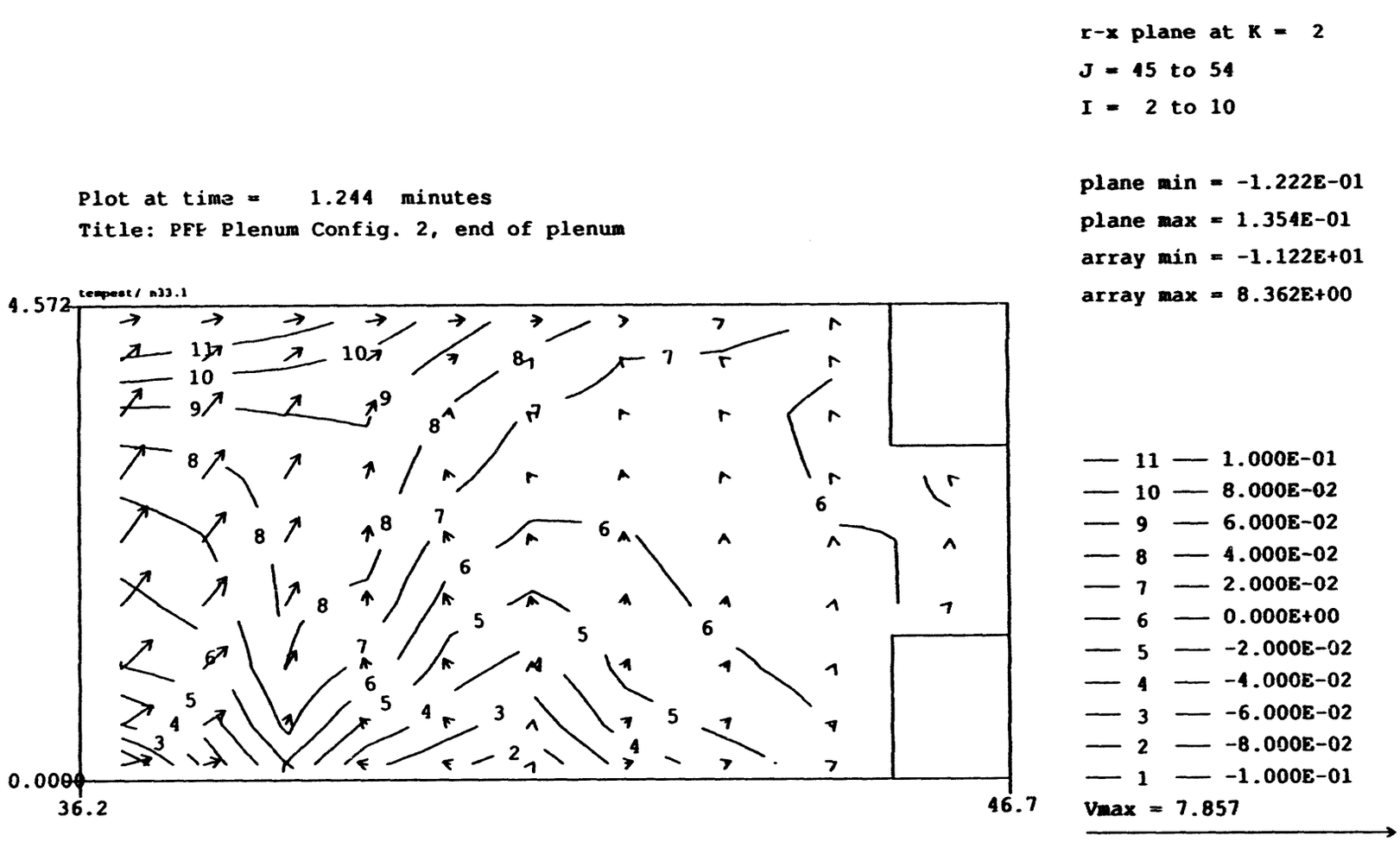

FIGURE 5.8. Floor-Level Horizontal and Vertical Velocities in the Southern Area of the Plenum for Fan Configuration 2

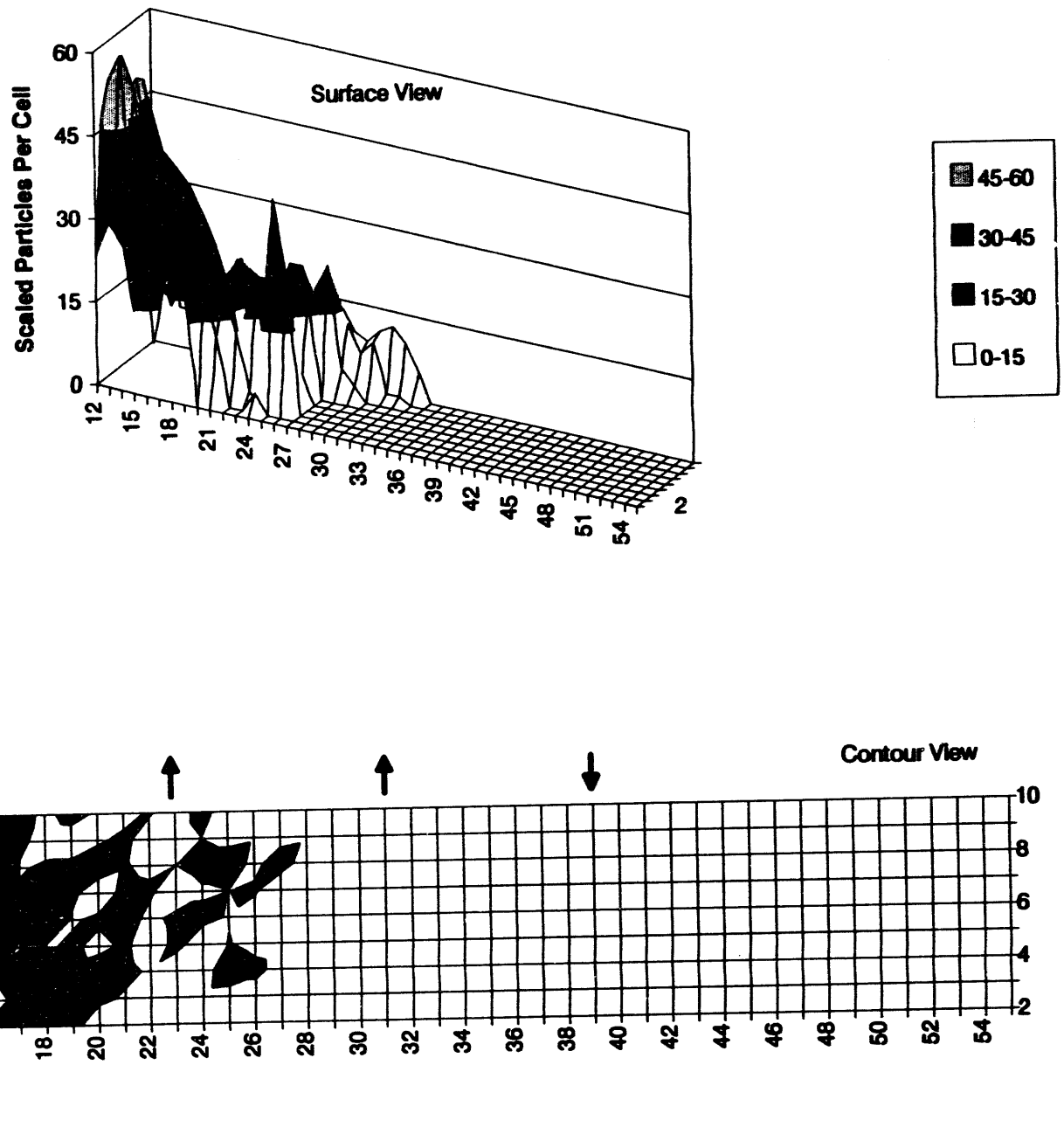

FIGURE 5.9. Deposition of 100-μm Particles in 234-5Z Effluent for Fan Configuration 1 After 50 s

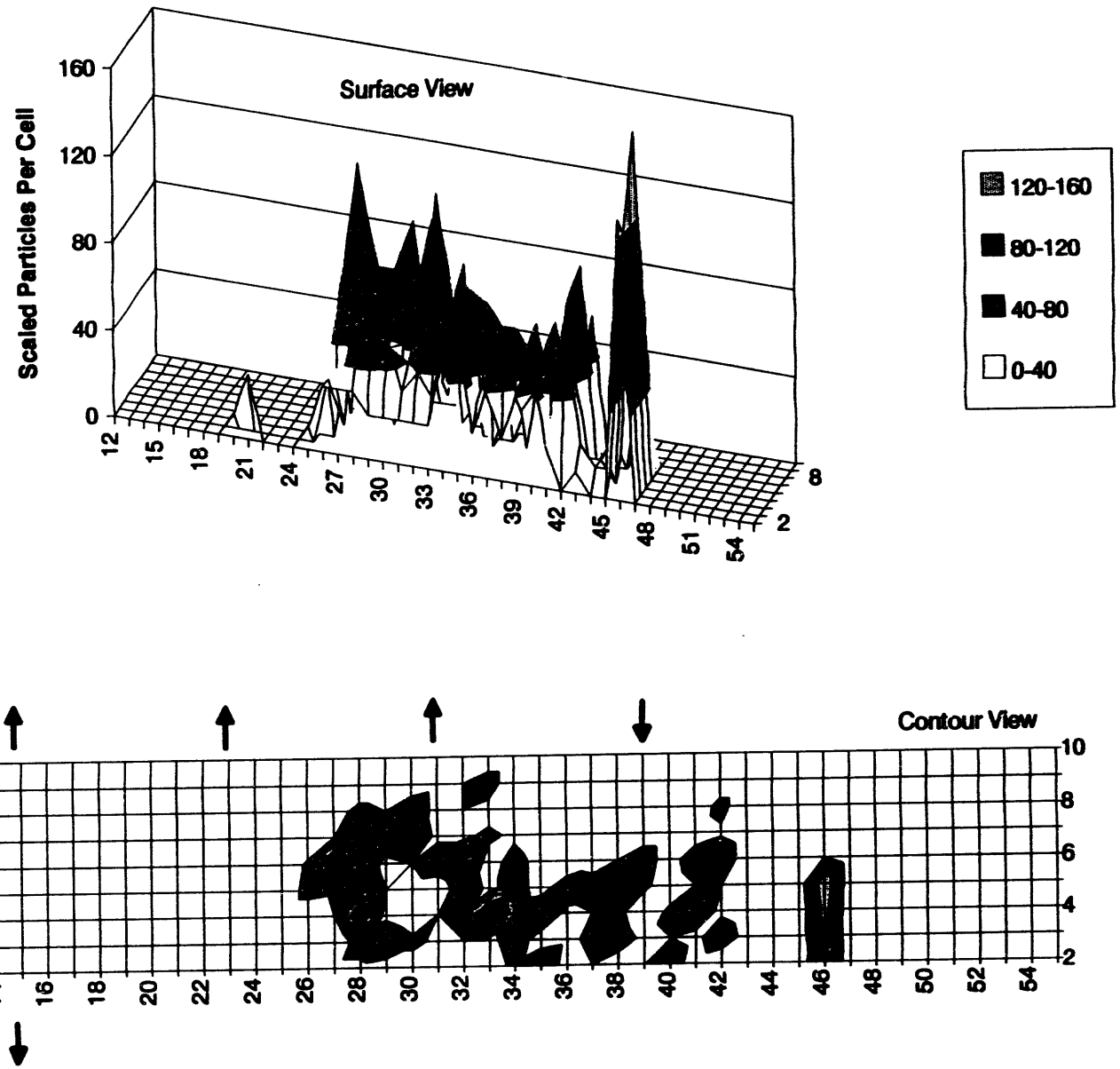

FIGURE 5.10. Deposition of 100-μm Particles in 232/236-Z Effluent for Fan Configuration 1 After 100 s

5.2.1 Tracer Particles

The first PART5 runs used tracer particles (non-depositing), and the results for particles coming from 232/236-Z and 234-5Z are summarized in Tables 5.1 and 5.2. The tables show the number of particles exhausted through each fan and the length of time required to exhaust 100% and 90% of the particles. (In these tables, information is arranged according to a plan view of the exhaust openings, with the north at the top of the table and east at the right of the table. Fan designations correspond to Figure 2.3.)

TABLE 5.1. Tracer Particle Ejection Times and Locations for Fan Configuration 1, 232/236-Z Injection Point

1000 particles injected. 200 s later, 20 particles (2%) still in flow. The ejected particles were, by fan:

West Side	East Side
EM1: 252 particles ejected at 9.8 to 164 s, 90% ejected by 23 s	EM5: 187 particles ejected at 11.5 to 21.1 s, 90% ejected by 16 s
	EM6: 0 particles ejected --- ---
	EM7: 541 particles ejected at 5.6 to 190 s, 90% ejected by 89 s

TABLE 5.2. Tracer Particle Ejection Times and Locations for Fan Configuration 1, 234-5Z Injection Point

8100 particles injected. 50 s later, 3 particles still in flow. The ejected particles were, by fan:

West Side	East Side
EM1: 1621 particles ejected at 0.51 to 49.7 s, 90% ejected by 22 s	EM5: 1816 particles ejected at 0.56 to 42.3 s, 90% ejected by 22 s
	EM6: 2141 particles ejected at 1.6 to 12.3 s, 90% ejected by 3.6 s
	EM7: 2519 particles ejected at 4.0 to 44.3 s, 90% ejected by 16 s

More than 90% of the tracer particles have a plenum residence time of 30 s or less, and more than 70% have a residence time of 9 s or less. (For comparison, the average plenum residence time is about 9 s.) Table 5.1 would indicate that, for this fan configuration anyway, contamination from 232/236-Z would have a longer residence time than that from 234-5Z and be unevenly ejected through the fans. The uneven distribution through the fans may result in uneven fan contamination. However, Table 5.2 indicates that contaminants coming from 234-5Z would be more uniformly distributed between the exhaust points.

5.2.2 Depositing Particles

The results from the PART5 100-μm particle runs are summarized in Tables 5.3 and 5.4 which show the exhaust distribution of particles.

The 100-μm particles that are exhausted typically have shorter residence times than tracer particles. Few of the exhausted 100-μm particles have residence times much longer than 24 s, the approximate time required for

TABLE 5.3. 100-μm Particle Ejection Times and Locations for Fan Configuration 1, 232/236-Z Injection Point

1000 particles injected. 100 s later, 14 particles (1.4 %) still in flow, 545 deposited. The ejected particles were, by fan:

West Side	East Side
EM1: 60 particles ejected at 10.2 to 31.9 s, 90% ejected by 22 s	EM5: 167 particles ejected at 11.2 to 24.9 s, 90% ejected by 16 s
	EM6: 2 particles ejected at 14 and 21 s
	EM7: 212 particles ejected at 5.3 to 21.0 s, 90% ejected by 10.5 s

TABLE 5.4. 100-μm Particle Ejection Times and Locations for Fan Configuration 1, 234-5Z Injection Point

8100 particles injected. 50 s later, 1 particle still in flow. 3369 deposited - 1168 deposited on the slope below the 234-5Z duct entry (in 0.01 to 5.5 s) and 2201 on the plenum floor (in 2.2 to 19.2 s). The ejected particles were, by fan:

West Side	East Side
EM1: 600 particles ejected at 0.51 to 41.2 s, 90% ejected by 13.6 s	EM5: 1150 particles ejected at 0.58 to 35.3 s, 90% ejected by 10.4 s
	EM6: 1129 particles ejected at 1.5 to 32.1 s, 90% ejected by 3.1 s
	EM7: 1851 particles ejected at 3.5 to 49.7 s, 90% ejected by 17.7 s

100-μm particles to settle from the top to the bottom of the plenum in still air (Table 4.1). The longer residence times that are seen are presumably the result of the updrafts through which these longer-lived particles have passed.

Another point of interest is the tendency of the 100-μm particles from 232/236-Z to be exhausted through fans other than EM6. Because this was also true for the tracers, it is likely that all sizes of particles coming from 232/236-Z would contribute to uneven contamination levels in the different fans, at least for this fan configuration.

Figures 5.9 and 5.10 show the deposition patterns for particles coming from 234-5Z and 232/236-Z. In the figures, the deposition is shown as number of particles deposited per floor cell, normalized to the number of particles injected and scaled with a convenient factor. The cells shown are not to scale, but are all equal sized. The coordinates shown can be used with Figure 4.1 to determine actual position.

Of the 3369 100-μm particles that were deposited from those injected at the 234-5Z location, 1168 particles (or 35% of the deposition) were located on the bottom of the sloping duct entering the plenum and are not shown in

Figure 5.9. The remaining 65% of the deposition was in the plenum proper and is shown in Figure 5.9. Most of the rest of the deposition from 234-5Z is just south of the slope, at the plenum entrance, but there is also a strong hint of a diagonal line of deposition that coincides with the diagonal line of convergence observed in Figure 5.2.

Deposition from 232/236-Z, Figure 5.10, follows a different pattern, with most of it spread over about half of the plenum area opposite the 232/236-Z plenum inlet. The 232/236-Z deposition stops just south of the same diagonal line that is the southern boundary of deposition for 234-5Z particles, presumably as a result of the floor-level convergence or stagnation line there. There is another line of deposition in the southwest part of the plenum. This deposition also appears to be caused by a stagnation area, one whose effect is increased by the low velocities throughout the south end of the plenum.

5.3 TEMPEST AEROSOL MODELING

Results from the many runs of TEMPEST (used as a continuum aerosol model) are shown in Figures 5.11 through 5.23. The TEMPEST runs listed in Table 5.5 explored the effects of particle size, point of injection, fan configuration, and longer injection time.

The contour plots in Figures 5.11 through 5.13 show the TEMPEST estimates of aerosol concentrations in the bottom cells (the bottom 1 ft) of the plenum. The figures do not show the sloped part of the plenum. Locations of the operating fans are shown by arrows; the numbers outside the plenum are TEMPEST cell numbers, and the numbers inside the plenum are mass fraction of aerosol times 10^{11}. For comparison, the inlet concentration of each aerosol size is 3.4×10^{-11} mass fraction (or "3.400," in the figures' notation). These results show bottom-cell concentrations of aerosol in air rather than true deposition. The figures can probably be best interpreted as where the aerosol would tend to accumulate if it did not stick to the floor where it first made contact but subsequently drifted along the floor before depositing.

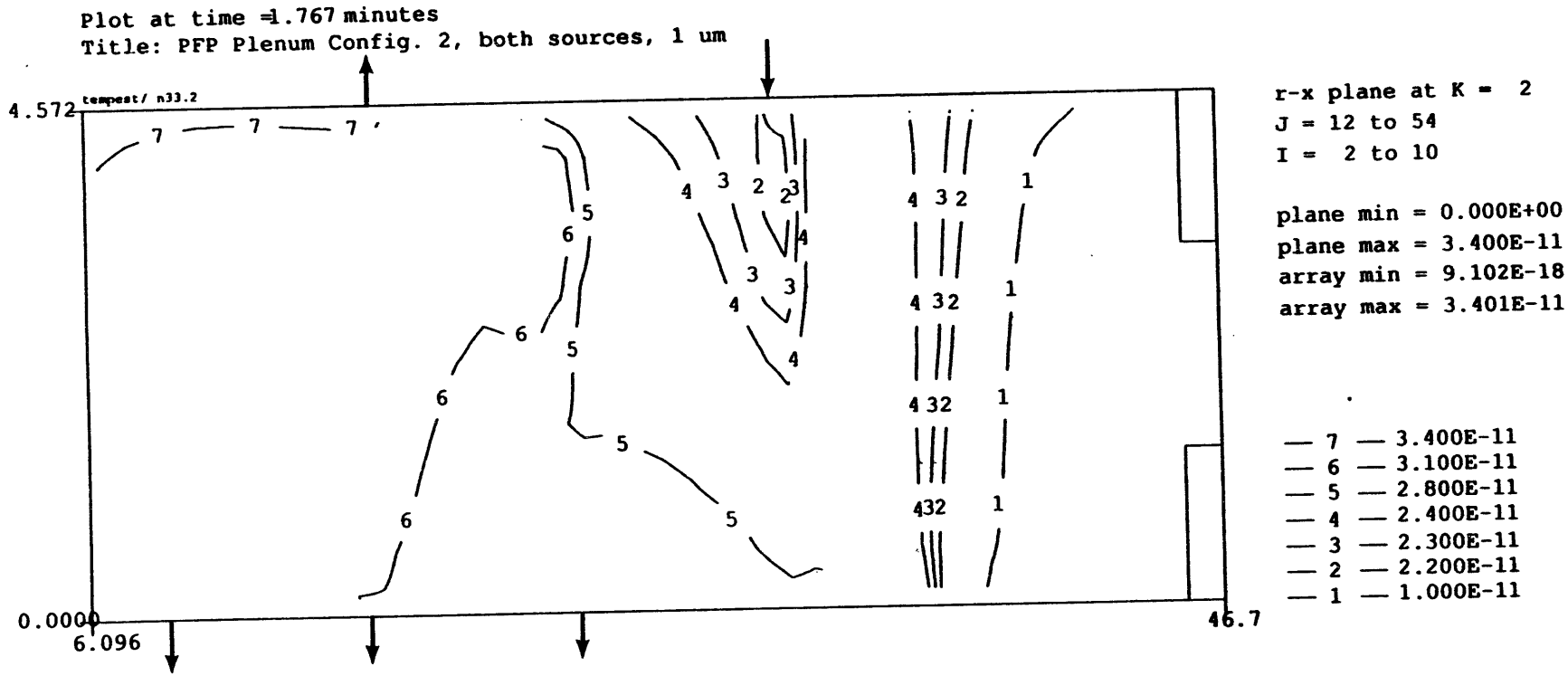

FIGURE 5.11. Near-Floor 1-μm Particle Concentration After 30-s Injection from 234-5Z and 232/236-Z for Fan Configuration 2

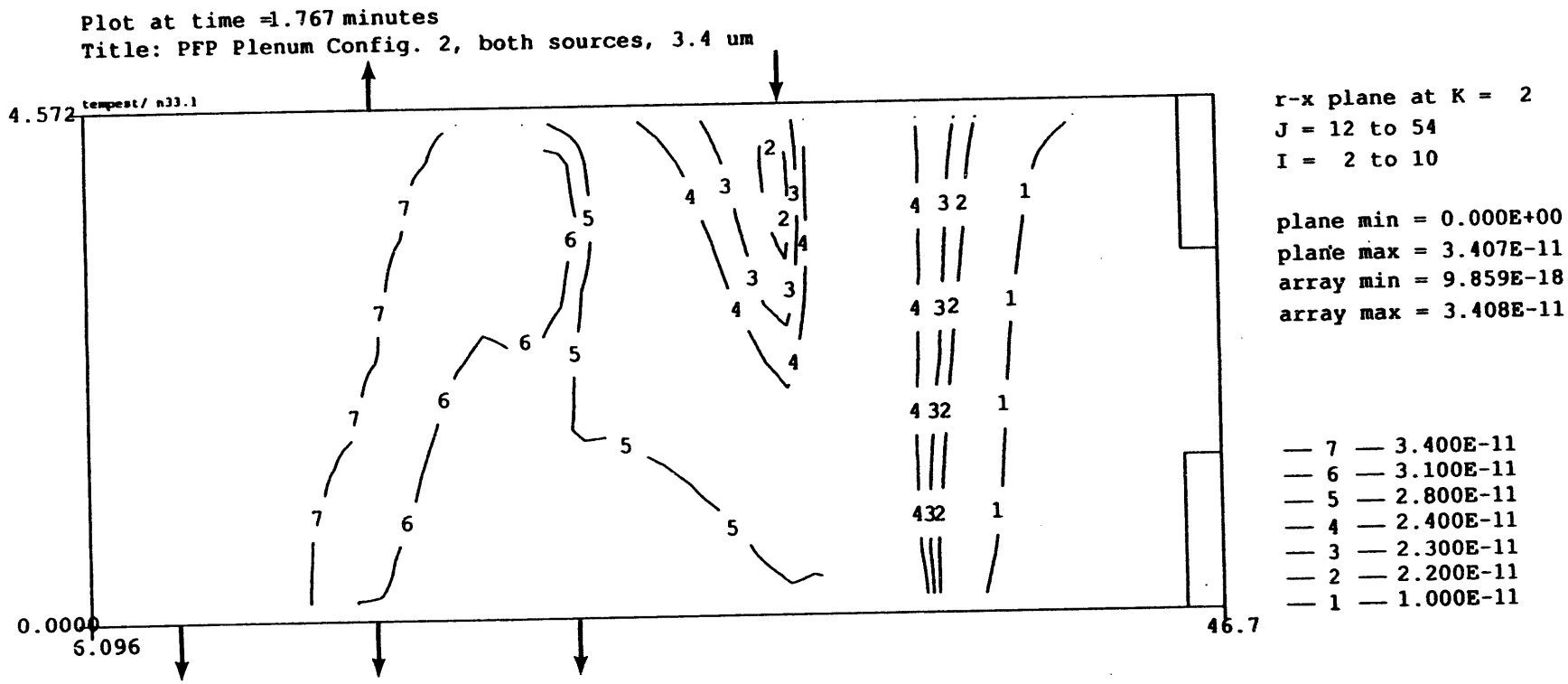

FIGURE 5.12. Near-Floor 3.4-μm Particle Concentration After 30-s Injection from 234-5Z and 232/236-Z for Fan Configuration 2

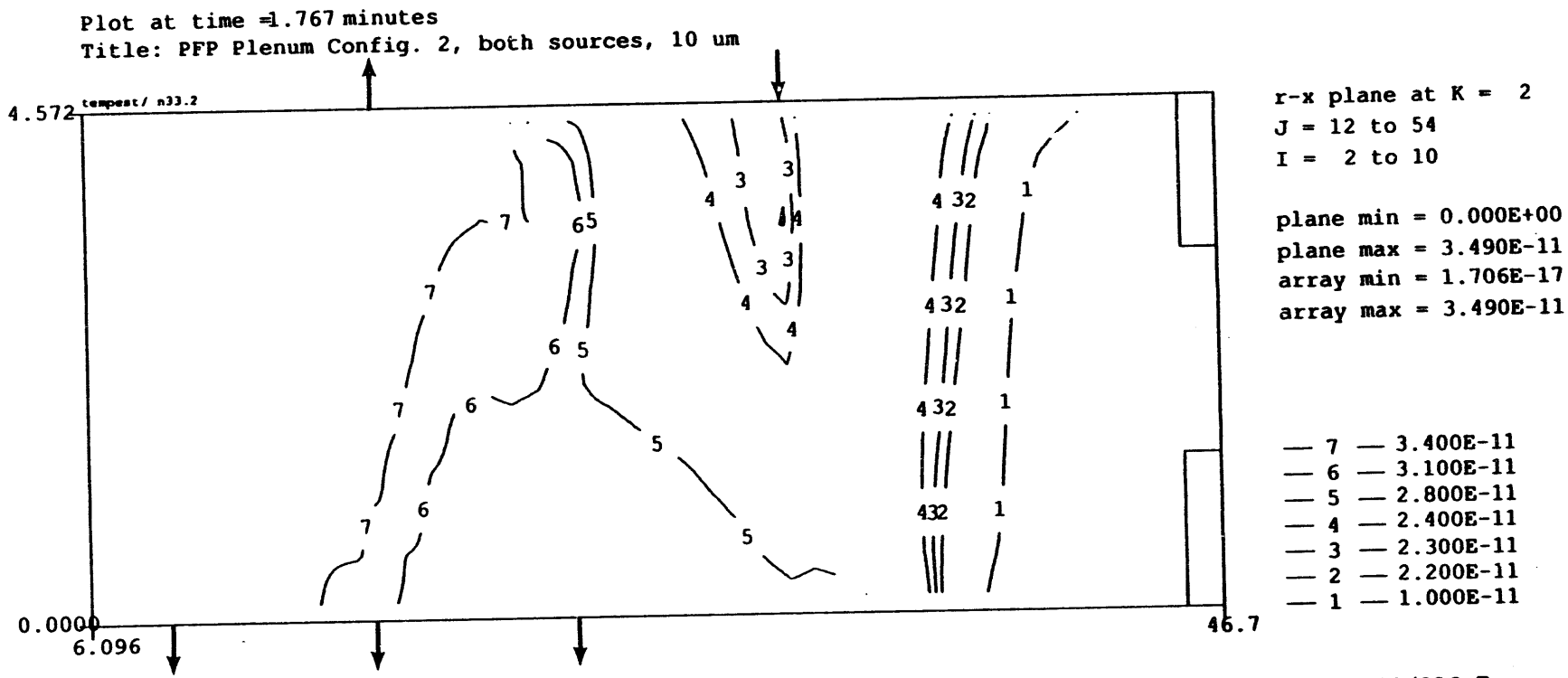

FIGURE 5.13. Near-Floor 10-μm Particle Concentration After 30-s Injection from 234-5Z and 232/236-Z for Fan Configuration 2

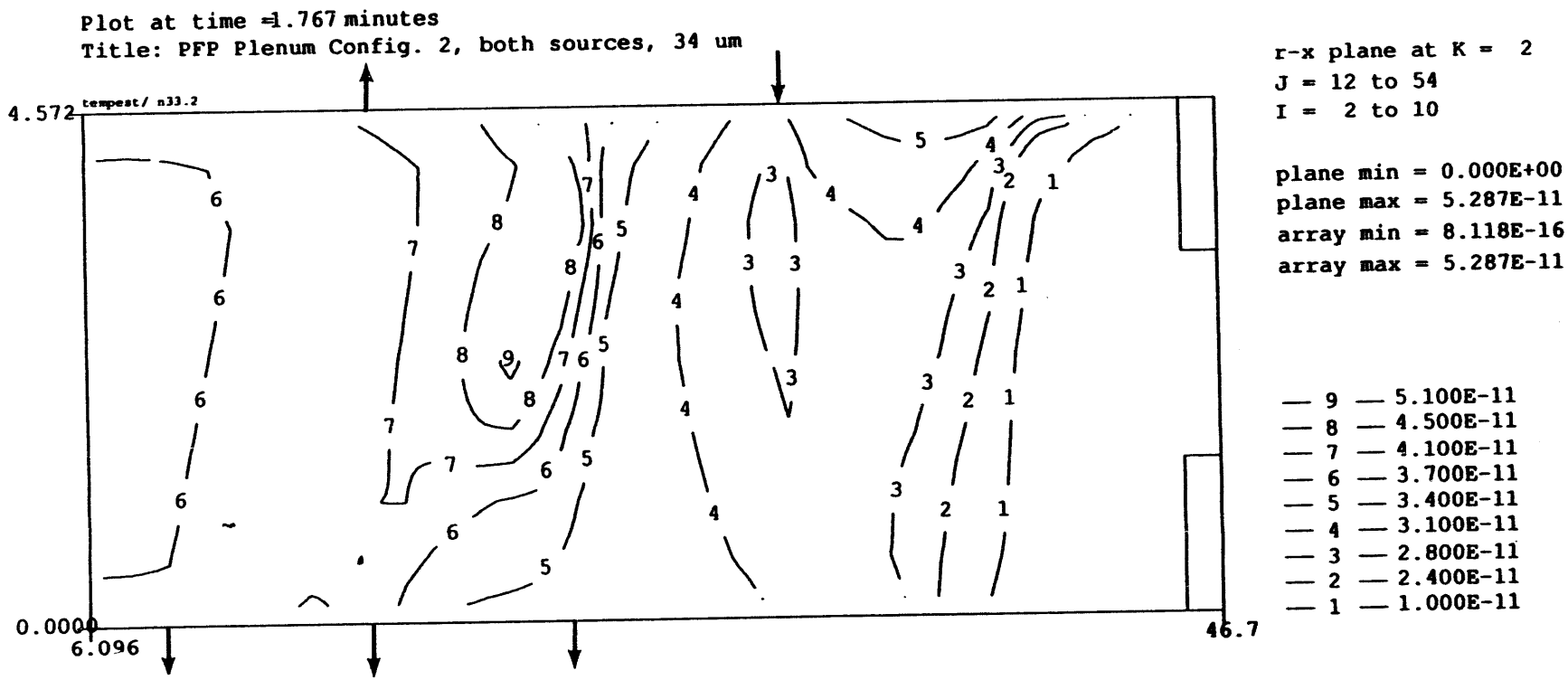

FIGURE 5.14. Near-Floor 34-μm Particle Concentration After 30-s Injection from 234-5Z and 232/236-Z for Fan Configuration 2

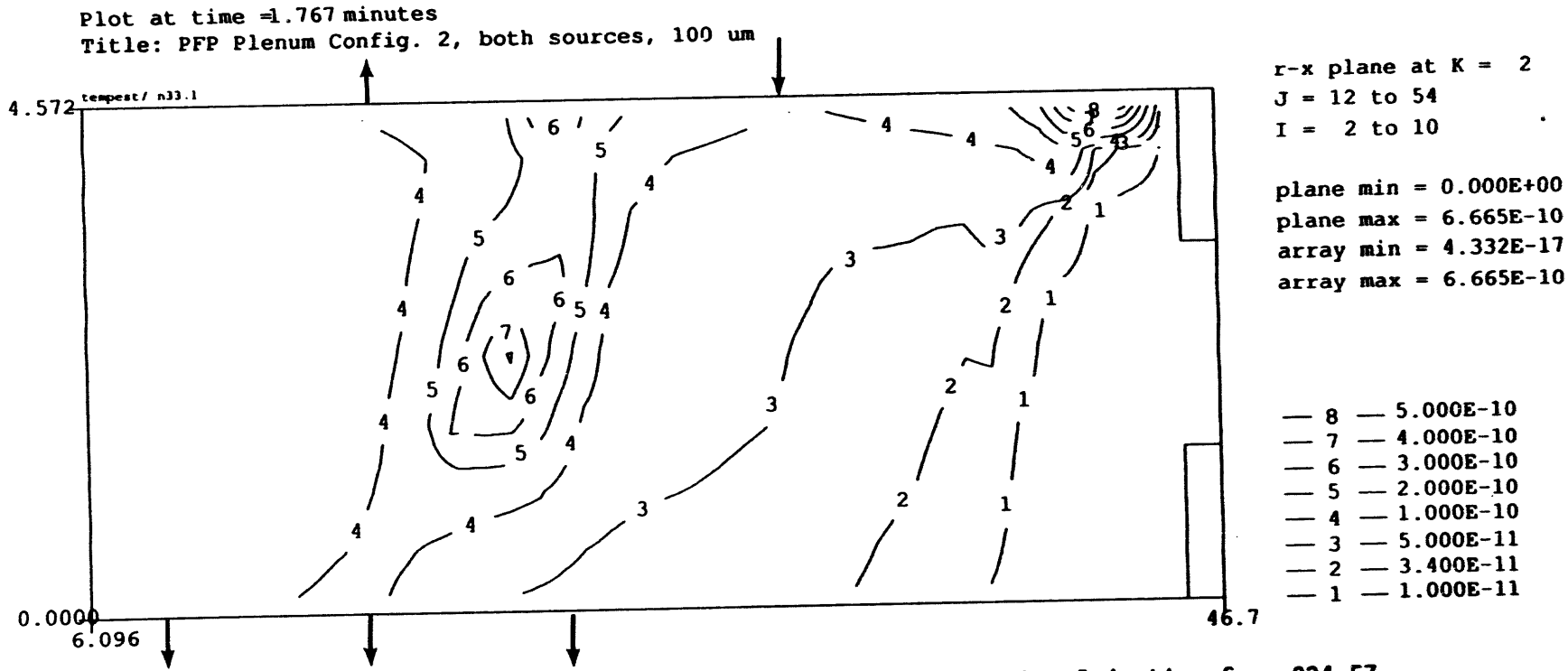

FIGURE 5.15. Near-Floor 100-μm Particle Concentration After 60-s Injection from 234-5Z and 232/236-Z for Fan Configuration 2

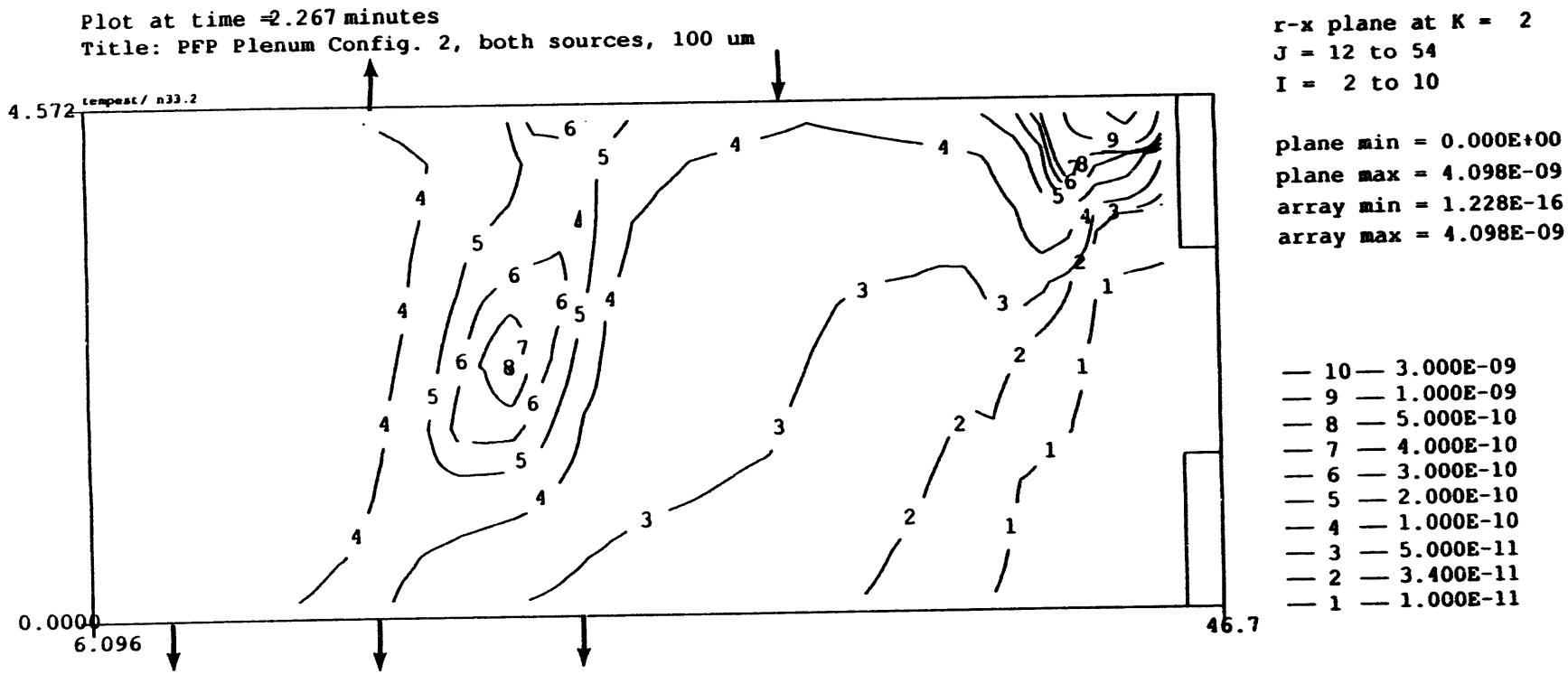

FIGURE 5.16. Near-Floor 100-μm Particle Concentration After 30-s Injection from 234-5Z and 232/236-Z for Fan Configuration 2

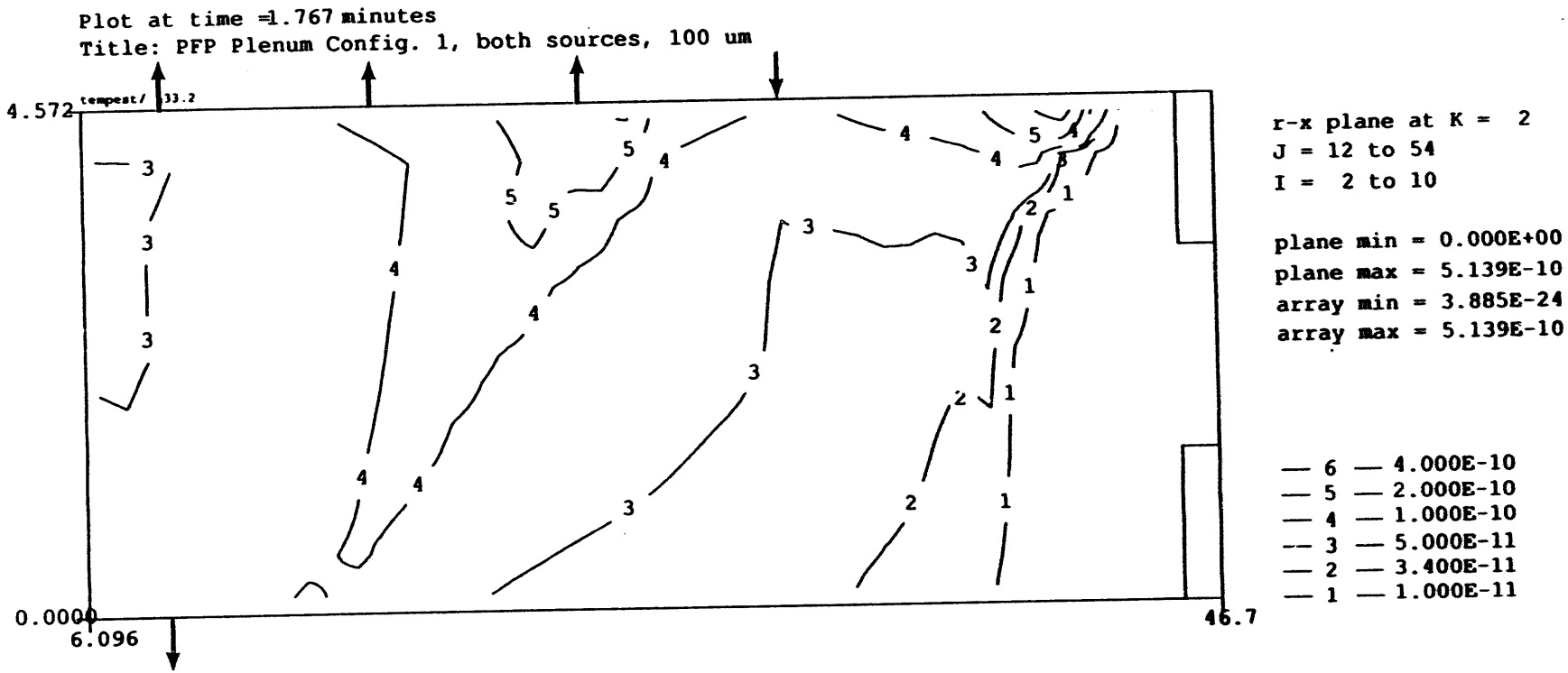

FIGURE 5.17. Near-Floor 100-μm Particle Concentration After 30-s Injection from 234-5Z and 232/236-Z for Fan Configuration 1

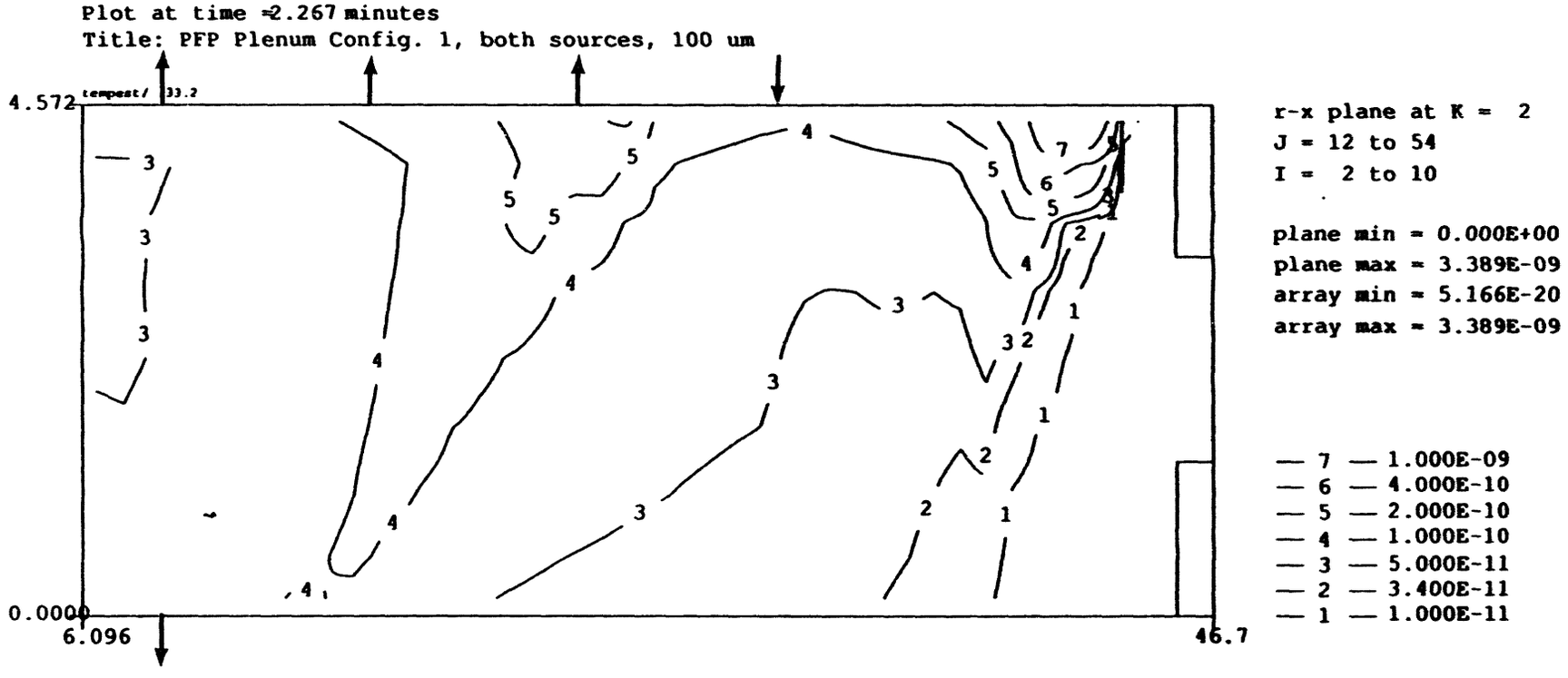

FIGURE 5.18. Near-Floor 100-μm Particle Concentration After 60-s Injection from 234-5Z and 232/236-Z for Fan Configuration 1

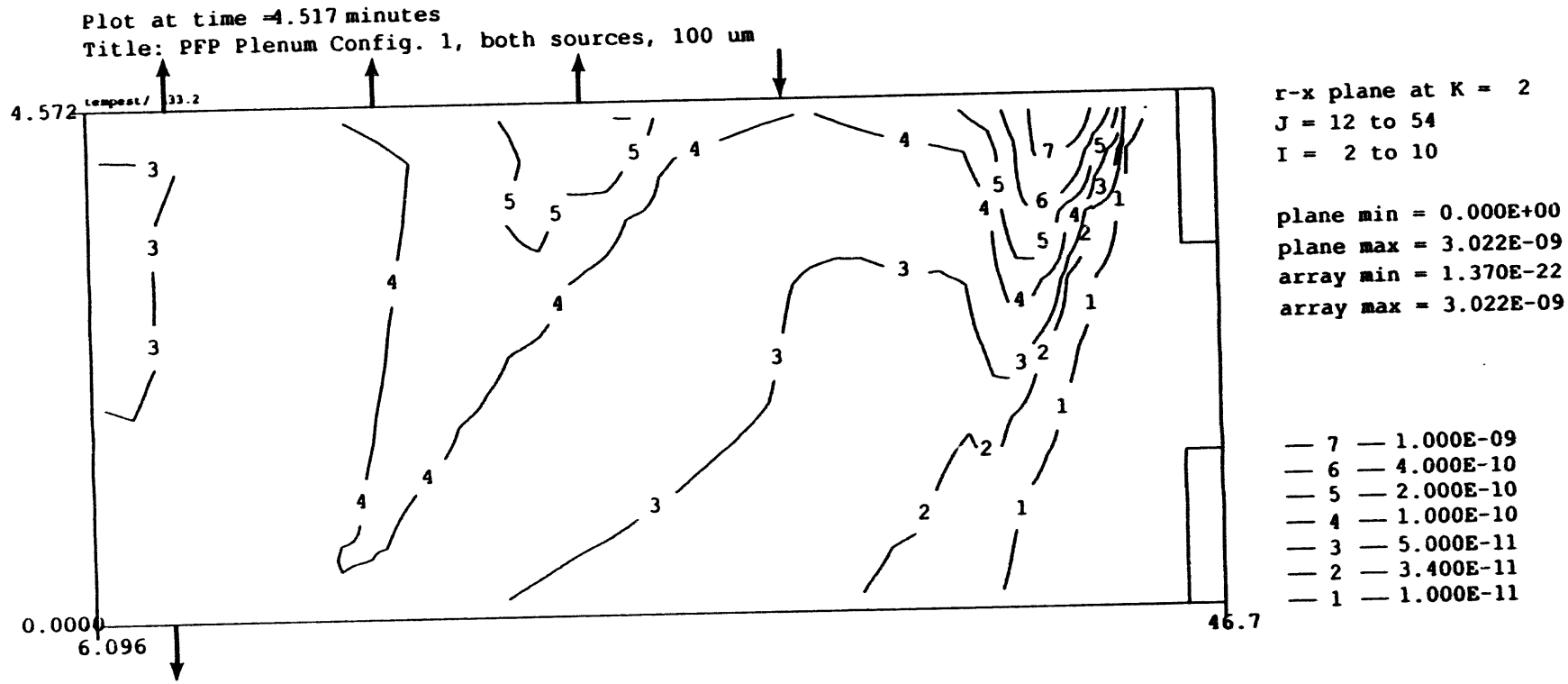

FIGURE 5.19. Near-Floor 100-μm Particle Concentration After 60-s Injection from 234-5Z and 232/236-Z for Fan Configuration 1 (extended to 215 s longer time)

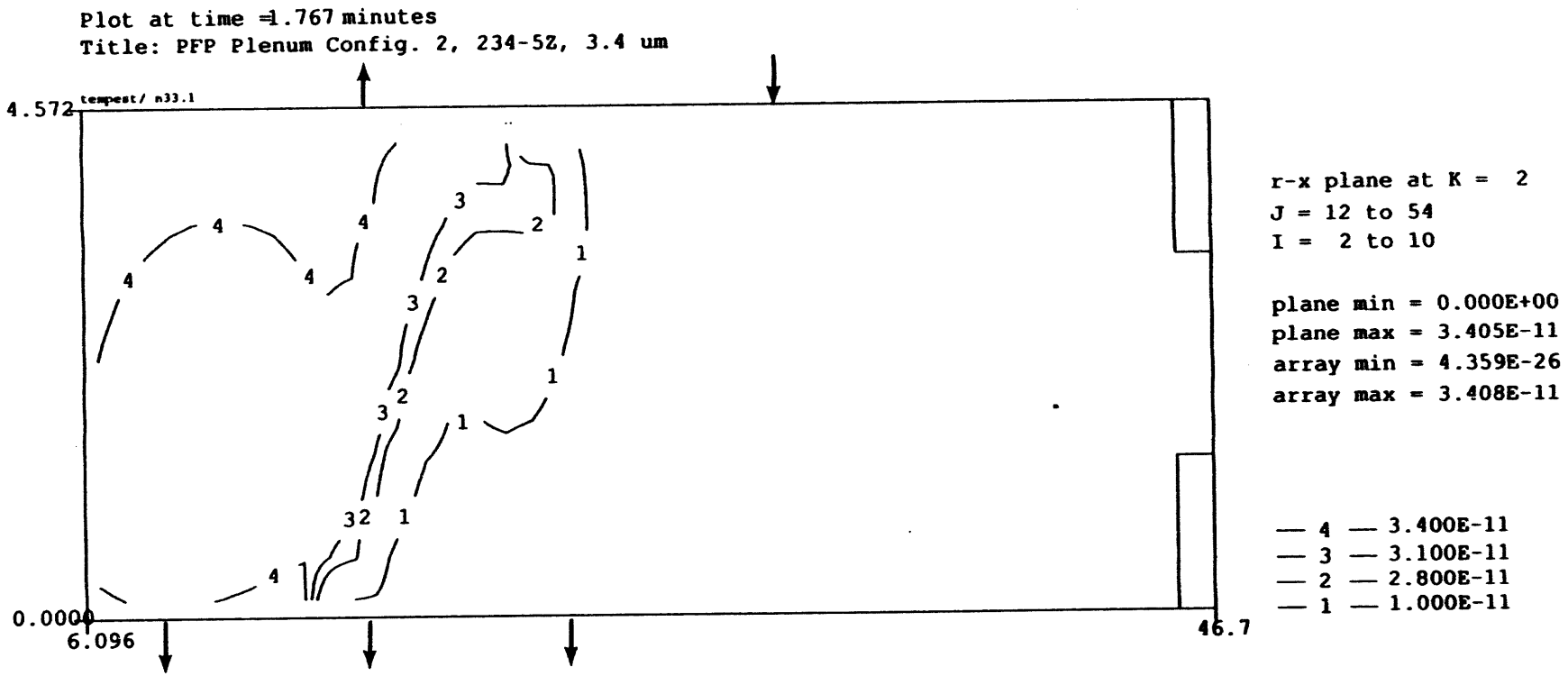

FIGURE 5.20. Near-Floor 3.4-μm Particle Concentration After 30-s Injection from 234-5Z Alone for Fan Configuration 2

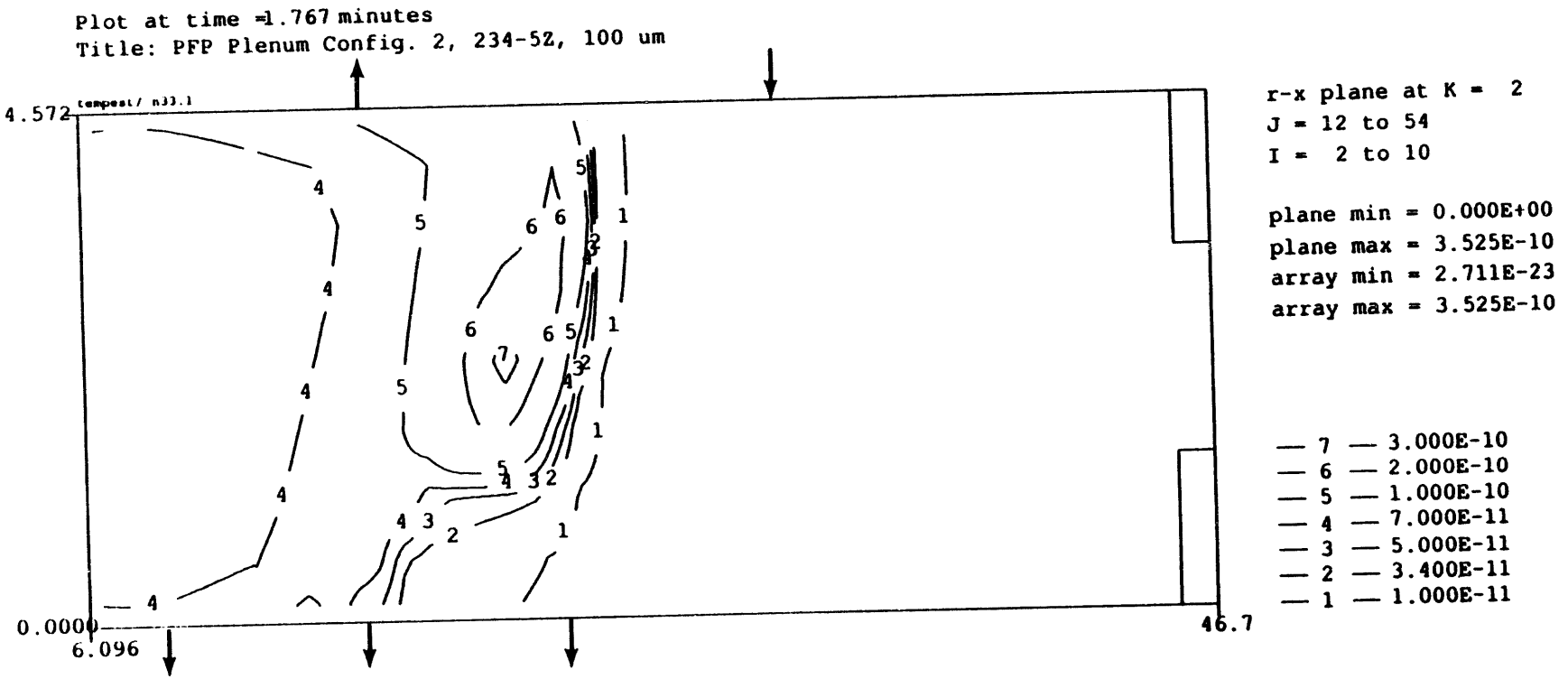

FIGURE 5.21. Near-Floor 100-μm Particle Concentration After 30-s Injection from 234-5Z Alone for Fan Configuration 2

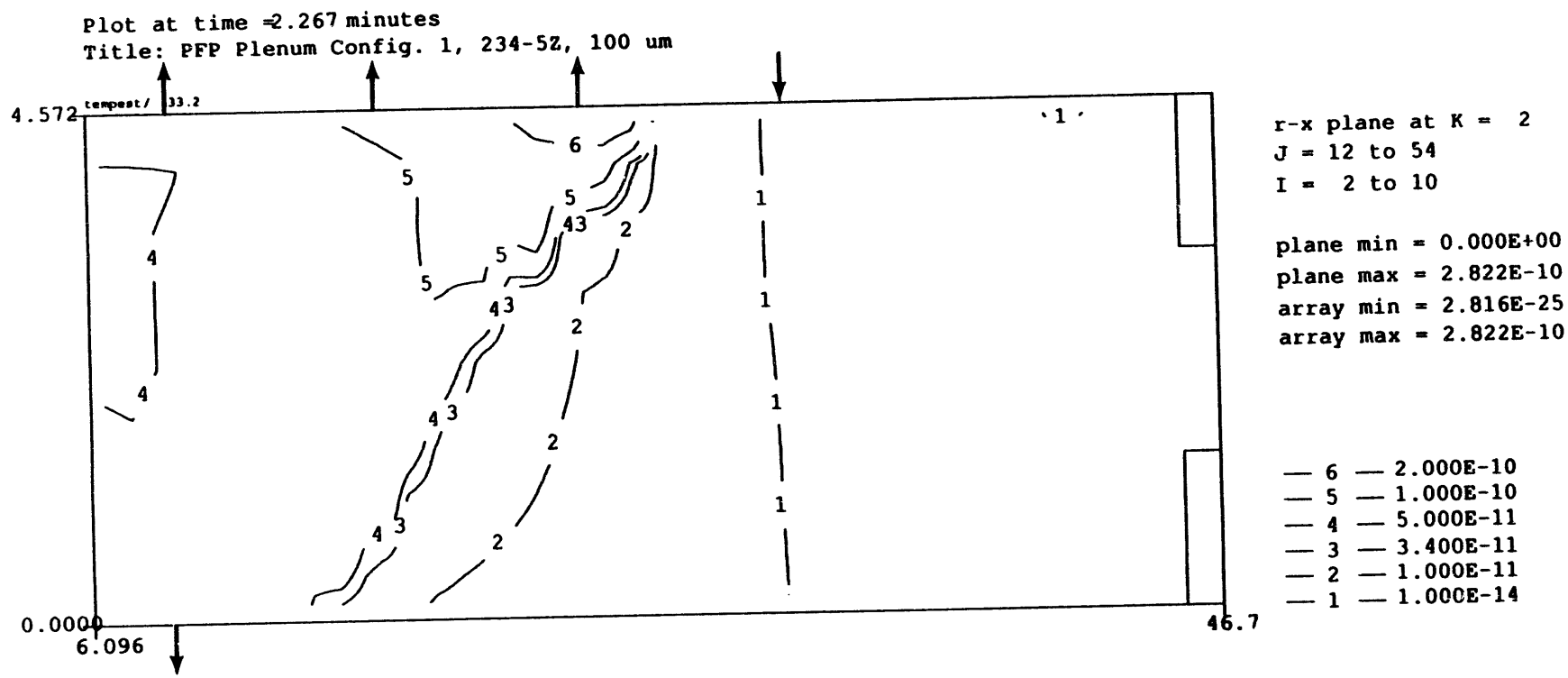

FIGURE 5.22. Near-Floor 100-μm Particle Concentration After 60-s Injection from 234-5Z Alone for Fan Configuration 1

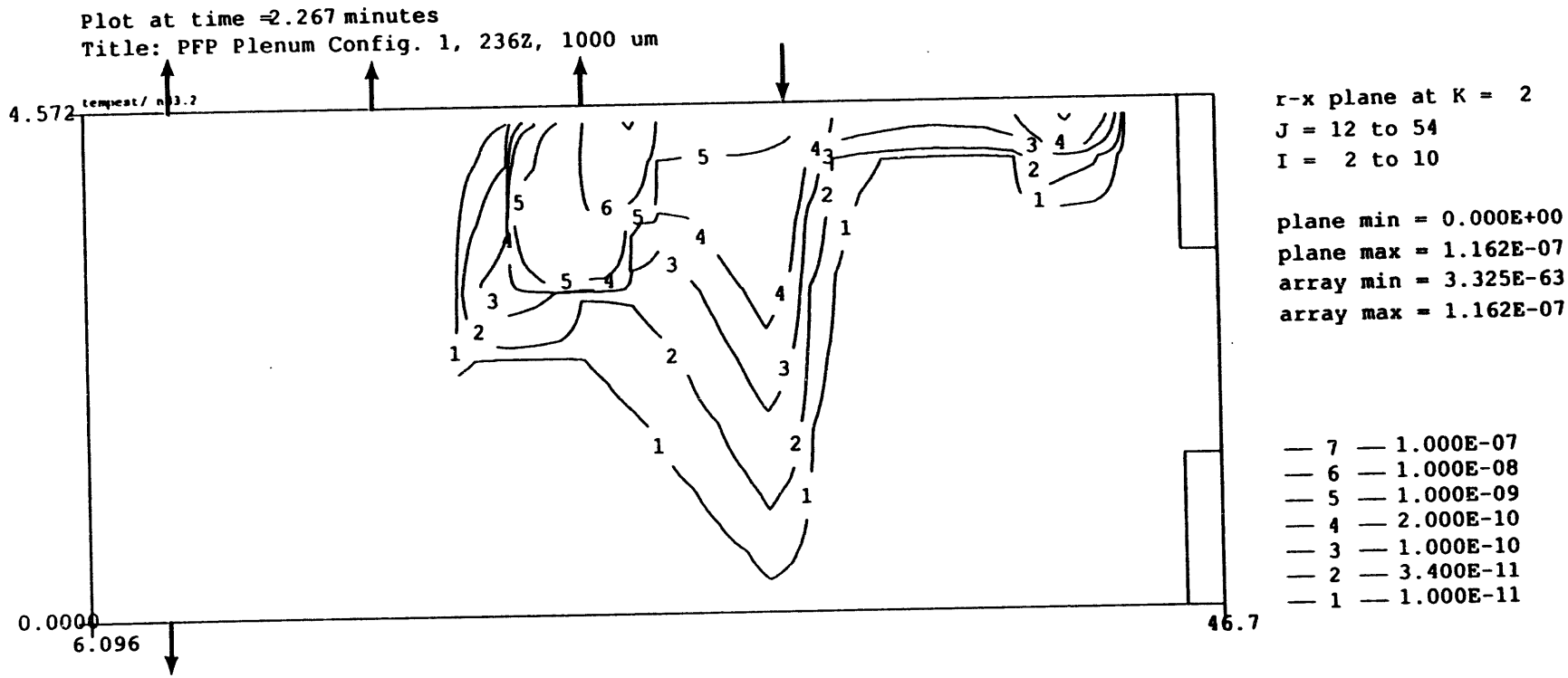

FIGURE 5.23. Near-Floor 1000-μm Particle Concentration After 60-s Injection from 232/236-Z Alone for Fan Configuration 1

TABLE 5.5. List of Figures Derived from TEMPEST Runs

Figure	Description
5.11	1-μm aerosol, 30 s time, both 234-5Z and 232/236Z, fan configuration 2
5.12	3.4-μm aerosol, 30 s time, both sources, fan configuration 2
5.13	10-μm aerosol, 30 s time, both sources, fan configuration 2
5.14	34-μm aerosol, 30 s time, both sources, fan configuration 2
5.15	100-μm aerosol, 30 s time, both sources, fan configuration 2
5.16	100-μm aerosol, 60 s time, both sources, fan configuration 2
5.17	100-μm aerosol, 30 s time, both sources, fan configuration 1
5.18	100-μm aerosol, 60 s time, both sources, fan configuration 1
5.19	100-μm aerosol, 60 s time, both sources, fan configuration 1 extended to 215 s
5.20	3.4-μm aerosol, 30 s time, only 234-5Z source, fan configuration 2
5.21	100-μm aerosol, 30 s time, only 234-5Z, fan configuration 2
5.22	100-μm aerosol, 60 s time, only 234-5Z, fan configuration 1
5.23	1000-μm aerosol, 60 s time, only 232/236-Z source, fan configuration 1

5.3.1 Methodology Validation

Almost all of the TEMPEST runs are based on velocity fields that were run for 76 or 80 s of flow time. Figures 5.18 and 5.19 show the effect on near-floor concentrations of using a velocity field generated from 215 s of simulated time rather than 30 s. The runs represented in these figures have identical inputs (particle size, injection time, and fan configuration); only the age of the flow field is different. A comparison of the two figures shows little difference in the concentration patterns from the two simulation times, thus validating the further use of the 76- and 80-s velocity fields.

Another methodology question that was considered was whether the predicted locations would change if injection was prolonged beyond the short times used in these runs. Because TEMPEST does not include a model for true deposition, i.e. particle sticking, there is a possibility that near-floor peak concentrations might move over time. The run that produced Figure 5.16 is an extension of the run in Figure 5.15. The 100-μm particle injection is carried a little further along in time, to 60 s duration of injection. The concentration maxima shown in Figure 5.15 (at 30 s) remain in the same locations in Figure 5.16 (at 60 s), and the southeast corner becomes the dominant location for near-floor particles. A comparison of Figures 5.15 and

5.16 provides some evidence that the locations of the concentration maxima do not vary with the duration of particle injection, validating the use of short injection intervals.

5.3.2 Effect of Fan Configuration

The effect of fan configuration was tested by comparing Figures 5.17 and 5.18, based on the first fan configuration, to Figures 5.15 and 5.16, which use the second fan configuration but are otherwise equivalent. All four figures show a near-floor maximum concentration in the southeast corner. For both fan configurations, the near-floor concentration maximum in the southeast corner of the plenum is in the same location at 60 s as it was at 30 s, suggesting that this maximum is a stationary accumulation for both fan configurations. In addition to this similarity, both configurations produce a diagonal band of high near-floor concentrations across the north part of the plenum. It appears that for deposition prediction purposes the two fan configurations are about equivalent.

5.3.3 Fan Configuration 2 Particle Accumulation

A comparison of Figures 5.11 through 5.16 (which are based on the second fan configuration) shows how the pattern of floor-level concentration changes as the particle settling velocity increases. For the largest particle size, 100 μm (Figure 5.16), there are concentration peaks in the north center, in the southeast corner, and just under the EM7 on the east wall. The peak in the southeast corner is the largest. Based on Figures 5.15 and 5.16, it is also the only peak that increases significantly over time. The second and third largest peaks are imbedded in a diagonal band of moderately high concentration, which joins with another moderate-concentration band along the south half of the east wall. The diagonal band is similar to that shown in the particle tracking analyses, and probably comes from the diagonal convergence zone (Figure 5.2). However, other areas that showed high deposition in the particle tracking runs (Figures 5.9 and 5.10), the north end of the plenum and the west half of the south end, do not show maxima in TEMPEST runs.

There are hints of similar spatial distributions for the smaller particles (Figures 5.11 through 5.14), but the trends are less clear. At 30 s injection time, the 34-μm particles are the smallest for which a southeast corner accumulation has begun to appear. The same is true for the maxima at the north central location and just under EM7. However, some form of the diagonal band of higher concentration is discernible for all particle sizes, even the 1-μm particles.

5.3.4 Fan Configuration 1 Particle Accumulation

Figures 5.17 through 5.19 show the near-floor concentrations for 100-μm particles, using the first fan configuration. Here the north-central concentration peak is absent, but the other peaks found for the second fan configuration are present. Figure 5.23 shows the near-floor concentration of 1000-μm particles (injected only from 232/236-Z) for the first fan configuration. The major peak for this particle size is near the EM7 on the east wall, and the other peaks, though suggested, are not well developed.

5.3.5 Large Particle Accumulation

Comparing Figure 5.19 to either Figure 5.21 or 5.22 indicates that the 232/236Z aerosol contributes a large amount of the near-floor aerosol concentration, in spite of the larger absolute amount of aerosol coming from 234-5Z. This comes about, as seen from the particle trajectory analyses, because of the lower velocity and more indirect exhaust path followed by the 232/236-Z flow. The 232/236Z aerosol produces a more rapid accumulation in the south plenum, as might be expected. However, there is a hint in Figure 5.22 that even aerosol from 234-5Z alone may in time accumulate in the southeast corner. In fact, over a longer time period the 234-5Z aerosol could be expected to produce accumulation in the south plenum. This was not indicated by the particle tracker analysis (using the PART5 model), in which the 234-5Z deposition location was solely at the north end of the plenum (Figure 5.9). With that model, deposition location was dependent on where particles first made contact, not on where they might have come to rest had there been some drift, bounce, or resuspension.

The high near-floor concentration in the southeast corner of the plenum is not a numerical artifact and should occur whether or not any aerosol comes from the 232/236-Z exhaust. The airflow into that corner comes mostly from the floor-level backwash from the 232/236-Z exhaust flow. The accumulation of near-floor aerosol results from near-stagnant horizontal flow carrying particles into the corner from all directions. The only flow leaving the cell goes upwards, but the upward velocity out of the corner is not fast enough to prevent particles from settling, unless the particles are less than about 7-μm AED in size. (Therefore fine particles may not be able to accumulate here, though larger ones can.) There appears to be no horizontal outflow from the corner, so the coarse particles cannot leave the corner; as a result the accumulation is continual and no upper limit equilibrium near-floor concentration is reached.

The smaller accumulations of 100-μm particles in the north center of the plenum and just under EM7 (see Figures 5.15 through 5.18) are also not numerical artifacts, but represent a different kind of situation where an equilibrium concentration has apparently been reached. The flow field for Fan Configuration 2 (Figure 5.3) contains a near-floor vortex (like a dust devil) centered on about the location of the concentration peaks in question. Because some flow does leave the vortex center horizontally, the particles in the flow are not trapped by their own settling velocity. Eventually the output flux (dependent on the concentration in the vortex) and the input flux become equal, so a maximum limiting concentration is attained.

5.3.6 Small Particle Accumulation

The 100-μm TEMPEST runs probably do not reliably indicate the locations where much finer particles (less than 5 μm) might tend to settle given a long enough time. As was just illustrated, what these runs do indicate is the location(s) where flows tend to converge horizontally at floor level and create an upward flow, which if slow enough, permits settling of fairly coarse particles at the convergence point. However, this same upward flow may tend to prevent deposition of the fine particles with their near-zero settling velocities.

The more likely locations for deposition of fines are the regions where there are near-stagnant slightly downward flows. Such flows are common throughout most of the south end of the plenum (south of the 232/236-Z entry point). Furthermore, in the southernmost 20 ft or so of the plenum, the near-floor horizontal airflows are slower than those required to cause saltation of large particles. (Saltation occurs when particles with AEDs of 100 μm or greater are incompletely resuspended, remaining within a few centimeters of the ground and repeatedly bouncing from it.) Since the typical resuspension mechanism for fine particles is momentum transferred from saltating larger particles, the rate of fines resuspension in the far south end of the plenum is likely to be considerably lower than elsewhere, allowing net deposition to occur.

6.0 CONCLUSIONS

Lacking information on particle resuspension and sticking in the PFP plenum, we must consider both the no-resuspension and the complete resuspension models as possible descriptions of the deposition patterns in the plenum. The two models have one element in common: the diagonal band of deposition across the north part of the plenum. However, the other predictions of peak deposition are different. If resuspension is complete, then the largest amount of deposition is predicted to occur in the southeast corner of the plenum as was shown in Figure 5.19. If there is no resuspension, then the southeast corner would be expected to be fairly clean, but the central and northern areas, and the sloped bottom of the incoming duct, would be areas of high deposition as shown in Figure 6.1 (an arithmetic sum of Figures 5.9 and 5.10).

Based on both models, almost all of the deposition would have come from large particles, over 10-μm AED. Particles fine enough to deposit by diffusion would have been likely to leave the plenum before much deposition could occur, according to the tracer particle tracker results. Historically, the most significant source of particles with greater than 10-μm diameter was probably contaminated rust from the old 236-Z duct. Because the 232/236-Z effluent is a more likely source of large particles, and because of the low velocity and indirect path to the fan inlets in that region, the deposition areas that it has produced in the southern part of the plenum are probably more significant than those produced in the north by the 234-5Z building effluent.

Another consideration in predicting deposition locations is one not susceptible to modeling. Operating personnel have observed evidence that during cold weather, water condenses from the (relatively) humid exhaust air on the inside of the uninsulated duct from the 234-5Z building. This being the case, particles that settled up-slope (in the duct or in the north part of the plenum) might very well be gradually carried down by the water. This wetted particulate material would be located more in the low spots in the floor than in areas indicated by deposition modeling. The plenum floor is believed to have a slight slope downward from north to south. The two most

predictable places for deposited material to end up would be the north end of the plenum, under the runoff from the duct, and the south end of the plenum, the overall low spot. Other local low spots, presently unidentified, could also contain runoff material.

It seems likely that for most particles, the deposition sites identified with the no-resuspension assumption may predominate. For particles that are large flakes or are "fluffy," as might be generated by filter breakthrough, the deposition sites identified assuming resuspension may be more realistic. Washdown by water to more southerly locations in the plenum may occur when sufficient moisture is present.

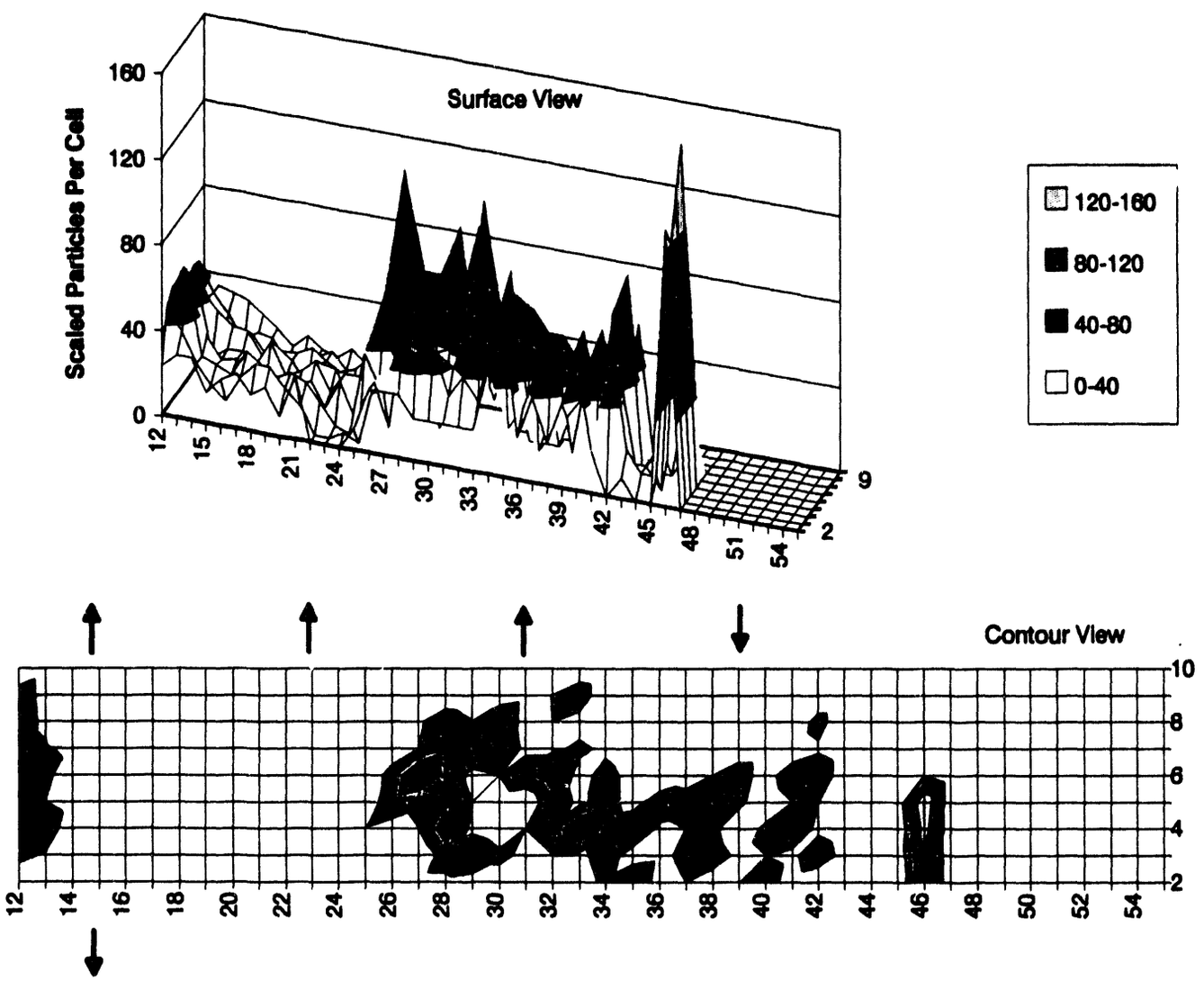

FIGURE 6.1. Predicted Locations of High Deposition

7.0 REFERENCES

Glissmeyer, J. A. 1992. *Experimental Performance Evaluation of Two Stack Sampling Systems in a Plutonium Facility.* PNL-8037, Pacific Northwest Laboratory, Richland, Washington.

Mishima, J., and L. C. Schwendiman. 1971. *Characterization of Radioactive Particles in the 234-5Z Building Ventilation Systems, Interim Report.* BNWL-B-105, Pacific Northwest Laboratories, Richland, Washington.

Mishima, J., and L. C. Schwendiman. 1973. *Characterization of Radioactive Particles in the 234-5Z Building Gaseous Effluent.* BNWL-B-309, Pacific Northwest Laboratories, Richland, Washington.

Trent, D. S., and L. L. Eyler. 1991. *TEMPEST: A Computer Program for Three Dimensional Time Dependent Computational Fluid Dynamics.* Battelle Memorial Institute, Columbus, Ohio.

APPENDIX A

SAMPLE TEMPEST INPUT FILES

1

* * * I N P U T R E C O R D I M A G E * * *

```
RECORD      COLUMN  1   5    1    1    2    2    3    3    4    4    5    5    6    6    7    7    8
no.                          0    5    0    5    0    5    0    5    0    5    0    5    0    5    0
   1            Title: PFP Plenum Airflow Distribution - Model 1
   2              input file: pfp.3c.inp
   3            size,   55   22   11
   4            note:   initially, run one step to check setup
   5            time,   1.    1
   6            prnt,
   7            note:   after modeling debugged, run more time steps, or restart and continue
   8            time,   1.       100              100
   9            prnt,                    2   10    2        10
  10            pres,  100            1-9
  11            rest,           1    1
  12            post,
  13            misc,           0
  14
  15            note:       GROUP 2 INPUT - CONTROL
  16            note:
  17            cont,sisy,besq,turb,mont,dtim,pace,
  18            cont,save,psav,msav,
  19            cont,read,
  20            aout,velr,velz,velx,
  21            plot,velr,velz,velx,
  22            dbug,data,qaed,size,ttbl,
  23
  24            note:       GROUP 3 INPUT - INTEGER DATA
  25            note:
  26            note:       PFP inflow
  27              40    1     1          2   10   22   22    2   10                  1  inflow
  28            note:       plenum volume
  29               0    1                2   54    2    8    2   10                  1  plenum
  30               0    1                2   50    9   21    2   10                  1  plenum
  31            note:       fan areas
  32              30    1               14   15   10   14    1    1                  1  fan W1
  33              30    1               14   15   10   14   11   11                  1  fan E1
  34              30    1               22   23   10   14    1    1                  1  fan W2
  35              30    1               22   23   10   14   11   11                  1  fan E2
  36              30    1               30   31   10   14    1    1                  1  fan W3
  37              30    1               30   31   10   14   11   11                  1  fan E3
  38              30    1               38   39   10   14    1    1                  1  fan W4
  39            note:       232Z/236
  40               0    1 4  2          38   39   10   14   10   10                  1  232/236Z
  41            note:       block out sloped wall
  42              50                    2   11    2    2    2   10                  1  45 wall
  43              50                    2   10    3    4    2   10                  1  45 wall
```

```
   50                    2    9    5    6    2   10                    1  45 wall
   50                    2    8    7    8    2   10                    1  45 wall
   50                    2    7    9   10    2   10                    1  45 wall
   50                    2    6   11   12    2   10                    1  45 wall
   50                    2    5   13   14    2   10                    1  45 wall
   50                    2    4   15   16    2   10                    1  45 wall
   50                    2    3   17   18    2   10                    1  45 wall
   50                    2    2   19   20    2   10                    1  45 wall
note:       block out corners of prow
   50                   54   54    2    8    2    4                    1  prowblck
   50                   54   54    2    8    8   10                    1  prowblck
note:       set up monitor cells
    9   12    6   15   12    6   28   12    6   41   12    6    1     5  mon. 1
   15    3    3   15   20    3   15    3    9   15   20    9    2     5  mon. 2
   28    3    3   28   20    3   28    3    9   28   20    9    3     5  mon. 3
   41    3    3   41   20    3   41    3    9   41   20    9    4     5  mon. 4

note:       GROUP 4 INPUT - FLOATING POINT DATA
note:
note:       gravitational orientation
   1.                                   90  180   90                    1es  orient
note:       option 2 input - R-coordinate, in feet
    1   11   2.                                                        1    3es R-coord
   12   13 3.25                                                       1    3es R-coord
   14   15 2.50                                                       1    3es   fan 1
   16   213.167                                                       1    3es R-coord
   22   23 2.50                                                       1    3es   fan 2
   24   293.167                                                       1    3es R-coord
   30   31 2.50                                                       1    3es   fan 3
   32   373.167                                                       1    3es R-coord
   38   39 2.50                                                       1    3es   fan 4
   40   503.045                                                       1    3es R-coord
   51   52 3.75                                                       1    3es R-coord
   53   54 4.33                                                       1    3es R prow
note:       option 1 input - X-coordinate, in feet
  1.0  1.0  1.5  2.0  2.0  2.0  2.0  2.0  1.5  1.0    1   10                5es X-coord
  1.0                                               11   11                5es X-coord
note:       properties - base air at 25C
                                  25.  20.  30.    2  1     11    1cg  6  air 25C
note:       initialize Temperature array
  25.                                1   55    1   22    1   11    9  Temper
note:       initialize Fans - velocity in ft/sec
             -43.7                 14   15   10   14    1    1    7es  fan W1
              43.7                 14   15   10   14   10   11    7es  fan E1
                0.                 22   23   10   14    1    1    7es  fan W2
              43.7                 22   23   10   14   10   11    7es  fan E2
                0.                 30   31   10   14    1    1    7es  fan W3
              43.7                 30   31   10   14   10   11    7es  fan E3
                0.                 38   39   10   14    1    1    7es  fan W4
             -31.3                 38   39   10   14   10   11    7es  232/23
note:       inflow PFP table
   0.   1.                                                            1   16  PFPinflo
```

```
 96                1+9   1.                                                  1   16  PFPinflo
 97              note:       232/236Z inflow table
 98                0.                                  -31.3                 2   16  236inflo
 99                1+9                                 -31.3                 2   16  236inflo
100                                                                                   enddata
```

1

Title: PFP Plenum Airflow Distribution - Model 2

PARAMETER LIST FOR CASE 08/26/91 17:24:08

number of time steps	, nsteps	6110	
total number of fluid cells	, nfluid	8130	
total number of solid cells	, nsolid	0	
total number of compt cells	, ntotal	8130	
total number radiation cells	, nrad	0	
total number constituents	, nsp	0	
number of cells in r-direction	, nr	55	
number of cells in z-direction	, nz	22	
number of cells in x-direction	, nx	11	
width of cells in r-direction	, dr	0.00000	metres (variable)
width of cells in z-direction	, dz	0.30480	metres
width of cells in x-direction	, dx	0.00000	metres (variable)
start of r-direction noding	, rstart	0.00000	metres
start of x-direction noding	, xstart	0.00000	metres
simulation time limit(opt'l)	, tstop	1.000E+14	seconds
gravitational comp r-direction	, grt	0.00000	m/sec2
gravitational comp z-direction	, gzt	-9.80000	m/sec2
gravitational comp x-direction	, gxt	0.00000	m/sec2
direction angle, r-axis	, thetar	90.00000	degrees
direction angle, z-axis	, thetaz	180.00000	degrees
direction angle, x-axis	, thetax	90.00000	degrees
slip condition	, sfact	-1.0000	
pressure acceleration factor	, pac	1.500	
continuity error criterion	, smax	1.000E-09	
maximum number pressure iters	, itmax	100	
crank-nichlsn implicit factor	, frnk	0.60	
time adder	, tadd	0.0000E+00	seconds
thermal time step limiter	, timp	5.000	
implicit time step limitation	, dtimax	1.0000E+15	seconds

automatic time step selection is used
initial time step, dt = 1.1884E-02 seconds
fract of max time step, cmax = 0.99

1

Title: PFP Plenum Airflow Distribution - Model 2

summary of problem dependent array size requirements

1

* * * I N P U T R E C O R D I M A G E * * *

```
RECORD      COLUMN  1   5    1    1    2    2    3    3    4    4    5    5    6    6    7    7    8
no.                      0    5    0    5    0    5    0    5    0    5    0    5    0    5    0
    1               Title: PFP Plenum Airflow Distribution - Model 2
    2                 input file: pfp.4d.inp
    3               size,   55   22   11
    4               note:   initially, run one step to check setup
    5               time,   1.    1
    6               prnt,
    7               note:   after modeling debugged, run more time steps, or restart and continue
    8               time,   1. 3000
    9               prnt,                    2   10    2        10
   10               pres,  100             1-9
   11               rest,           1    1
   12               post,
   13               misc,           0
   14
   15               note:       GROUP 2 INPUT - CONTROL
   16               note:
   17               cont,sisy,besq,turb,mont,dtim,pace,
   18               cont,save,psav,msav,
   19               cont,read,
   20               aout,velr,velz,velx,
   21               plot,velr,velz,velx,
   22               dbug,data,qaed,size,ttbl,
   23
   24               note:       GROUP 3 INPUT - INTEGER DATA
   25               note:
   26               note:       PFP inflow
   27                  40    1    1          2   10   22   22    2   10                  1  inflow
   28               note:       plenum volume
   29                   0    1               2   54    2    8    2   10                  1  plenum
   30                   0    1               2   50    9   21    2   10                  1  plenum
   31               note:       fan areas
   32                  30    1              14   15   10   14    1    1                  1  fan W1
   33                  30    1              14   15   10   14   11   11                  1  fan E1
   34                  30    1              22   23   10   14    1    1                  1  fan W2
   35                  30    1              22   23   10   14   11   11                  1  fan E2
   36                  30    1              30   31   10   14    1    1                  1  fan W3
   37                  30    1              30   31   10   14   11   11                  1  fan E3
   38                  30    1              38   39   10   14    1    1                  1  fan W4
   39               note:       232Z/236
   40                   0    1 4  2         38   39   10   14   10   10                  1  232/236Z
   41               note:       block out sloped wall
   42                  50                   2   11    2    2    2   10                  1  45 wall
   43                  50                   2   10    3    4    2   10                  1  45 wall
```

```
   50                    2    9    5    6    2   10                        1  45 wall
   50                    2    8    7    8    2   10                        1  45 wall
   50                    2    7    9   10    2   10                        1  45 wall
   50                    2    6   11   12    2   10                        1  45 wall
   50                    2    5   13   14    2   10                        1  45 wall
   50                    2    4   15   16    2   10                        1  45 wall
   50                    2    3   17   18    2   10                        1  45 wall
   50                    2    2   19   20    2   10                        1  45 wall
note:       block out corners of prow
   50                   54   54    2    8    2    4                        1  prowblck
   50                   54   54    2    8    8   10                        1  prowblck
note:       set up monitor cells
    9  12    6   15   12    6   28   12    6   41   12    6    1    5  mon. 1
   15   3    3   15   20    3   15    3    9   15   20    9    2    5  mon. 2
   28   3    3   28   20    3   28    3    9   28   20    9    3    5  mon. 3
   41   3    3   41   20    3   41    3    9   41   20    9    4    5  mon. 4

note:       GROUP 4 INPUT - FLOATING POINT DATA
note:
note:       gravitational orientation
  1.                                  90  180   90                        1es  orient
note:       option 2 input - R-coordinate, in feet
    1  11   2.                                                            1   3es R-coord
   12  13 3.25                                                           1   3es R-coord
   14  15 2.50                                                           1   3es   fan 1
   16  213.167                                                           1   3es R-coord
   22  23 2.50                                                           1   3es   fan 2
   24  293.167                                                           1   3es R-coord
   30  31 2.50                                                           1   3es   fan 3
   32  373.167                                                           1   3es R-coord
   38  39 2.50                                                           1   3es   fan 4
   40  503.045                                                           1   3es R-coord
   51  52 3.75                                                           1   3es R-coord
   53  54 4.33                                                           1   3es R prow
note:       option 1 input - X-coordinate, in feet
  1.0 1.0  1.5  2.0  2.0  2.0  2.0  2.0  1.5  1.0    1   10                    5es X-coord
  1.0                                              11   11                    5es X-coord
note:       properties - base air at 25C
                                  25.  20.  30.    2  1     11    1cg  6  air 25C
note:       initialize Temperature array
  25.                                              1   55    1   22    1   11    9  Temper
note:       initialize Fans - velocity in ft/sec
             -43.7                                14   15   10   14    1    1    7es  fan W1
                0.                                14   15   10   14   10   11    7es  fan E1
             -43.7                                22   23   10   14    1    1    7es  fan W2
              43.7                                22   23   10   14   10   11    7es  fan E2
             -43.7                                30   31   10   14    1    1    7es  fan W3
                0.                                30   31   10   14   10   11    7es  fan E3
                0.                                38   39   10   14    1    1    7es  fan W4
             -31.3                                38   39   10   14   10   11    7es  232/23
note:       inflow PFP table                                                  1   16  PFPinflo
  0.   1.
```

```
 96                1+9   1.                                                  1   16  PFPinflo
 97              note:       232/236Z inflow table
 98                0.                                  -31.3                 2   16  PFPinflo
 99                1+9                                 -31.3                 2   16  PFPinflo
100                                                                                   enddata
1
     Title: PFP Plenum Airflow Distribution - Model 1

     P A R A M E T E R   L I S T   F O R   C A S E                  05/22/91          12:39:29

     number of time steps          , nsteps  - - -       (variable)
     total number of fluid cells   , nfluid  - - - 8130
     total number of solid cells   , nsolid  - - -    0
     total number of compt cells   , ntotal  - - - 8130
     total number radiation cells  , nrad- - - - -    0
     total number constituents     , nsp - - - - -    0
     number of cells in r-direction, nr  - - - - -   55
     number of cells in z-direction, nz  - - - - -   22
     number of cells in x-direction, nx  - - - - -   11
     width  of cells in r-direction, dr  - - - - -   0.00000 metres (variable)
     width  of cells in z-direction, dz  - - - - -   0.30480 metres
     width  of cells in x-direction, dx  - - - - -   0.00000 metres (variable)
     start of r-direction noding   , rstart  - - -   0.00000 metres
     start of x-direction noding   , xstart  - - -   0.00000 metres
     simulation time limit(opt'l)  , tstop - - - - 1.000E+02 seconds
     gravitational comp r-direction, grt - - - - -   0.00000 m/sec2
     gravitational comp z-direction, gzt - - - - -  -9.80000 m/sec2
     gravitational comp x-direction, gxt - - - - -   0.00000 m/sec2
     direction angle, r-axis       , thetar  - - -  90.00000 degrees
     direction angle, z-axis       , thetaz  - - - 180.00000 degrees
     direction angle, x-axis       , thetax  - - -  90.00000 degrees
     slip condition                , sfact - - - -  -1.0000
     pressure acceleration factor  , pac - - - - -   1.500
     continuity error criterion    , smax  - - - -   1.000E-09
     maximum number pressure iters , itmax - - - - 100
     crank-nichlsn implicit factor , frnk  - - - -   0.60
     time adder                    , tadd  - - - - 0.0000E+00 seconds
     thermal time step limiter     , timp  - - - -   5.000
     implicit time step limitation , dtimax  - - - 1.0000E+15 seconds


          automatic time step selection is used
          initial time step,        dt = 1.0734E-02 seconds
          fract of max time step, cmax =   0.99
1
     Title: PFP Plenum Airflow Distribution - Model 1

                         summary of problem dependent array size requirements
```

APPENDIX B

VELOCITY TIME HISTORIES

APPENDIX B

VELOCITY TIME HISTORIES

To assess whether sufficient simulation time was allowed for TEMPEST to generate steady-state velocity fields, the velocity as a function of time at several fixed computational cells was monitored. These monitor cells were located as shown in Figure B.1. The remaining Figures B.2 through B.7 show the velocities as a function of time. Velocities are shown for each component direction, with the U component corresponding to J in Figure 5.1, W to I, and V to K, respectively.

Most of the calculations were carried out to 75 - 80 s. At this point, steady-state conditions appeared to have been achieved as can be observed in the following figures. However, because we felt some concern that an adequate steady state had not been reached in the south end of the plenum, presumed to be one of the major potential deposition locations, a longer velocity-field run was made for the first fan configuration, carrying the calculations out to 215 s of simulation time. The near-floor concentrations for this better-converged velocity field were compared to those for the 80-s velocity field (Figures B.1 and B.2, respectively). The similarity between the two sets of results confirmed the adequacy of the 80-s field for use in the rest of the study. The velocity field used for the second fan configuration was 76s "old," and was considered to be adequate by analogy to the first.

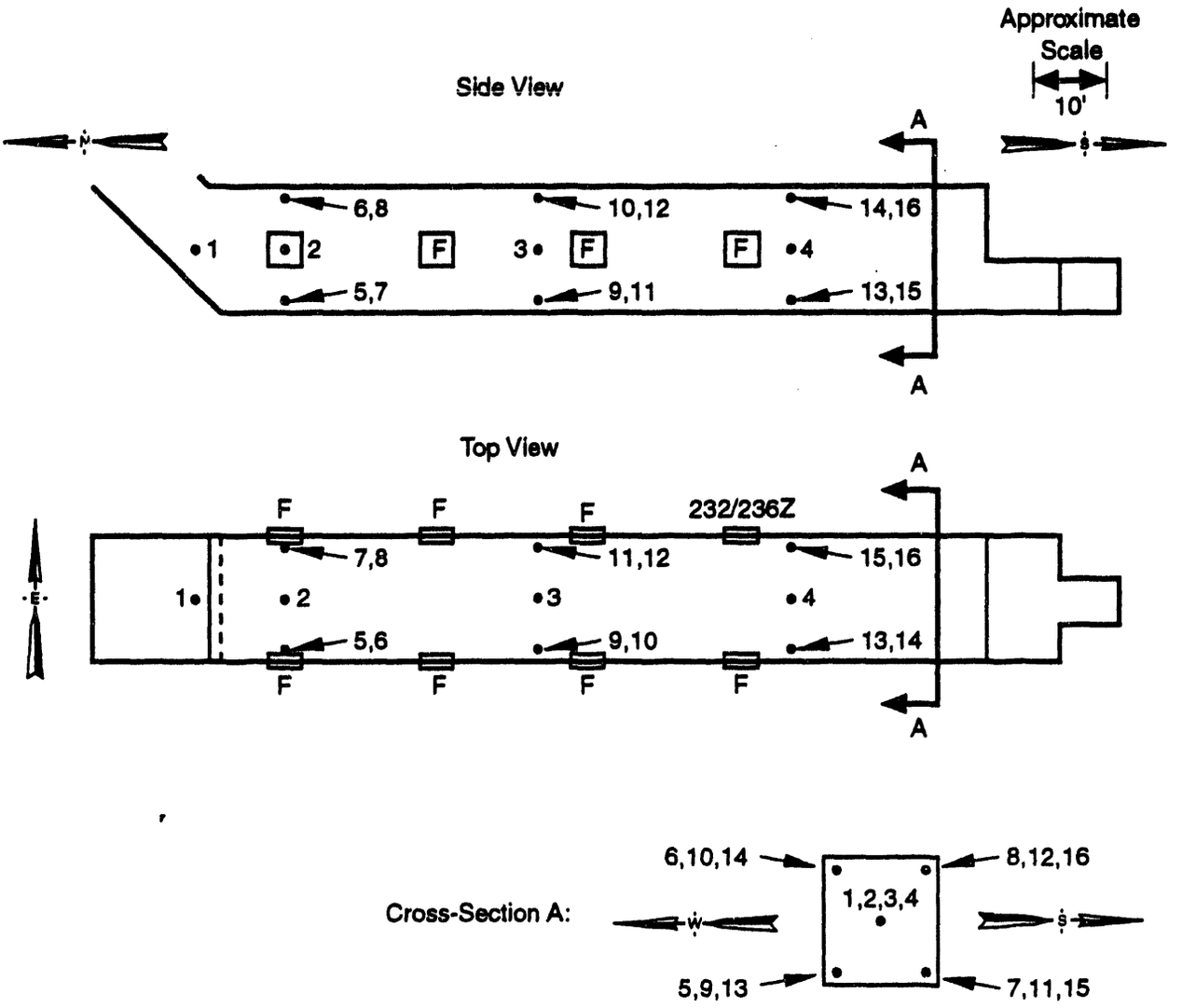

FIGURE B.1. Map of Locations of Convergence Monitor Cells

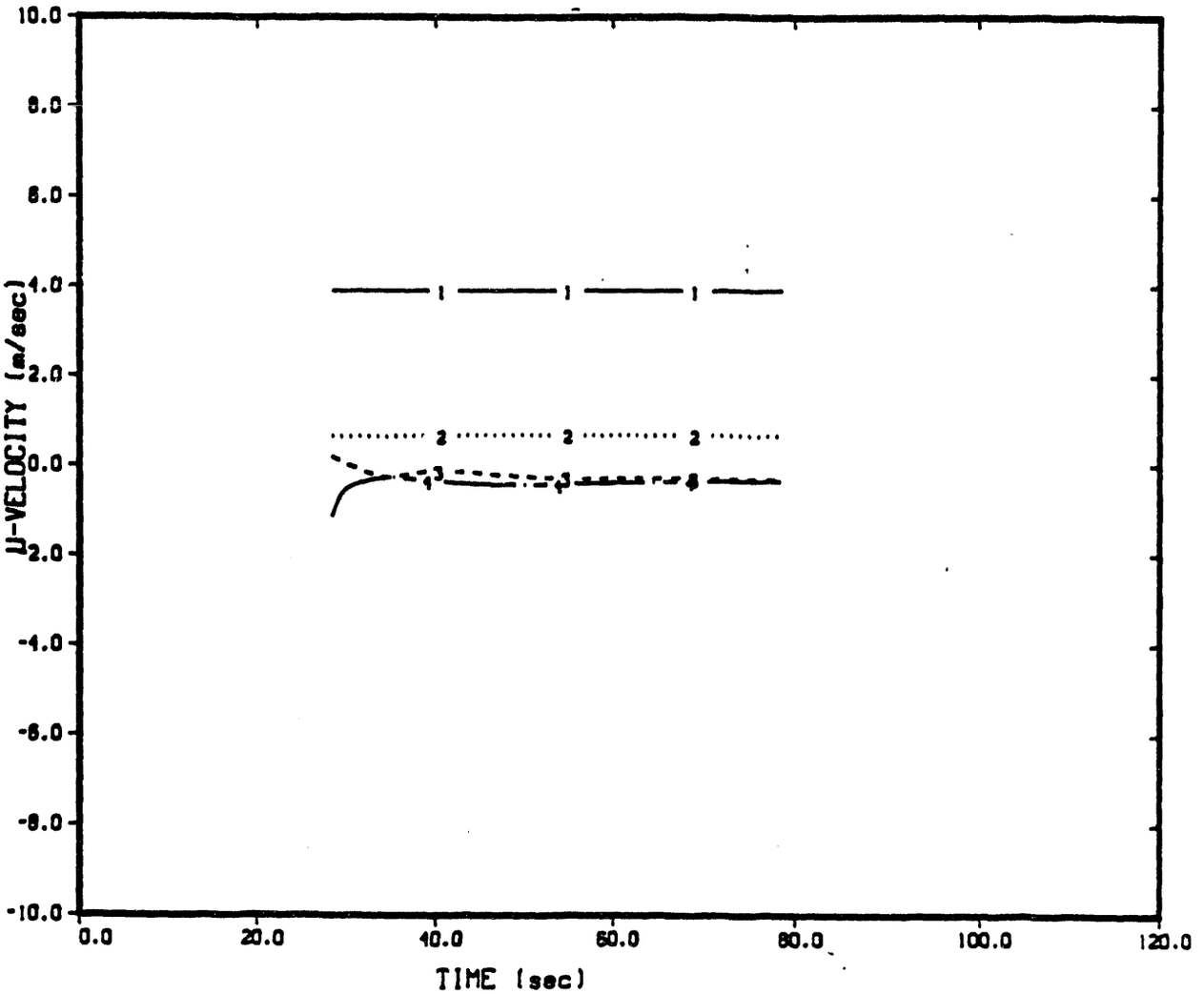

FIGURE B.2. Development Over Time of the Lengthwise Velocity Components at Monitor Cells 1 Through 4 for Fan Configuration 1

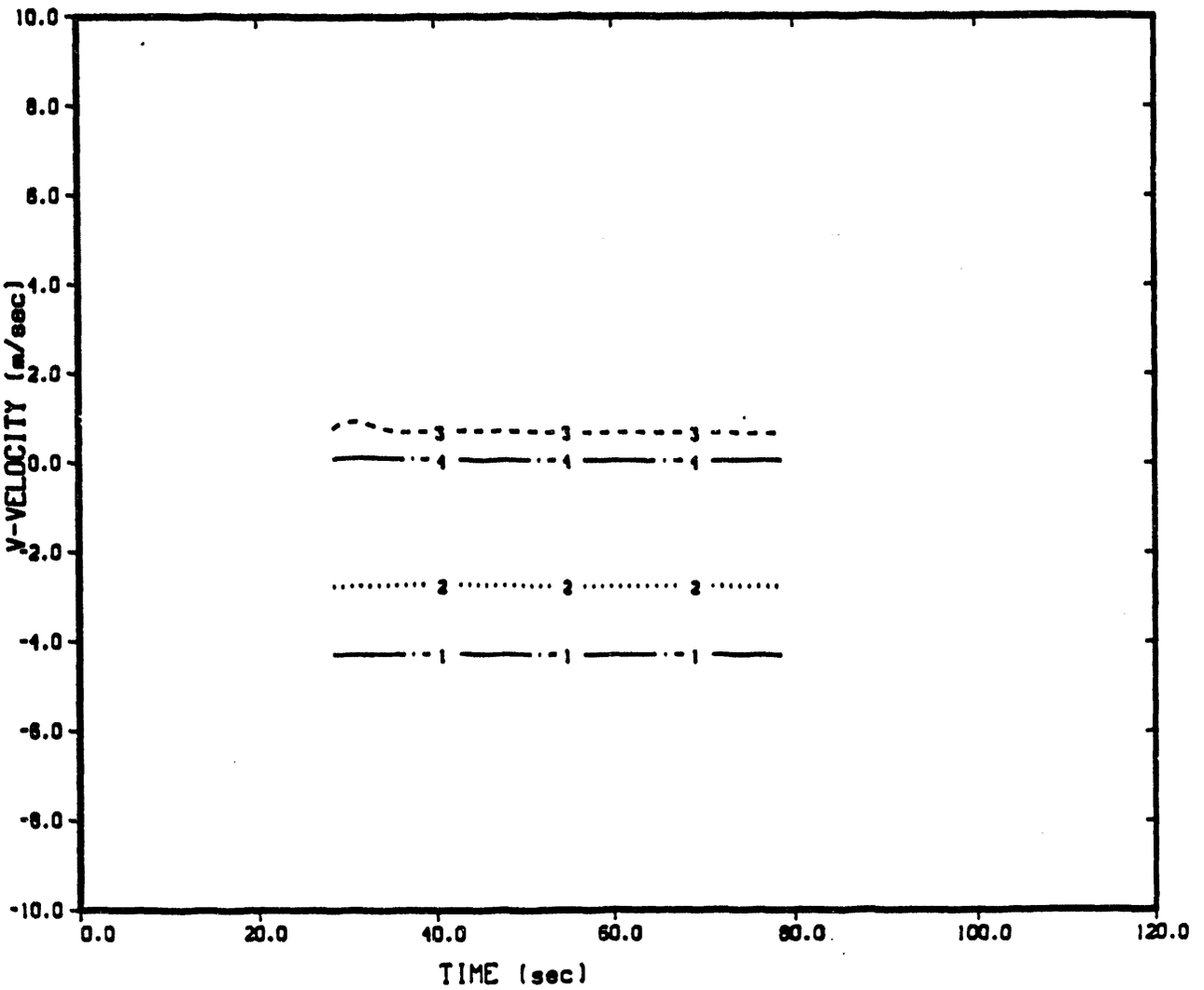

FIGURE B.3. Development Over Time of the Vertical Velocity Components at Monitor Cells 1 Through 4 for Fan Configuration 1

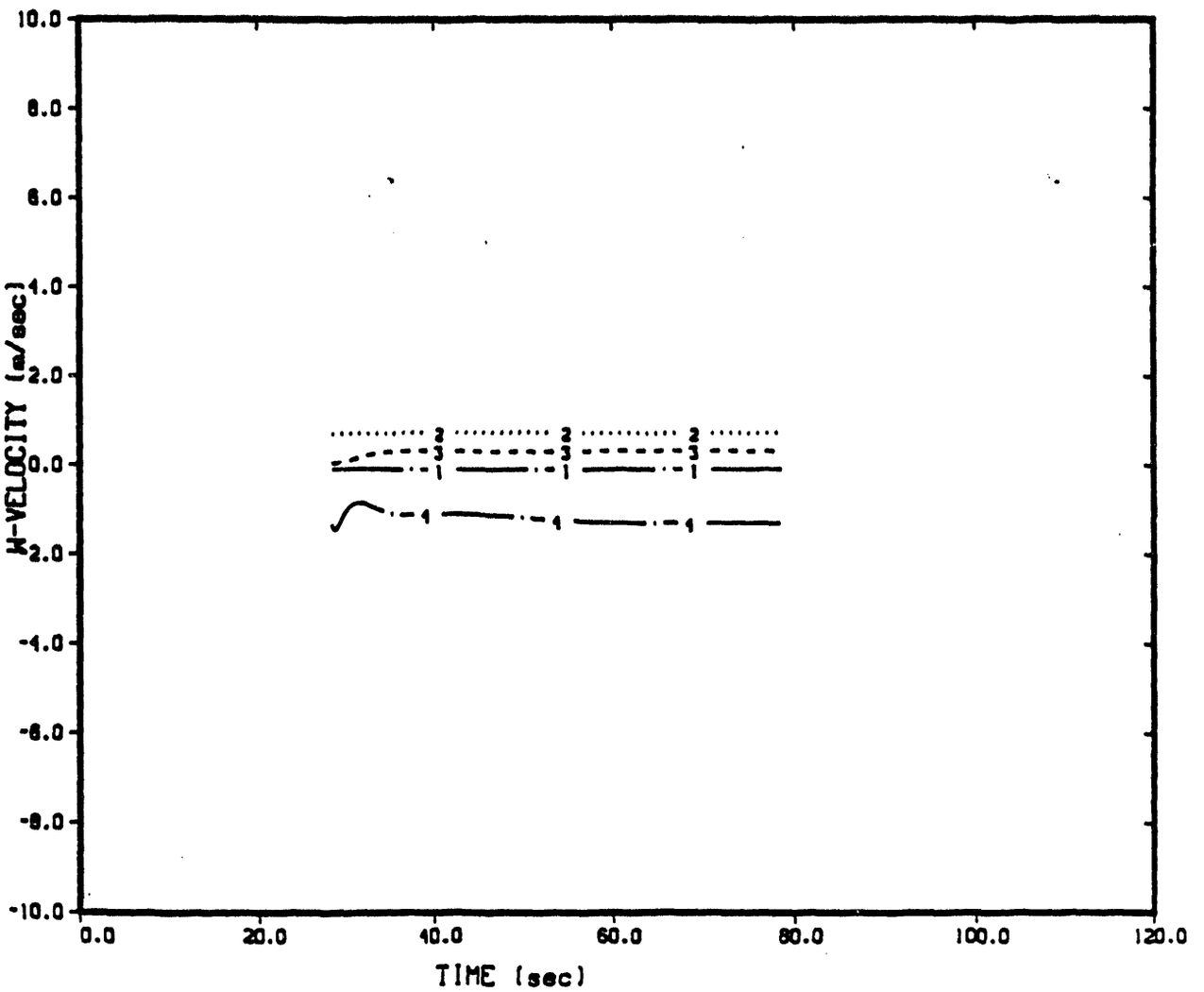

FIGURE B.4. Development Over Time of the Widthwise Velocity Components at Monitor Cells 1 Through 4 for Fan Configuration 1

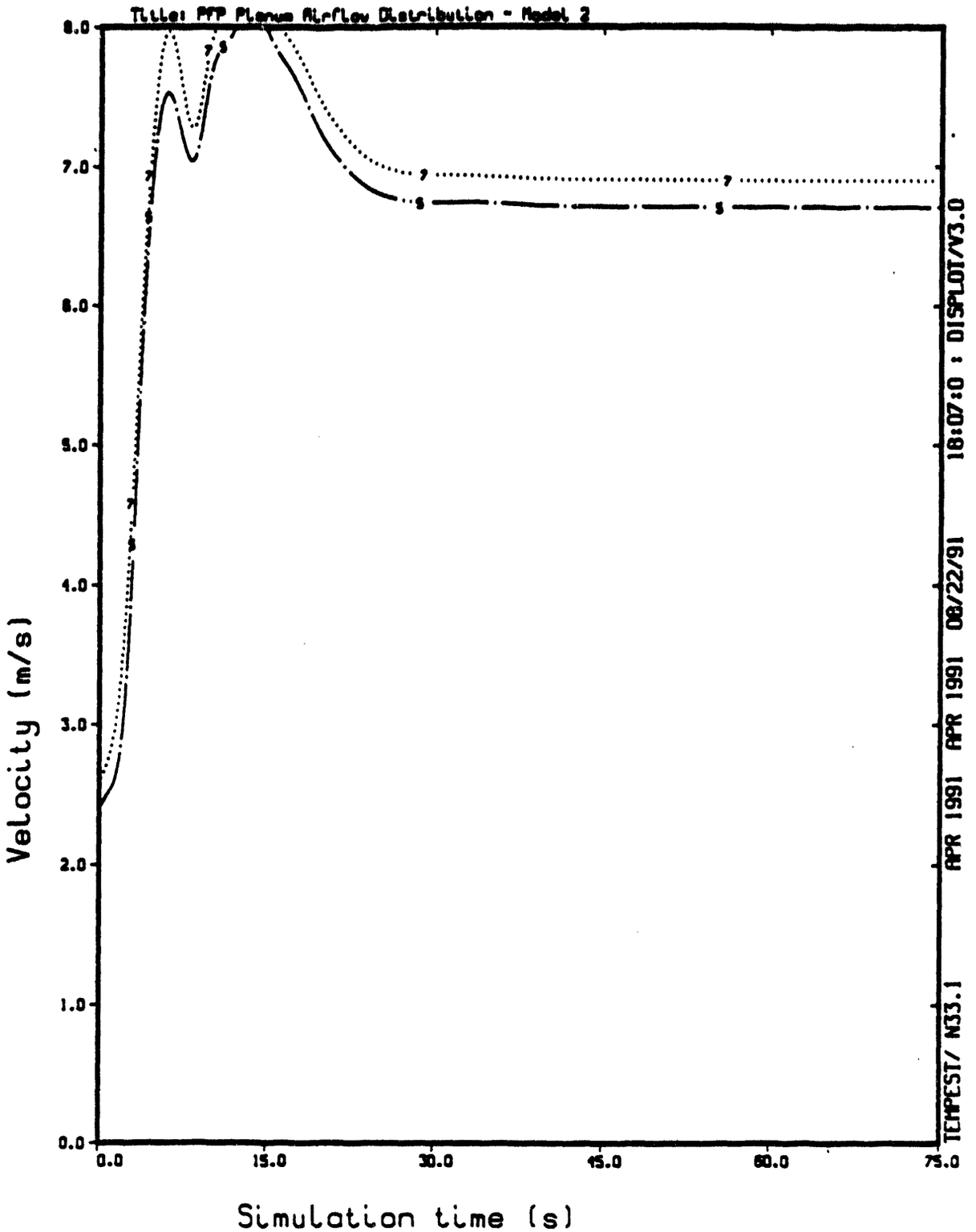

FIGURE B.5a. Development Over Time of the Lengthwise Velocity Components at Monitor Cells 5 and 7 for Fan Configuration 2

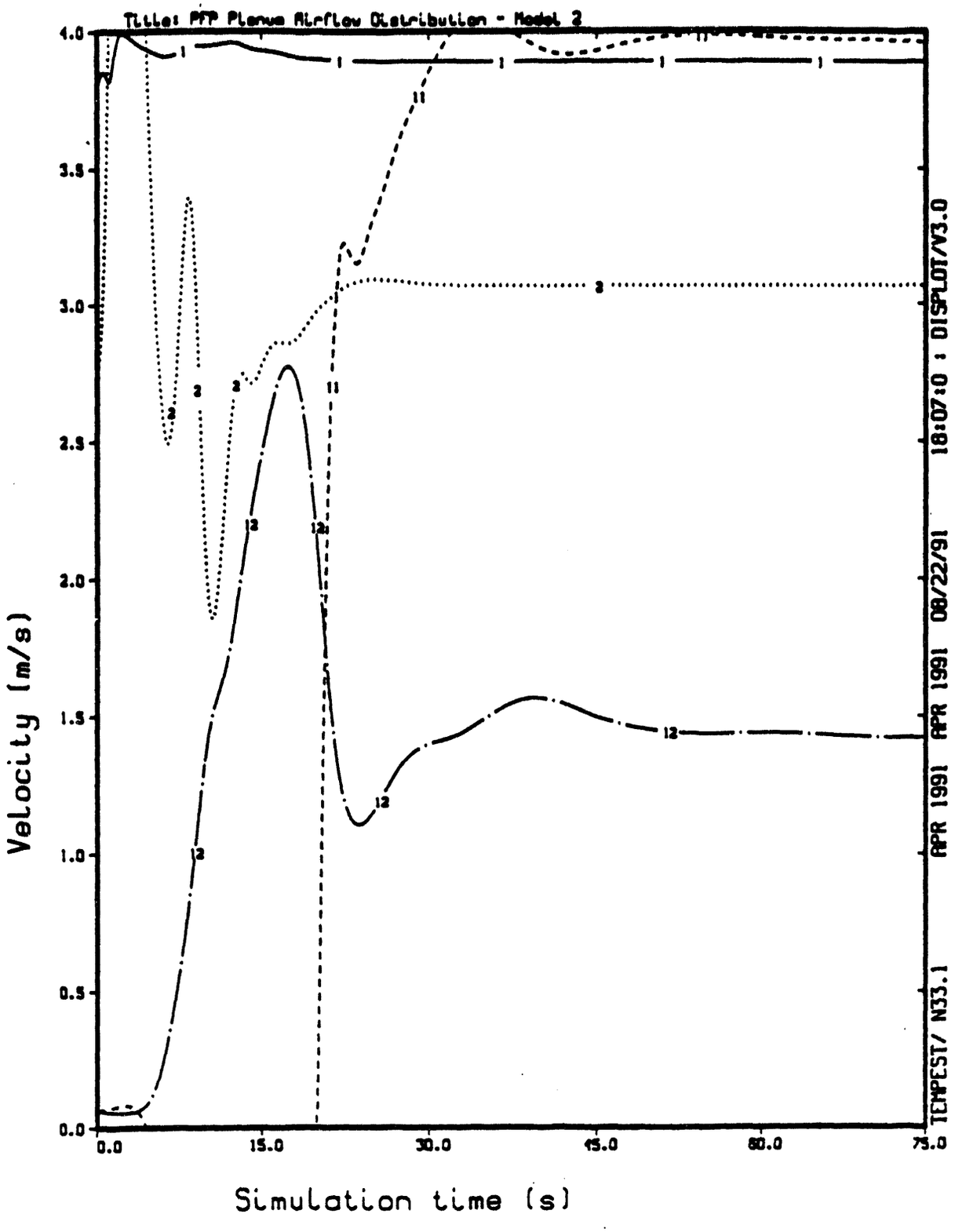

FIGURE B.5b. Development Over Time of the Lengthwise Velocity Components at Monitor Cells 1, 2, 11, and 12 for Fan Configuration 2

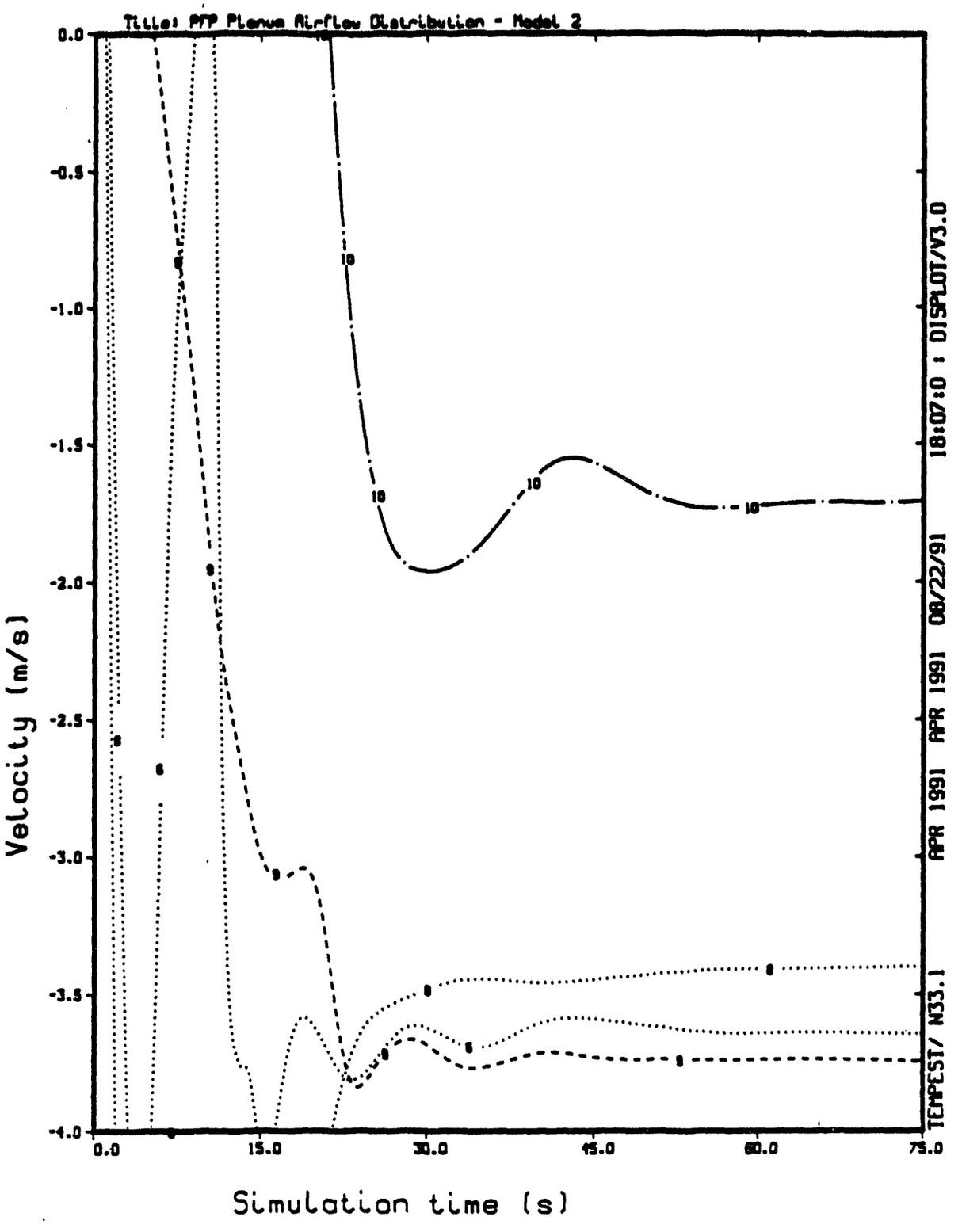

FIGURE B.5c. Development Over Time of the Lengthwise Velocity Components at Monitor Cells 6, 8, 9, and 10 for Fan Configuration 2

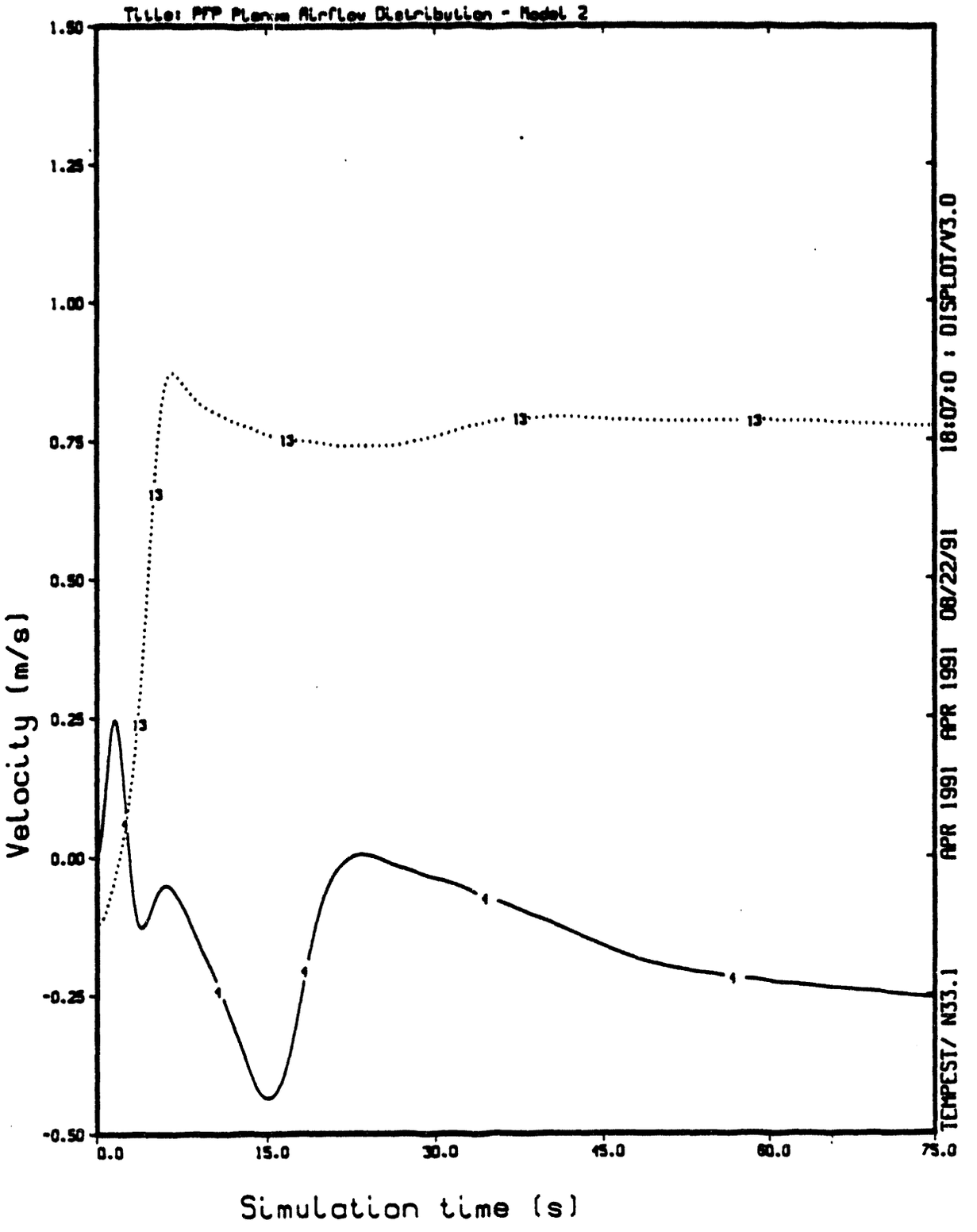

FIGURE B.5d. Development Over Time of the Lengthwise Velocity Components at Monitor Cells 4 and 13 for Fan Configuration 2

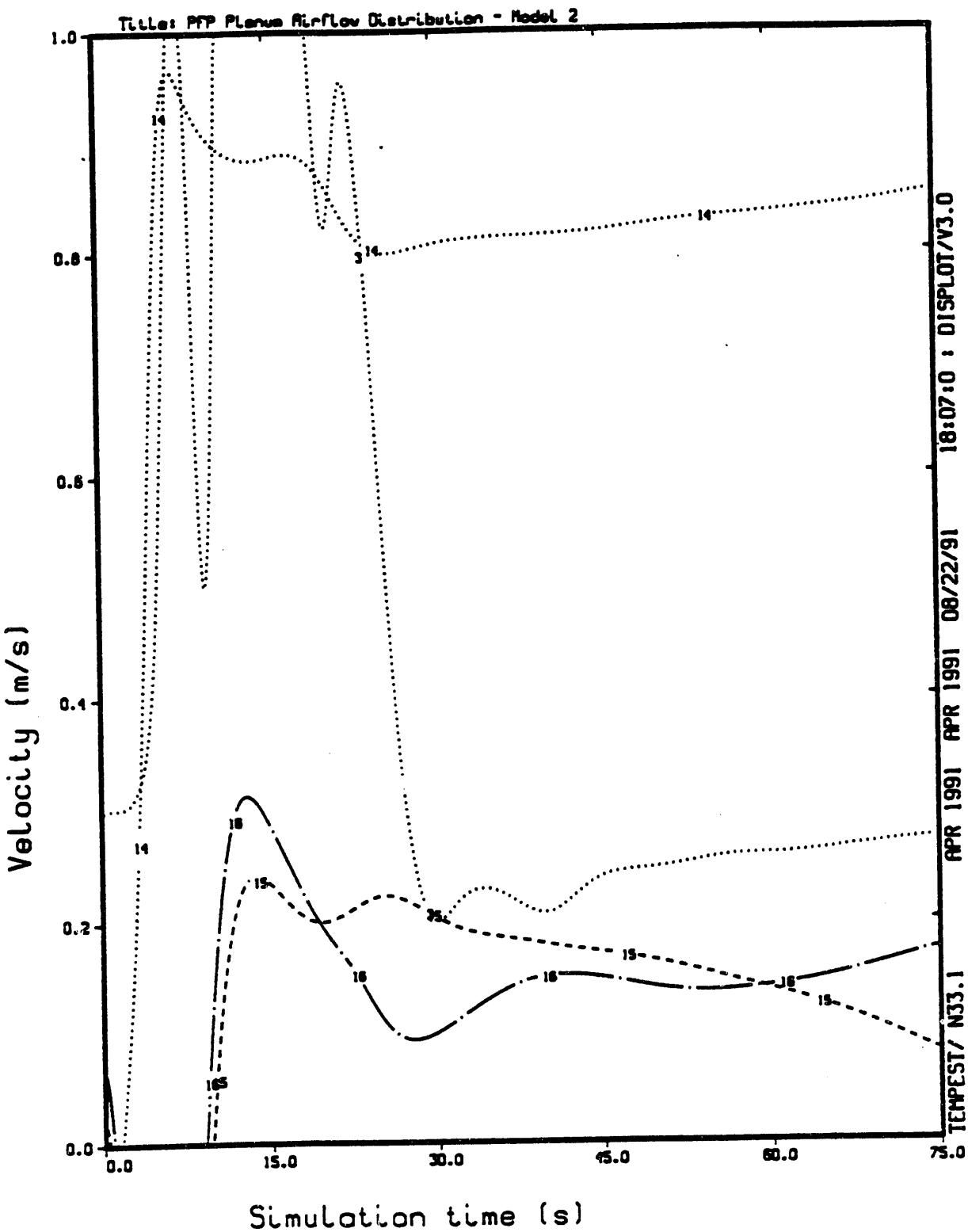

FIGURE B.5e. Development Over Time of the Lengthwise Velocity Component at Monitor Cells 3, 14, 15, and 16 for Fan Configuration 2

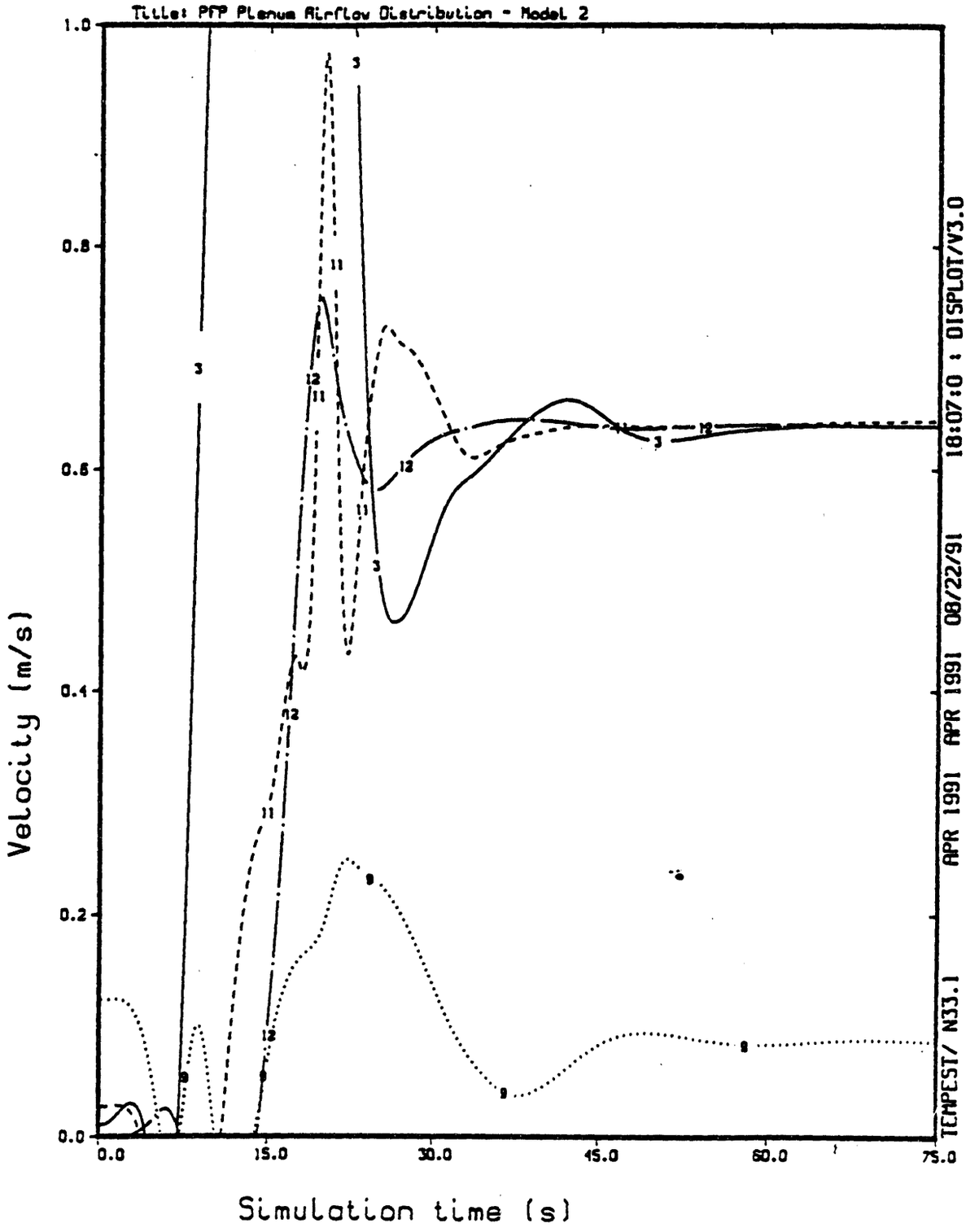

FIGURE B.6a. Development Over Time of the Vertical Velocity Component at Monitor Cells 3, 9, 11, and 12 for Fan Configuration 2

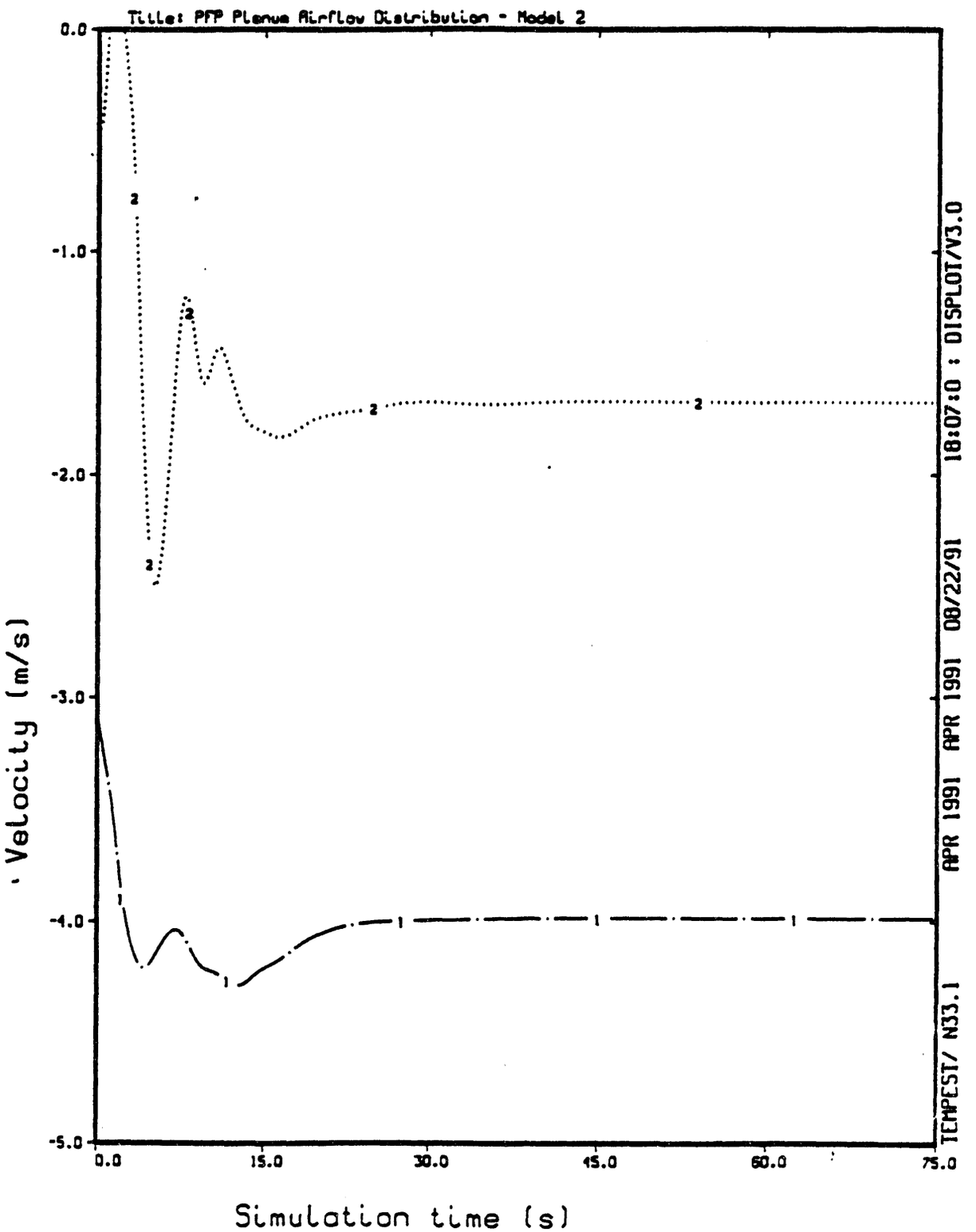

FIGURE B.6b. Development Over Time of the Vertical Velocity Component at Monitor Cells 1 and 2 for Fan Configuration 2

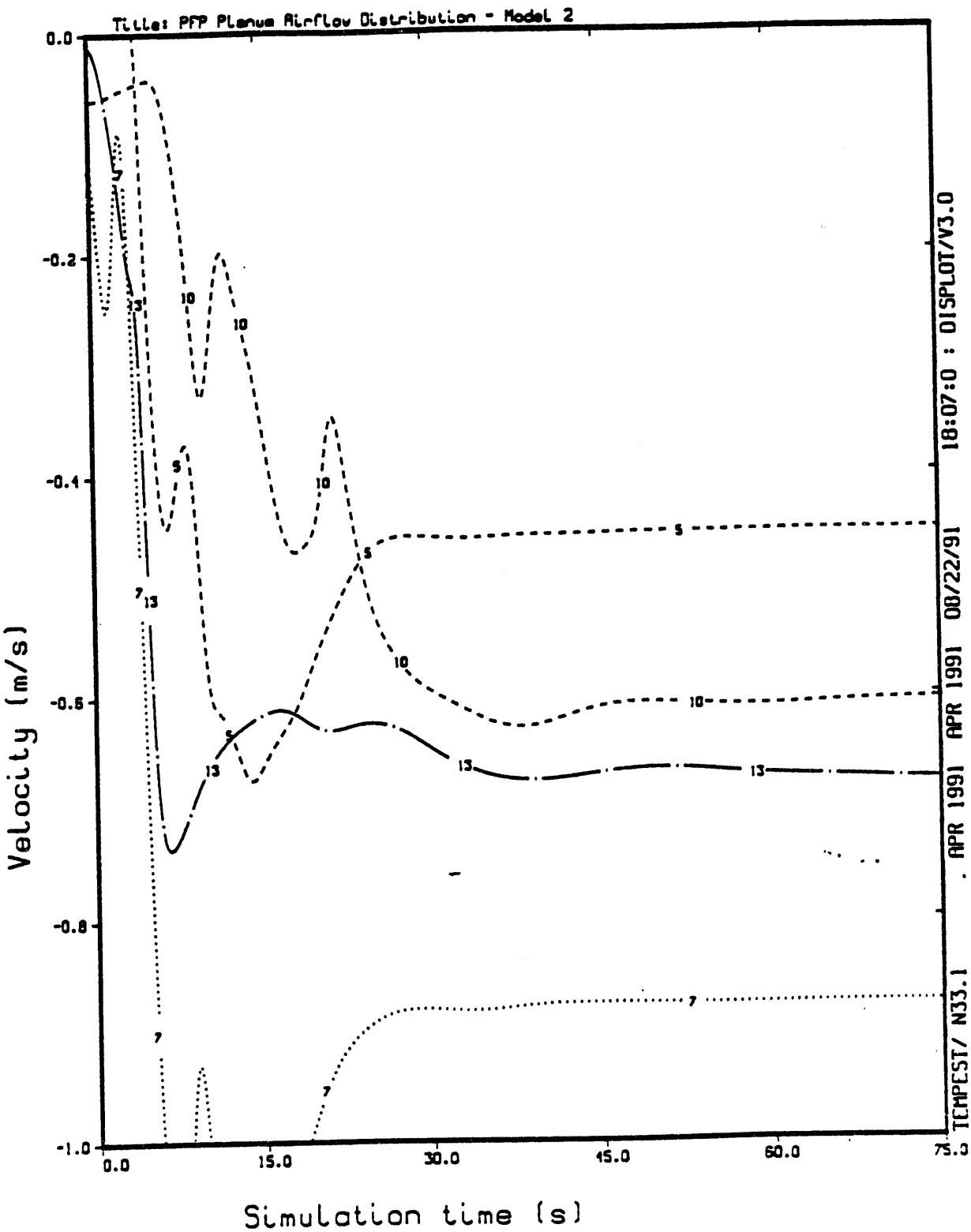

FIGURE B.6c. Development Over Time of the Vertical Velocity Component at Monitor Cells 5, 7, 10, and 13 for Fan Configuration 2

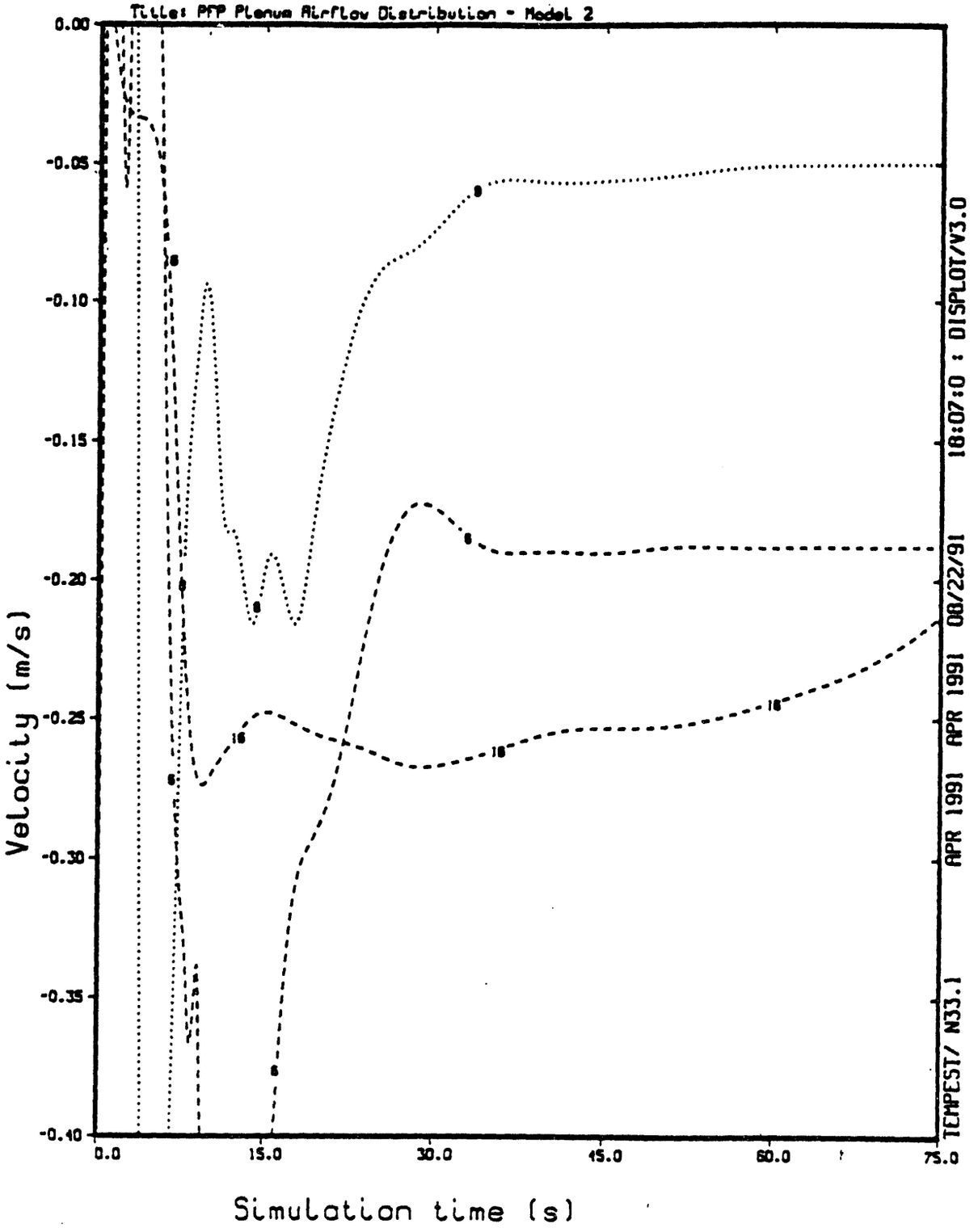

FIGURE B.6d. Development Over Time of the Vertical Velocity Component at Monitor Cells 6, 8, and 16 for Fan Configuration 2

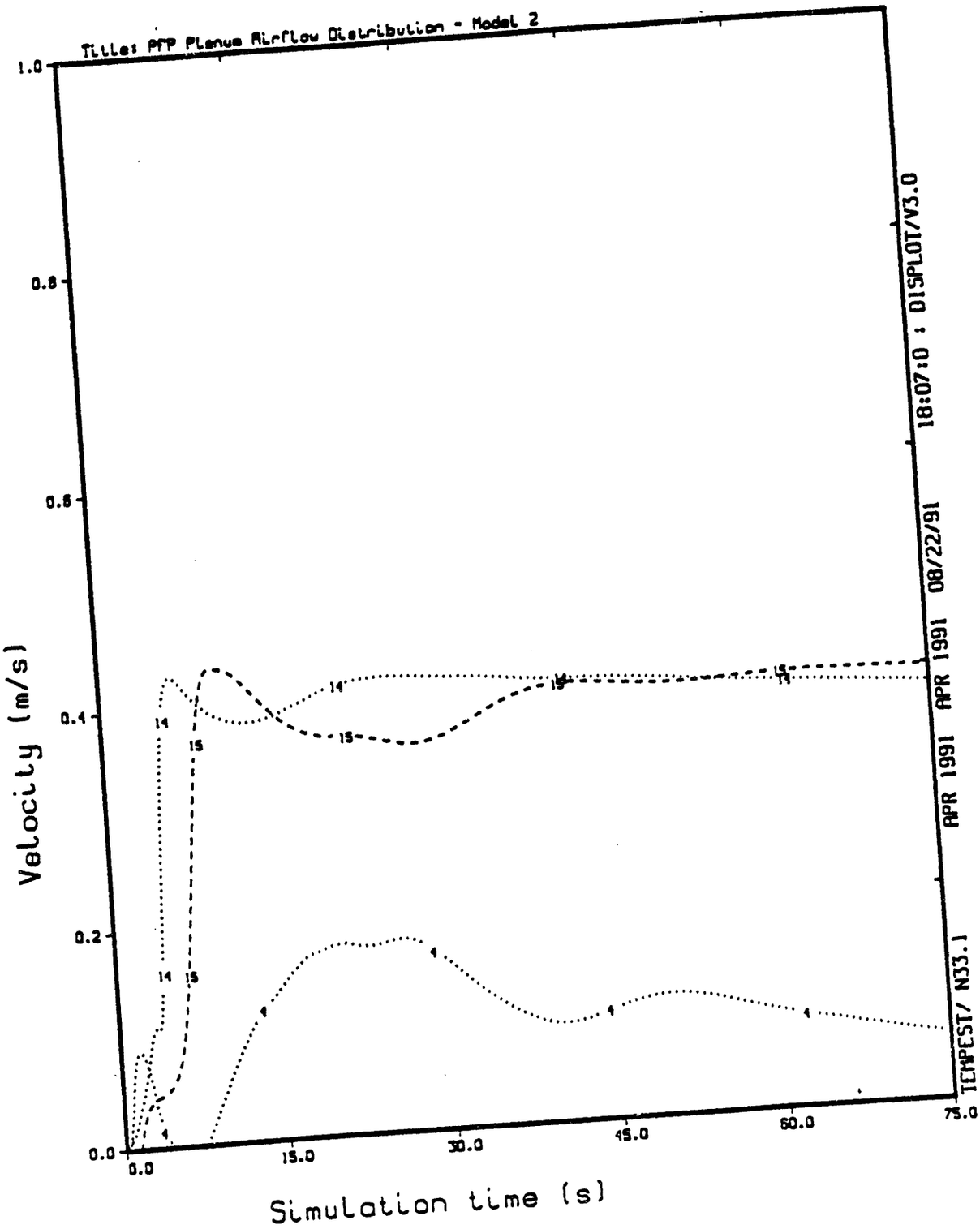

FIGURE B.6e. Development Over Time of the Vertical Velocity Component at Monitor Cells 4, 14, and 15 for Fan Configuration 2

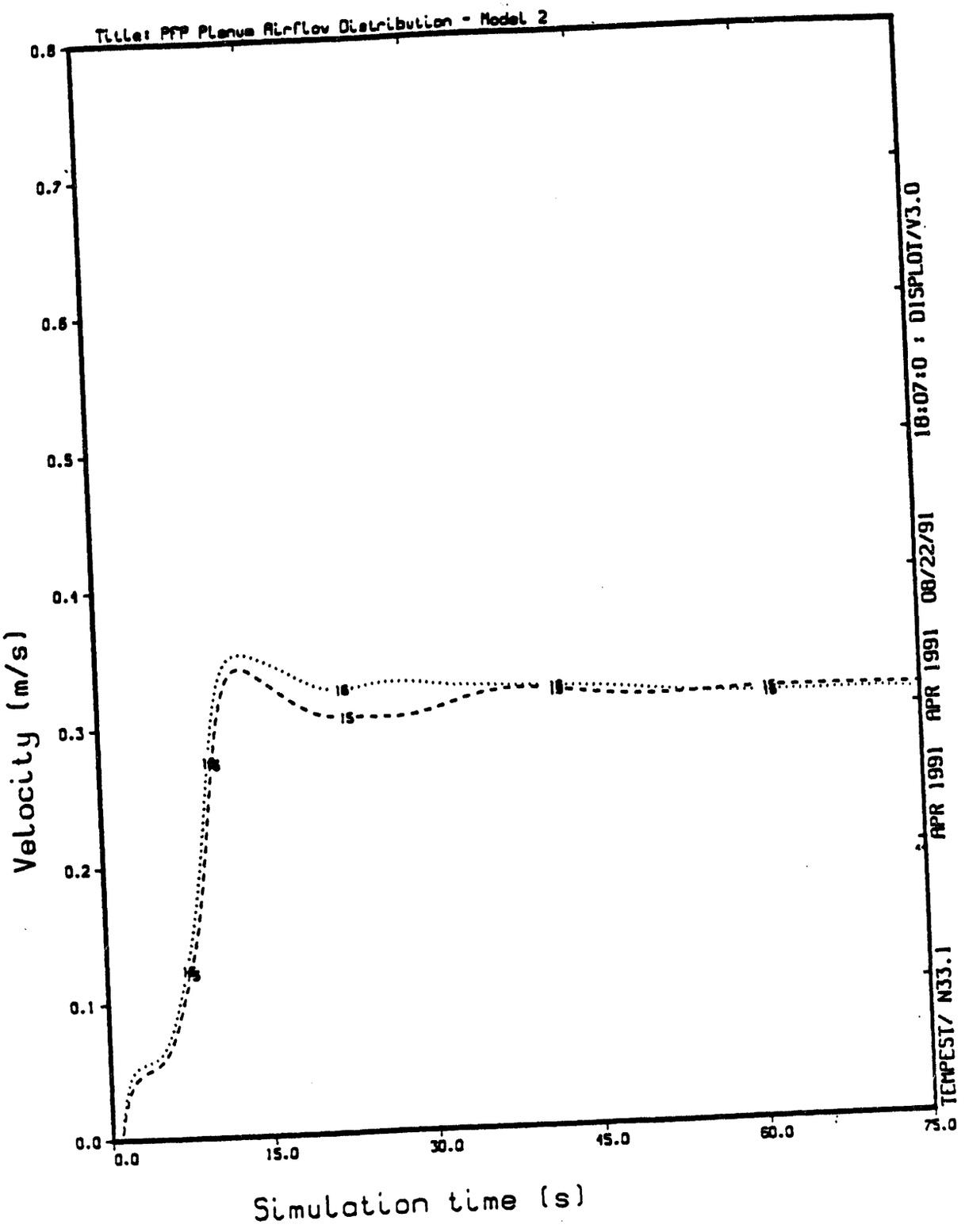

FIGURE B.7a. Development Over Time of the Widthwise Velocity Component at Monitor Cells 15 and 16 for Fan Configuration 2

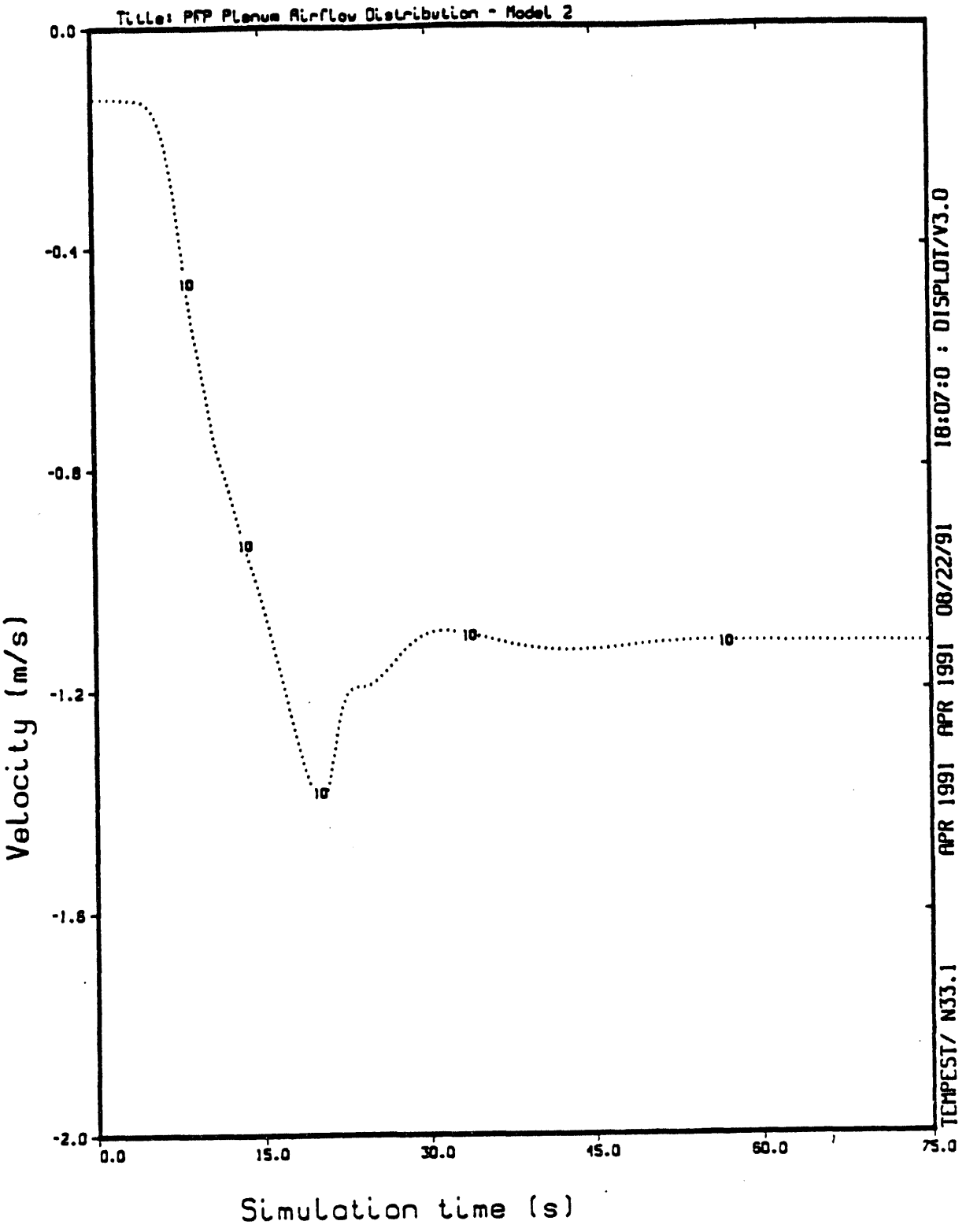

FIGURE B.7b. Development Over Time of the Widthwise Velocity Component at Monitor Cell 10 for Fan Configuration 2

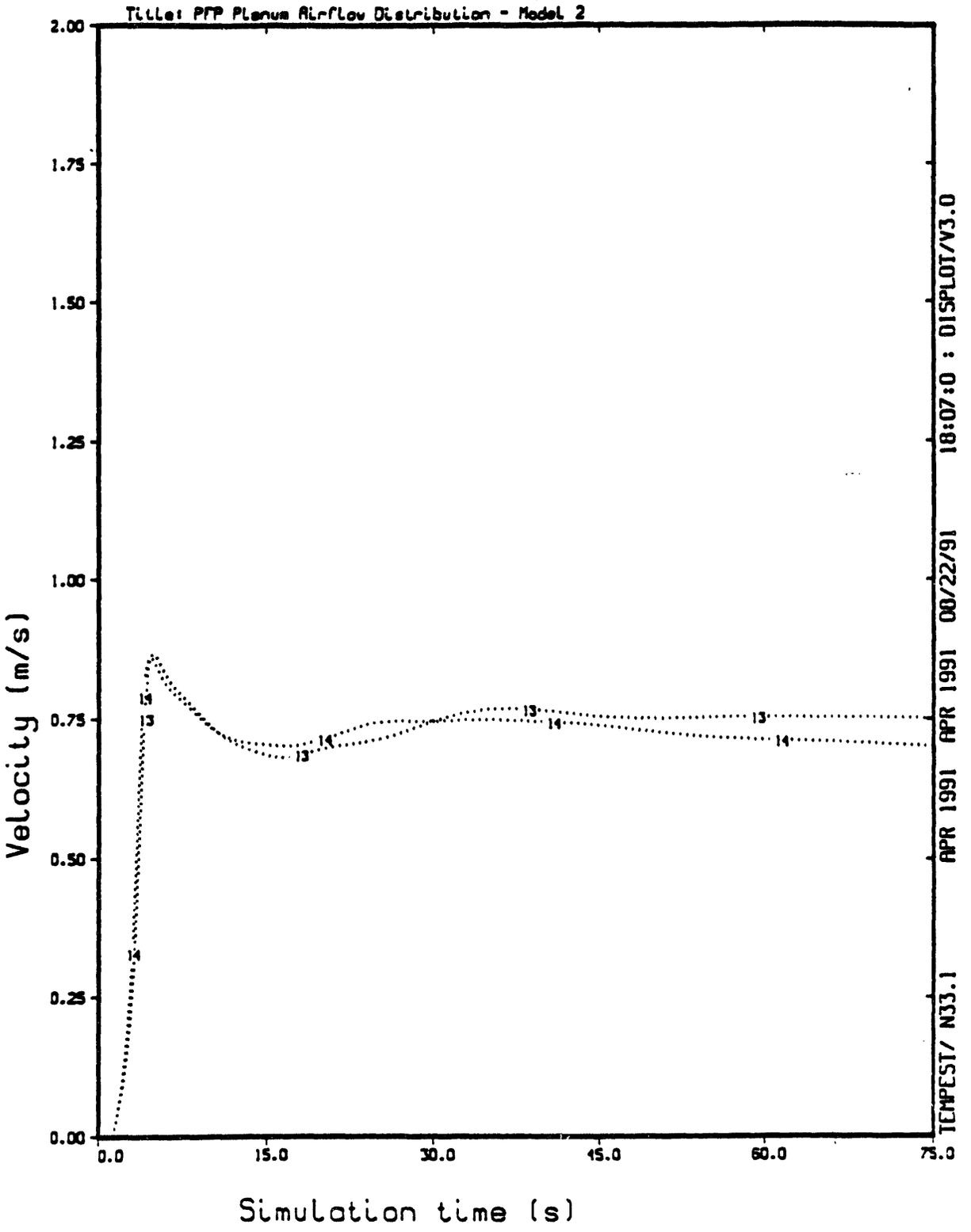

FIGURE B.7c. Development Over Time of the Widthwise Velocity Component at Monitor Cells 13 and 14 for Fan Configuration 2

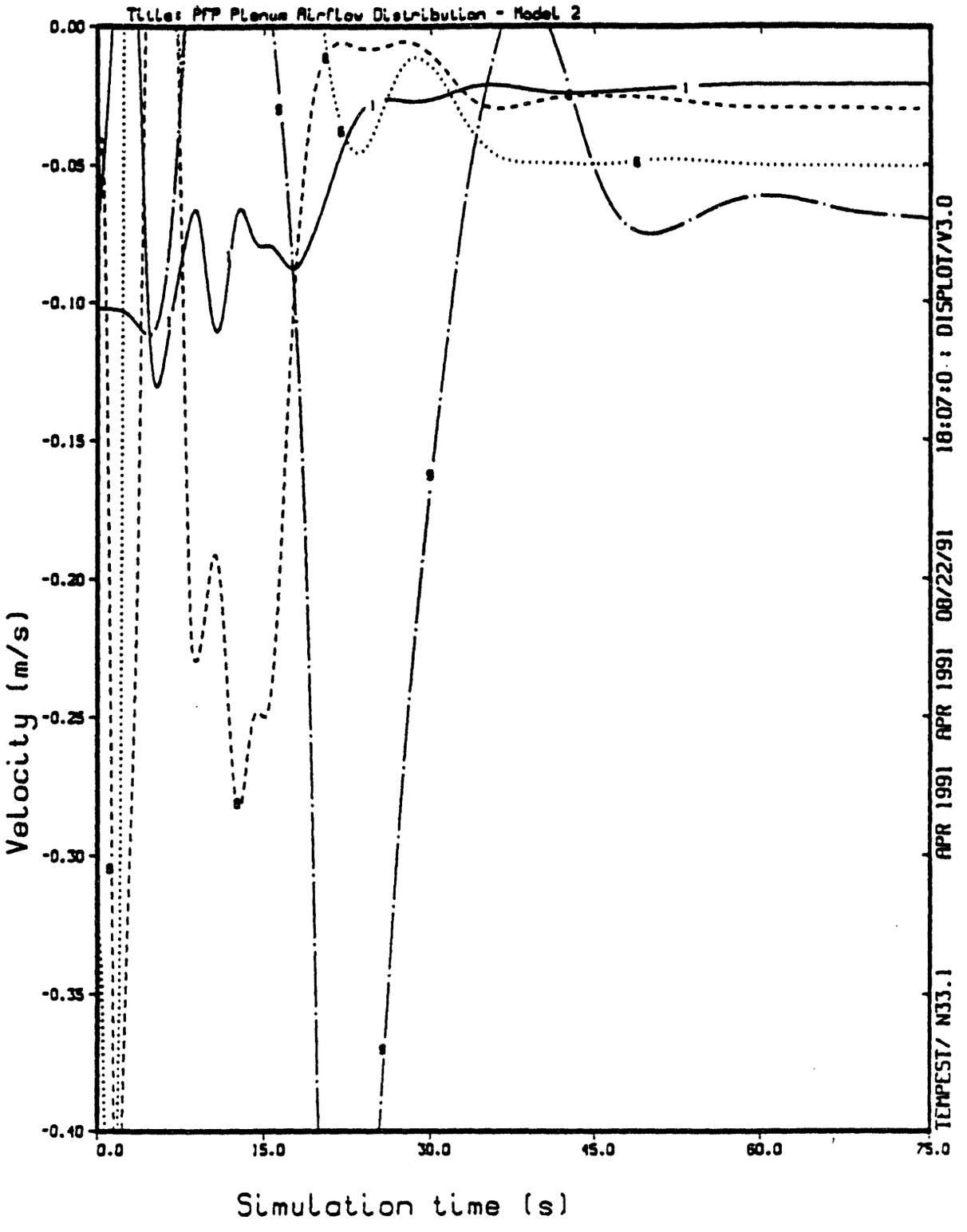

FIGURE B.7d. Development Over Time of the Widthwise Velocity Component at Monitor Cells 1, 6, 8, and 9 for Fan Configuration 2

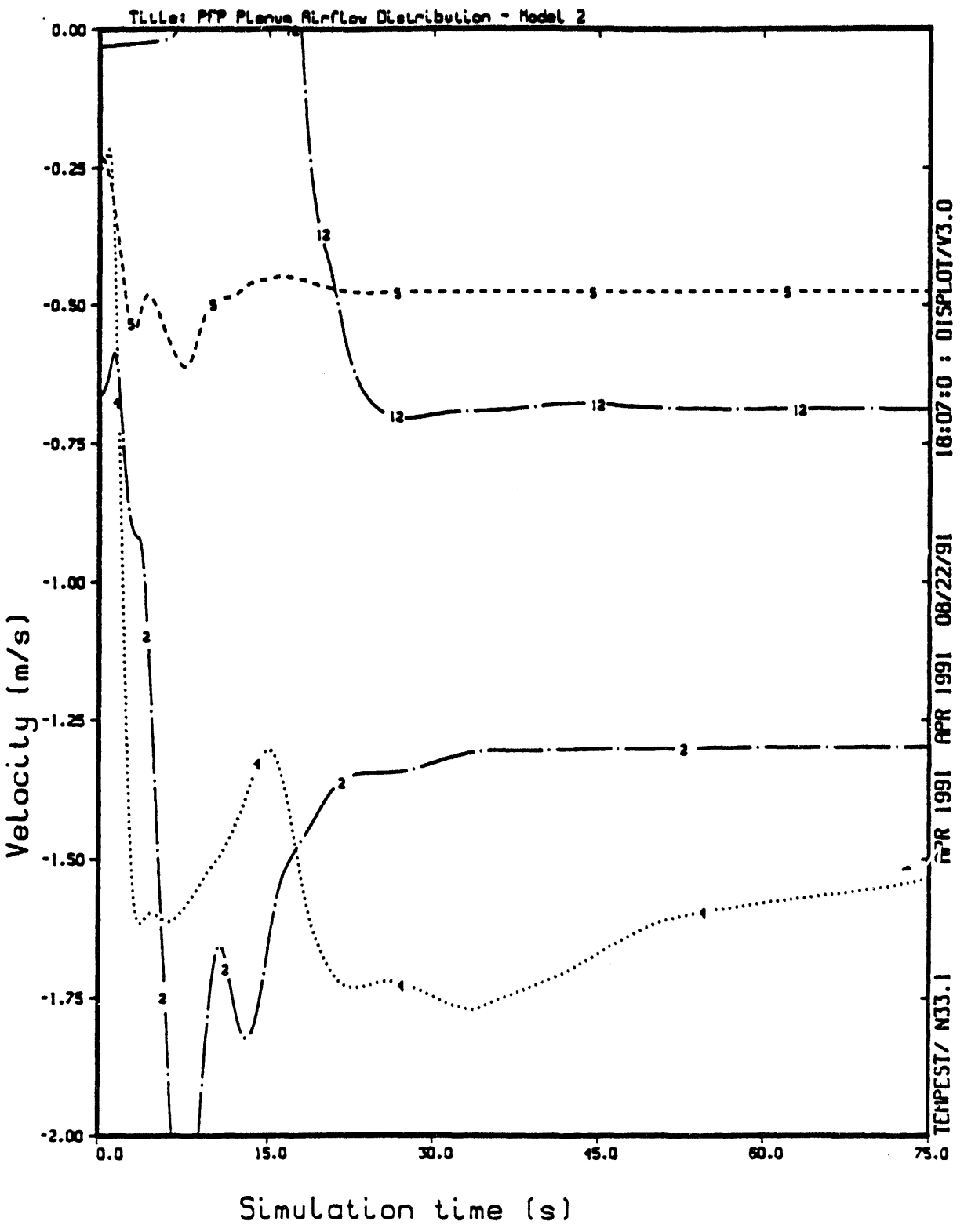

FIGURE B.7e. Development Over Time of the Widthwise Velocity Component at Monitor Cells 2, 4, 5, and 12 for Fan Configuration 2

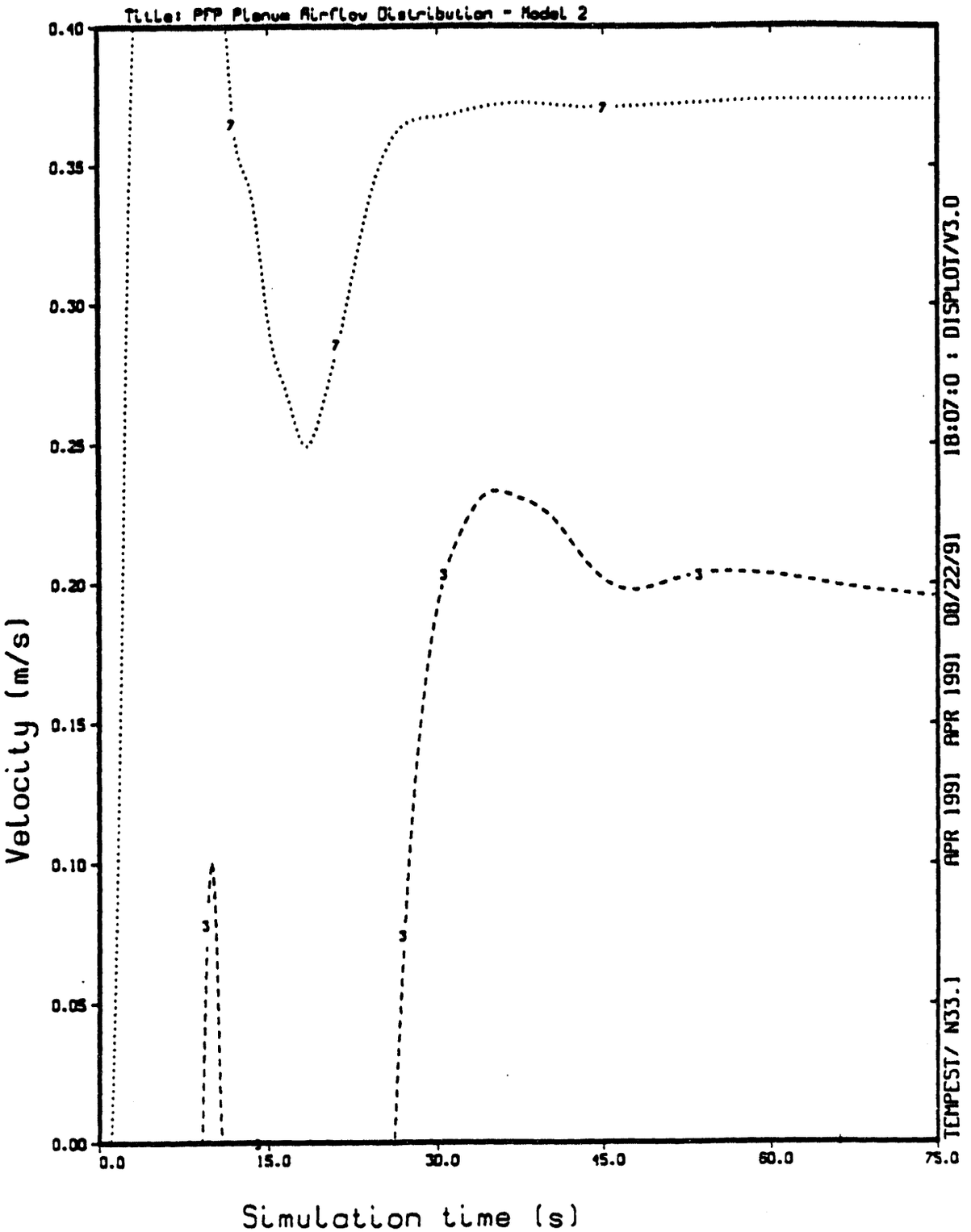

FIGURE B.7f. Development Over Time of the Widthwise Velocity Component at Monitor Cells 3 and 7 for Fan Configuration 2

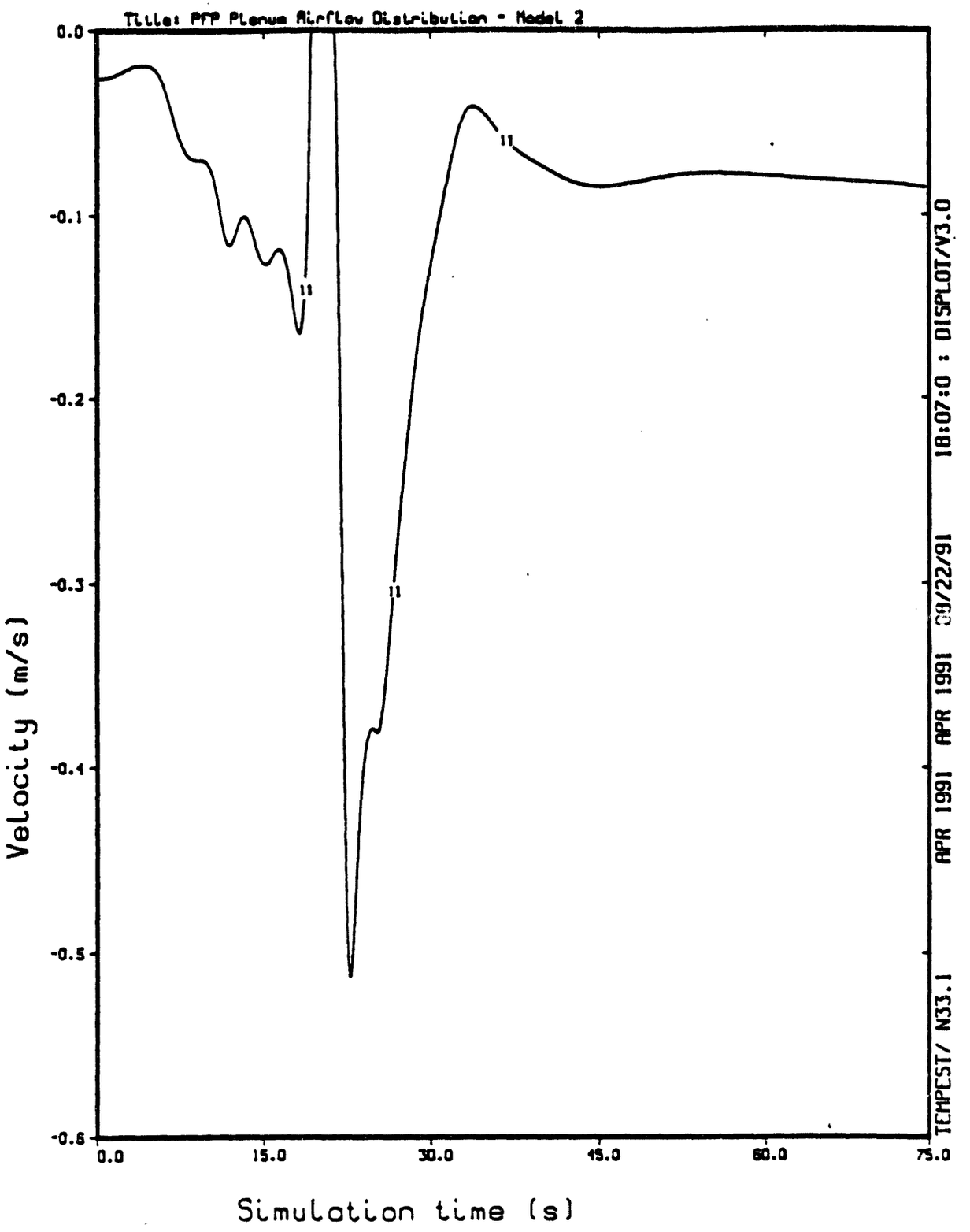

FIGURE B.7g. Development Over Time of the Widthwise Velocity Component at Monitor Cells 11 for Fan Configuration 2

PNL-8681
UC-702

DISTRIBUTION

No. of Copies

OFFSITE

12 DOE/Office of Scientific and Technical Information

ONSITE

2 DOE Richland Operations Office

D. W. Templeton
J. E. Mecca

15 Westinghouse Hanford Company

E. C. Vogt
G. A. Glover
C. M. Kronvall
J. D. Dick
G. M. Stevens
D. J. McBride
J. A. Teal
R. E. Barker
F. C. Han
G. A. Westsik (5)
A. L. Ehlert

No. of Copies

17 Pacific Northwest Laboratory

L. A. Mahoney (2)
J. A. Glissmeyer (5)
M. Y. Ballinger
C. S. Sloane
B. J. Tegner
Publishing Coordination
Technical Report Files (5)

Routing

R. M. Ecker
M. J. Graham
P. M. Irving
C. S. Sloane
P. C. Hays/B. J. Tegner (last)

DATE
FILMED
8/12/94
END